Addis Ababa University
Addis Ababa Institute of Technology
School of Mechanical & Industrial Engineering

Design and Simulation of Institutional Solar-powered Cookstove Using Thermal Storage System

A Thesis Submitted to the School of Graduate Studies of Addis Ababa Institute of Technology, Addis Ababa University in partial fulfillment for the Degree of Master of Science in Mechanical Engineering

(Thermal engineering)

By: Tihun Birhanu Beyene

Advisors: Abdulkadir A. (PhD) & Kamil D. (PhD)

Addis Ababa, Ethiopia
June, 2023

Addis Ababa University
Addis Ababa Institute of Technology
School of Graduate Studies
School of Mechanical and Industrial Engineering

Design and Simulation of Institutional Solar-powered Cookstove Using Thermal Storage System

By

Tihun Birhanu Beyene

Approved by the Board of Examiners:

Abdulkadir A. (PhD)	____________________	____________________
Kamil D. (PhD)	____________________	____________________
Advisor Name	Signature	Date
____________________	____________________	____________________
Internal Examiner	Signature	Date
____________________	____________________	____________________
External Examiner	Signature	Date
Dr. Araya Abera	____________________	____________________
School Dean	Signature	Date
Dr. Sosina Mengistu	____________________	____________________
Associate Direct for PG Program	Signature	Date

DECLARATION

I hereby declare that the work which is being presented in this thesis entitled Design and Simulation of Institutional Solar-powered Cookstove Using Thermal Storage System is original work of my own, has not been presented for a degree of any other university and all the resource of materials used for this thesis have been duly acknowledged.

________________________ ____________

Tihun Birhanu Beyene Date

This is to certify that the above declaration made by the candidate is correct to the best of my Knowledge.

Abdulkadir A. (PhD) Date

Kamil D. (PhD) Date

ACKNOWLEDGMENT

This thesis would not have been feasible without the help and encouragement of a few unique people. As a result, I'd like to thank everyone who helped me complete this MSc program in any form.

First and foremost, I want to express my gratitude to God. He has provided me with strength and encouragement during the difficult process of finishing my thesis. I am eternally grateful for His unending love, mercy, and grace.

Next, I'd like to thank my advisers, Dr. Abdulkadir Aman and Dr. Kamil Dino, for their assistance and inspiration throughout the study. Their invaluable advice and enthusiasm for the research topic were the driving forces behind my everyday efforts. It is an honor to convey my heartfelt gratitude to my late mother, father, and siblings for their love and support. I'd like to thank and honor my friends for their continued encouragement and inspiration during this journey. Abi Thank you so much for your encouragement; may God continue to bless you. Last but not least, I would like to thank the School of Mechanical and Industrial Engineering (AAiT- AAU).

Thank you for your encouragement and guidance in getting me to where I am now. May the Highest continue to bless you all!

ABSTRACT

The world's demand for energy is rising quickly, yet conventional energy supplies are also declining. Future energy demands must thus be supplied and increased securely and efficiently. One of the most pressing issues of the twenty-first century is the sustainable production and use of renewable energy. A dependable supply of clean, affordable energy for everybody must be addressed. Because of that, this study determined if a solar-powered institutional cook stove with thermal energy storage that uses commercial SHELL THERMIA OIL B as the heat transfer medium as well as 40% KNO_3+60% $NaNO_3$ potassium nitrate salt (Solar Salt) as PCM for institutional food preparing was feasible. A mixture of 41L HTF (bulk temperatures up to 320*°C*, and film temperature up to 340*°C*) and 42 sealed copper tubes (Internal diameter 62.611 mm, 2 mm thickness 300 mm height) carrying a total of 60 kg of PCM (melting point range of 210-220°C and the Latent heat fusion 108.67 KJ/Kg)is used to store heat. The HTF was filled in the storage compartment to cover the copper tubes and is assumed to fit within cylinder jackets that wrap around the tubes and also operate as a heat transfer medium. A heater having 4500 W and 220 V input power from photovoltaic system with temperature control device is immersed inside storage during the charging phase. The ANSYS software is used to simulate the proposed model's thermal storage unit's transient behavior. ANSYS Workbench was utilized in a step-by-step fashion to model the process. A pressure-based solver was employed for melting/solidification processes, and for pressure-velocity coupling, the Semi-implicit pressure-linked equation technique was used. Grid independence assessment is also performed in order to choose the ideal grid size with the best solution and the lowest computing cost. The thermal storage's performance was assessed utilizing constant heat flux. The developed model's numerical study was solved numerically using an enthalpy-porosity approach and validated against experimental data. The results demonstrated that the CFD simulation using ANSYS Fluent for the stove was appropriately validated. Based on the simulation results, a performance investigation was carried out. The thermal storage was able to store 53.5MJ of energy in 3.8889 hours of charging time. The overall cooking, charging, and discharging efficiencies were 61.46%, 71.52%, and 85.62%, respectively. In the case of a convective heat transfer coefficient of 244 W/m^2 K, the phase change material and heat transfer fluid demonstrated good heat retention of 5 h. Finally, the results indicate expanding the application of solar cooking at the institutional level is visible.

TABLE OF CONTENTS

LIST OF FIGURES

LIST OF TABLES

NOMENCLATURE AND ABBREVIATIONS

Nomenclature

m	Mass
m_i	Initial mass
m_f	Final mass
hc	Convective heat transfer coefficient
Pr	Prandtl number
v	Kinematic viscosity
K	Thermal conductivity
A	Area
T	Temperature
V	Volume
η	Efficiency
ρ	Density
g	Gravitational acceleration
Ra	Rayleigh number
Nu	Nusselt number
h	Enthalpy
a_m	Melted fraction
Q_{Total}	Total energy stored
Q_{PCM}	Energy stored in PCM
Q_{HTF}	Energy stored in HTF

Abbreviations

SHS	Sensible Heat Storage
LHS	Latent Heat Storage
WHO	World Health Organization
CO_2	Carbon di oxide
CO	Carbon monoxide

PCM	Phase Change Material
LPG	Liquefied Petroleum Gas
PNG	Petroleum and natural gas
GHG	Greenhouse Gas
PV	Photovoltaic
CFD	Computational Fluid Dynamics
HTF	Heat Transfer Fluid
ETSC	Evacuated Tube Solar Collector
ETC	Evacuated Tube Collector
TES	Thermal Energy Storage
SC	Solar Cooker
FPCU	Flat Plate Collector Unit
SBC	Solar Box Cooker
WBT	Water Boiling Test
EPCMs	Encapsulated Phase Change Materials
PR	Performance Ratio
PSI	Peak Solar Insolation
DC	Direct Current
AC	Alternating Current
RMSE	Root Mean Square Error
MNRE	The Ministry of New and Renewable Energy
LHTES	Latent Heat Thermal Energy Storage
MOWIE	Ministry of Water Irrigation and Energy,Ethiopia
CDM	Clean Development Mechanism
REDD+	Reduced Emissions from Deforestation and Forest Degradation
WB-FCPF	World Bank Forest Carbon Partnership Facility

CHAPTER 1: INTRODUCTION

1.1 Background

Humankind completely relies based on carbon based fuels, accounting for more than 80% of world energy use. Its volatile cost, as well as its future inadequacies, necessitate a global shift. Cooking accounts for a substantial portion of family and institutional energy use, relying mostly on other polluting sources include coal, wood, and kerosene due to their minimum cost and ease of availability. The extensive usage of these resources produces major health and environmental issues. This is a more typical issue in isolated rural locations when Non-commercial fuels such as agricultural waste, firewood, and cow dung supply the energy needed for cooking. (Lizaso, 2020).

In rich nations which includes the USA, cooking contributes to around 37%-53% of the entire energy use (Aramesh et al., 2019). Cooking consumes a large portion of domestic energy usage in developing nations like South America, Africa, and Asia (Narayan & Doytch, 2017). Furthermore, according to research (SNV, 2018), biomass is still the major energy source, and cooking remains Ethiopia's greatest energy user. According to the most current MOWIE national balance of energy, Biomass provided 89% of the total energy supply. Resulting in massive volumes of GHG emission and deforestation. This demonstrates the necessity for ecologically friendly cooking methods that utilize clean energy resources. (Lentswe et al., 2021).

Energy availability benefits the quality of life, people's and society's, long-term survival, as well as well-being (Lambert et al., 2014). Two critical aspects of energy management that should be explored together for long-term development and ecological benefit are energy conservation and the consumption of renewable energy sources (Indora & Kandpal, 2019a). Renewable energy technologies provide usable energy by transforming natural events into usable forms of energy.

Solar energy is quickly becoming among the greatest environmentally friendly energy sources available. The average energy from the sun towards the earth is 1367 W/m^2, ranging from 1412

W/m^2 at the end of December to 1322 W/m^2 at the beginning of July. It has several applications, which may be split into two categories: electricity generation and heat production. Cooking with solar energy is one of the most basic, inexpensive, and appealing thermal uses.

Aside from the fact that solar energy is a fluctuating source, solar-powered stoves with storage have the advantage of allowing cooking to take place even when there is little or no sunshine. As a result, several studies have established that using thermal energy storage devices in solar cookers is preferable (Karthick & Sivalakshmi, 2019).

LHS, SHS, thermochemical energy storage, or a combination of these can all be utilized to store thermal energy. In the case of SHS, thermal energy is stored by increasing the temperature of a storage medium. In contrast, LHS requires a phase transition to store or release energy at certain temperatures. Thermochemical storage functions by transferring energy from an exothermic process and recovering heat from an endothermic reaction (Kajumba et al., 2020).

Preparation of food is done both at the institutional and family levels and it requires a large quantity of energy daily (Indora & Kandpal, 2019b). Institutional cooking is cooking done for a group of people who get their meals from the same kitchen. In the instance of institutional cooking, the number of meals might range from as few as 20-25 to thousands at a time. These kitchens frequently use commercial fuels (mainly fossil fuels) to fulfill cooking energy needs (Indora & Kandpal, 2018c). According to the World Health Organization (WHO), hazardous gas emissions (such as CO2, CO) during burning of commercial and non-commercial cooking fuels cause 3.8 million deaths (WHO, 2018). It is more severe in institutional kitchens than in domestic kitchens because a greater volume of fuel is burned with greater intensity for cooking in bulk. Clean cooking solutions are thus essential to decrease indoor air pollution while simultaneously protecting the ecosystem. Clean cooking technologies may involve both the effective usage of traditional fuels in improved cook stoves and cooking using clean energy sources (Craig & Dobson, 2015).

The theoretical, technological, and economic potential of solar cooking may be measured at different levels at an institutional level (Sharma et al., 2016). The theoretical capacity of solar energy systems fundamentally determines their highest utilization capacity for a given end application. Technical capacity, on the contrary, considers elements including solar abundance, any temporal imbalance in energy consumption, and the ability of the solar energy system to satisfy future demands. Economic potential considers affordability and financial sustainability into account. Therefore, the theoretical and technological potentials of solar energy consumption for institutional cooking will be explored in this study.

1.2 Problem statement

Institutional cooking is cooking done for beneficiaries in a centralized kitchen, and this kitchen requires a large volume of fuel to be combusted at a high intensity for mass cooking (Indora & Kandpal, 2018b). According WHO, 3.8 million fatalities occur as a result of dangerous gas emissions (including CO, CO_2) during the burning of commercial and non-commercial fuels for cooking (WHO, 2018). However every day, a large quantity of energy is required for institutional cooking which is one of the key elements influencing the amount of global energy expenditure and GHG emission. Because the energy used for cooking is so important, Solar cooking is regarded as one of the most simple, practical, and popular choices for utilizing solar energy (Indora & Kandpal, 2019a). Solar cookers can give a clean, alternative cooking option. However, institutional level use of solar cooking takes considerations such as any time difference between energy demand and solar resource availability, as well as any time imbalance between energy demand and energy supply, and the capabilities of the solar energy system to satisfy perceived demands. Solar cookers must be combined along thermal energy storage technologies to overcome this issue. This function will help to reduce the imbalance with in the supply of solar energy and consumption of cooking energy. Furthermore, storage aids the storage of extra solar energy throughout the daytime to be utilized later in the night or early in the next morning (Tesfay et al., 2019). The suggested design and simulation of an institutional clean cook stove would optimize and Look into the potential for employing solar energy for institutional cooking in terms of performance, theoretical potential, and technical feasibility.

1.3 Research objectives

1.3.1 General objective

The overall goal of the research is to design, and simulate an institutional cook stove with TES system. The performance of the developed institutional cook will be validated using existing institutional cook stove and national standard. The pot to be used has a diameter of around 580 mm for the preparation of sauce – 'wot'.

1.3.2 Specific objectives:

- Calculate the amount of energy needed for cooking;
- Design an institutional thermal storage cook stove with standard solar cooker;
- Model validation
- Simulation of the institutional thermal storage system coupled with standard solar cooker;
- Validate the test results with institutional cook stove results tested with the international standard test protocol ISO 19867-1: Laboratory Test Standard.

1.4 Research questions

- ✓ How long can the energy that is stored in thermal storage be used?
- ✓ What is the type of specific thermal storage and PCM used for efficient storage for this specific application?
- ✓ How much is the overall cooking, charging, and discharging efficiencies of the designed institutional cook stove?

1.5 Significance of the study

Cooking is Ethiopia's most energy-intensive end-use. Wood (biomass) is used to cook in almost all Ethiopian houses, and commercial and social establishments like bakeries, restaurants, schools, detention facilities, colleges, and hospitals. As a result, Ethiopia is one of four nations with the greatest biomass utilization, indoor air pollution illness burden, and use of non-renewable fuels from biomass (Negash et al., 2021). As a result, the adoption of clean energy sources like solar energy for preparing food at the institutional level may considerably reduce reliance on conventional fuels while also reducing human challenges, environmental damage, and global warming. Ethiopia might have benefited from carbon funding offered by the CDM, REDD+, and the WB-FCPF through GHG reductions associated with increased biomass fuel use efficiency due to the implementation of clean cookstoves. Apart from being a clean resource, several developing nations have enough solar radiation to explore using solar power for cooking to replace traditional fuels. As the economy grows rapidly and energy consumption rises, all civilizations require energy services to provide basic human needs such as lighting, cooking, space comfort, transportation, communication, and the operation of productive processes. As a result, it is highly desired to promote solar cooking at educational institutions, community groups, and businesses that serve a large number of people. This opens up prospects for economies of scale, which might lead to solar cooking being an ecologically and economically advantageous sector.

1.6 Scope and Limitations

1.6.1 Scope of the Study

The research aims to design and simulate institutional solar (PV) powered cook stoves with thermal energy storage devices for water-boiling applications. This work includes the sizing of PV systems, specifically for Addis Ababa weather conditions, the investigation of energy demand for the specified amount of water, the selection of appropriate materials for thermal storage, CFD (computational fluid dynamics) simulation of thermal storage with ANSYS fluent 19.2 that satisfies the heat demand of boiling the specified amount of water, and finally the validation of the model with experimental work from (Bhave & Thakare, 2018) is performed.

1.6.2 Limitation of the Study

The major focus of this study is a numerical simulation analysis that was restricted to a charging and discharging behavior of a thermal energy storage (Combination of PCM and HTF). However, the simulation of the entire system (consisting of PV, charge controller, inverter, heater and thermal storage coupled with the cooking pot having water to boil), the simulation of boiling water, simulation of PV output depending up on the solar radiation fluctuation and the experimental study were not included.

1.7 Organization of the thesis

This thesis is organized into six chapters, the first of which is an introduction. The introduction provides some background for the issue of institutional solar-powered cook stoves. Chapter 2 examines some of the literature on solar cookers with thermal storage systems, both at the household and institutional levels, and related thermal storage technologies, to identify appropriate material candidates for TES, an efficient configuration of LHS, and various LHS performance enhancement techniques.

The method used to complete the study and the design of the institutional solar-powered cook stoves with thermal storage system, are discussed in Chapter 3. The suggested model is described in depth: energy demand determination, PV sizing, thermal storage sizing, and storage material selection.

The numerical approach, encompassing the physical model, computational domain, grid generation, mathematical modeling, grid independence test, and model validation, is covered in Chapter 4.

The results and discussion are provided in Chapter 5, including the efficiency attained and a comparison of the simulation result with previous studies. Chapter Six concludes the thesis in terms of the objective and makes recommendations for further work.

CHAPTER 2: LITERATURE REVIEW

2.1 History of Solar Cooking

Cooking is an essential way for humans to prepare food for survival. A solar cooker, on the other hand, is a gadget that prepares food by utilizing energy from sun as its primary heat source and allowing the food to be prepared. Food was consumed in its natural state before the era of civilization because heating food was an unknown activity (Panwar et al., 2012). Because of the beginning of civilization, humankind began to cook food, and cooking has persisted due to the benefits and enjoyment it provides humans.

Tschirnhausen, was the 1st to call for solar cooking, experimenting with boiling water in clay pots by concentrating the sun's energy rays with huge lenses. Following the initial solar cooker experiment in 1767, Horace de Saussure, a Franco-Swiss scientist, was the first to construct a tiny greenhouse (box-type solar cooker) out of five glass cans putting one in the other on a black plateau used to cook fruits (Panwar et al., 2012). Later, De Saussure continued his research, experimenting with different materials, adding insulation, and cooking at various altitudes. He began investigating solar energy about 250 years ago, during the Pre-Era of the solar cooking movement.

Sir John Herschel traveled to South Africa in 1830 with an insulated book solar cooker (Sawarn et al., 2021). Mouchot created the first parabolic solar cooker in the same period in history 1869. In 1876, a British soldier named Adams built a panel solar cooker for seven troops in India that could cook vegetables and meat in two hours (Singh et al., 2021). In 1894, China created a restaurant where ducks were grilled and served using a solar cooker. Later in the 1940s, in the United States, Telkes researched a variety of sun cookers, including the heat storage kind. Sri M.K. Ghosh invented the first profit-oriented solar box cooker in India in 1945. In 1973, Kerr in the United States constructed many solar cookers utilizing basic, low-cost materials with great thermal inertia, concentrating and non-focusing or box-type solar cookers were included. 1979 Dr. Metcalf and Marshall Longuin used a solar box cooker to pasteurize water. However, because of its high cost and inefficiency, it was not socially acceptable.

In the 1980s, the rising expense of nonrenewable fuels regard to their financial value as well as wellness and ecological costs prompted governments in both developing and industrialized nations to encourage solar cooking. Following the promotion, the governments of India and China were the first to broaden the national promotion of solar box cookers, and extensive research was conducted at the time (Singh et al., 2021). Mullick introduced the two performance assessment measures known as figures of merit (F1 and F2) as a testing technique for solar cookers (box type) in 1987 India. Following this, other researchers conducted a variety of investigations on solar cooking technologies. Lately, intensive efforts have been undertaken, to increase the cooking power capacity of solar based cookers. Several researchers have carried out several analytical, computational, as well as experimental investigations on innovative solar cookers designs.

Domanski et al. (1995) Used PCM as medium for storage to investigate the possibility of cooking during evening hours. They attempted to analyze the cooker ability to perform with respect to PCM melting and solidification times throughout various scenarios. The sun's intensity, cooking medium mass, and the thermos-physical parameters of the PCM were discovered to have a considerable influence on cooker capability. Finally, upon discharge, the total efficiency of the cooker was determined to be 3-4 times larger compared to that of heat-pipe and steam solar cookers, that may be used for at home cooking.

A natural convection solar cooker with a FPC and short-term coconut oil TES was built. Flat-plate collector was solar cooker's power source having a double-glazed selective surface. At the very top point of the thermo-syphon cycle, there was a tank of oil in which two culinary vessels were submerged to allow for excellent heat transmission between fluid used for operation and the cooking vessels Readings of about 150°C were possible between 10:00 and 14:00 hrs due to high solar exposure. (Hararsingh et al., 1996).

Sahoo and Buddhi (1997) Created and evaluated a solar cooker using materials that store latent heat. Stearic acid was utilized to store latent heat, and an absorber plate was employed to speed up the cooking process.

A cylindrical PCM storage device was designed and constructed for solar cooking as well as late-night storing. They conducted many trials in which the amount of PCM within the storage container was varied. The study's purpose was to enhance the length of late-night cooking and the thermal efficiency of the device, and they discovered excellent results (Sharma et al. (2000).

Kumar Rakesh et al. (2001) Created an ETSC-based community-type solar pressure cooker. It was made up of an ETSC and a pressure cooker that served as both a cooking and TES device. A heat exchanger linked the two units together. The collector absorbed the incident solar irradiance and increased the working fluid temperature inside the tubes. The evaporated fluid climbed into heat exchange system and, through condensation, transferred energy to water circulating in the heat exchanger's secondary cycle. The heat transfer process was then restarted once the condensed fluid was returned to the collecting tubes.

A hot BSC with engine oil as a storage medium was conceived, built, and tested to prepare food in the evening hours (N.M. Nahar, 2003). Double-walled devise with the area between it containing 5.0 kg of old engine oil and glass wool protection was used. During the day, the greatest stagnation temperature attained within the cooking compartments of the hot BSC with store material was identical to that of the SC without storage, but from 17:00 to 24:00 hours, the value was 23° C higher for the storage SC. Finally, the storage solar cooker's efficiency was determined to be 27.5%.

Buddhi et al. (2003) Created a LHS unit by three-reflector for a SBC. They employed acetanilide as a PCM for evening cooking. The authors concluded from the testing findings that cooking tests were carried out effectively for evening cooking until 20:00 hours using 4.0 kg PCM utilized in the storage.

(S.D. Sharma et al., 2005) Built an indirect solar stove based on an ETSC coupled to a PCM. Figure 2.1 depicts a diagram of the indirect solar stove. During the day, warm water transported its energy to the PCM. The results of the experiments revealed that cooking might be done in the evening.

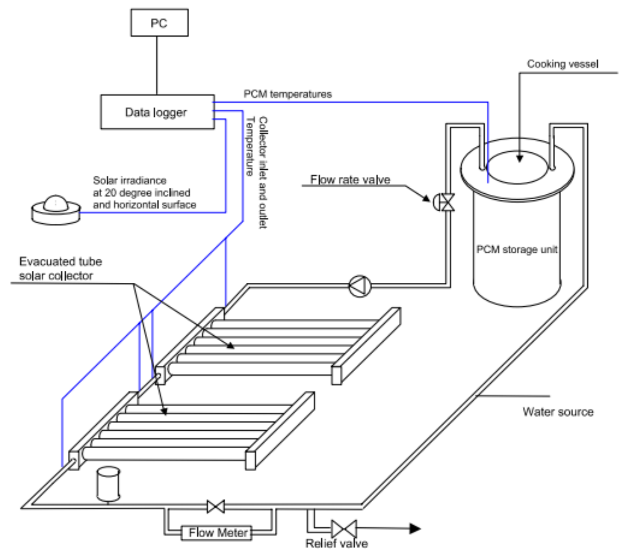

Figure 2.1: Solar cooker based on ETSC with PCM storage unit

(Shrestha & Byanjankar, 2007) examined the experimental thermal capability of a BSC utilizing stone pebbles as TES material in Nepal. To compare to a SC with stone pebbles, a cooker without pebbles was evaluated. The experimental findings of the empty load and loaded testing demonstrated that by inserting stone pebbles within the cooker, the cooking time could be extended by roughly two hours after midday, making the cooker suitable for evening meals due to the stored heat.

Hussein et al. (2008) Investigated a unique indirect solar cooker with an outside elliptical cross section, wickless heat pipes, a flat-plate solar collector, and integrated interior PCM thermal storage and cooking. They employed two plane reflectors to increase the amount of sunlight hitting on the cooker's collector, and magnesium nitrate hexahydrate is used as the PCM within the cooker's interior cooking unit. Following that, (Badran et al., 2010) constructed a movable solar stove and water warmer utilizing a parabolic concentrator.

2.2 Classification of solar cookers

Several solar cooker configurations are available across the world. Beginning with the launch of the pioneering solar cooker in 1767. Scientists and manufacturers have consistently improved. As a result, identifying solar cookers based on their configuration is difficult (Cuce

& Cuce, 2013). However, solar cookers are categorized according to how thermal energy is delivered to the cooking vessel as direct or indirect solar cookers, as illustrated in Figure 2.2. Furthermore, because solar energy is unpredictable, solar cookers are divided into solar cookers with thermal storage and without thermal storage.

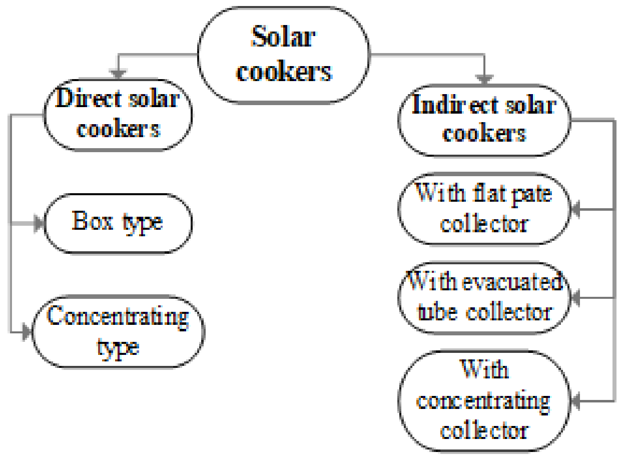

Figure 2.2: Solar cooker classification

2.2.1 Direct solar cooker

Solar radiation is actively engaged in the culinary process in direct solar cooking systems, and by far the most widespread kinds of direct sun cookers are concentrated and box types.

Box-type SC features an isolated box with a clear glass lid. Reflectors are generally placed within the box to guide the sun's rays toward the box (Saxena et al., 2011). Figure 2.3 shows an illustrative drawing of a box-type SC. The interior tray within the body of the cooker has been darkened since black absorbs the most heat. One face of the box is constructed of glass, enabling solar energy to pass through. Solar energy with shorter wavelengths can penetrate through the glass coating. There are two glass coating to limit heat loss, and a rubber strip keeps a box sealed. To retain heat and combat heat loss, insulation layers are utilized around the box's body and the black plate within the box (Sawarn et al., 2021).

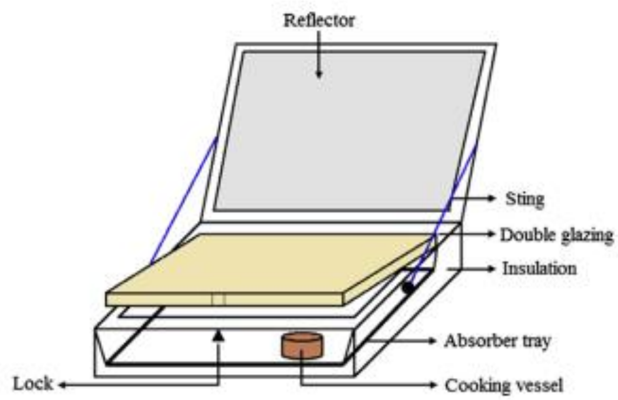

Figure 2.3: Solar box cooker Components

Concentrator SC, also known as parabolic reflector direct SCs, focus the reflecting solar energy in a point, where it may be used for cooking. The body of the SC is made up of multiple reflective surfaces set up in a parabolic shape. This entire system is held together by metal structure having castor wheels, allowing it to move around during the day to change the reflective body to concentrate on the cooking vessel. The cooking pan is placed on a structure elevated above the reflecting body in the middle (a focal point of the reflector). The reflective component collects solar energy and then projects it to the bottom of the vessel used for cooking, causing it to heat up and transfer it to the food within. Figure 2.4 depicts the ideal layout of a parabolic dish-type SC.

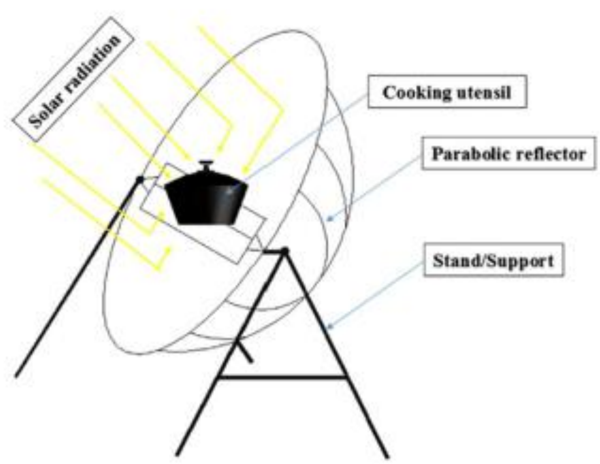

Figure 2.4: Concentrating solar oven with parabolic reflector

Mekonnen et al. (2020) Performed experimental testing and capability evaluation for the SK14 solar cooker in Ethiopia. The flat iron and reflecting aluminum plates with a reflecting value of 0.9 was used to build the cooker. In the no-load test, the stagnation temperature, the highest temperature within the cooker, as well as the first figure of merit seemed 188 °C,212 °C, and 0.22 °C/W/m2, respectively, whereas the standard cooking power, thermal efficiency, cooking power, and second figure of merit became 375.8 W, 46.4%, 635 W, and 0.625, respectively.

(Senthil, 2021) investigates the use of PCM to increase the productivity of a parabolic dish SC. A cooker is constructed with two concentrating cylinders filled with fines and paraffin wax to increase output during limited daylight hours.

2.2.2 Indirect solar cooker

In an indirect system SC, the radiation from the sun warms a specific fluid, called HTF that distributes heat to the cooking vessel. Indirect solar cookers are classified based on the kind of collector used, which might be a FPC, evacuated tube collector, or parabolic concentrator. Several sorts of research have been reported along these lines. In one of such study, (Kumaresan et al., 2018) investigates the experimental capability of the FPCU combined with the LHTES system to change the traditional way of LPG-based or biomass cooking. The HTF and PCM are Therminol 55 and D Mannitol in the experimental setup. Furthermore, they used ANSYS Fluent software to perform CFD analysis to investigate the heat transfer behavior throughout the cooking time. The CFD analysis findings are confirmed with experimental data, and the heat transfer coefficient (average) throughout the food preparation process is determined to be around 100 W/m^2 K.

A SC based on an ETC with a PCM was designed (Kumar et al., 2018). Water is employed as the fluid that operates in the evacuated tubes, and acetanilide (PCM) is used to transmit the stored energy to the cooking container during the day until late at night. In addition, the use of a reflector improves the capability of the SC. As a consequence, in the case of a large load, the SC with a reflector performs better than the SC missing a reflector. Figure 2.5 depicts a schematic of a SC with an ETC and PCM storage.

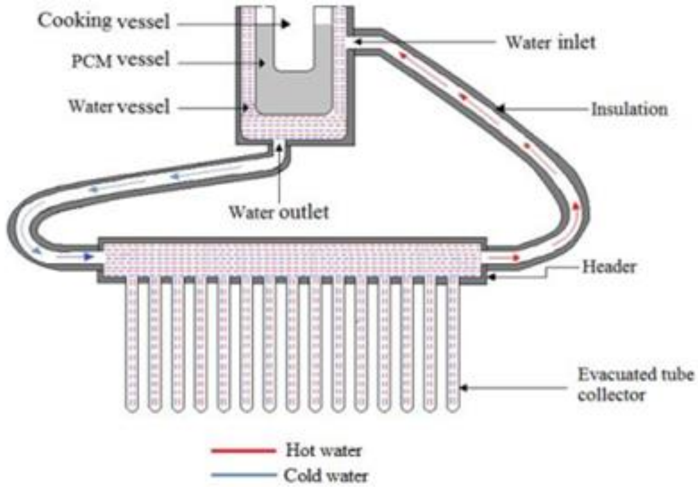

Figure 2.5: Solar stove with ETC and PCM storage unit.

(Tesfay et al., 2016) Studied a concentrator-type SC having PCM as thermal storage and heat transfer cycle appropriate for bulk-temperature usage. The technology is specifically intended for Injera baking applications. The store is coupled to a polar-mounted concentrator with a non-movable receiver and steam HTF. In a closed thermosiphon loop, steam flows naturally between the evaporator and condenser. The thermosiphon loop is intended to simplify heat transmission methods across long distances, and Figure 2.6 depicts the whole system schematic.

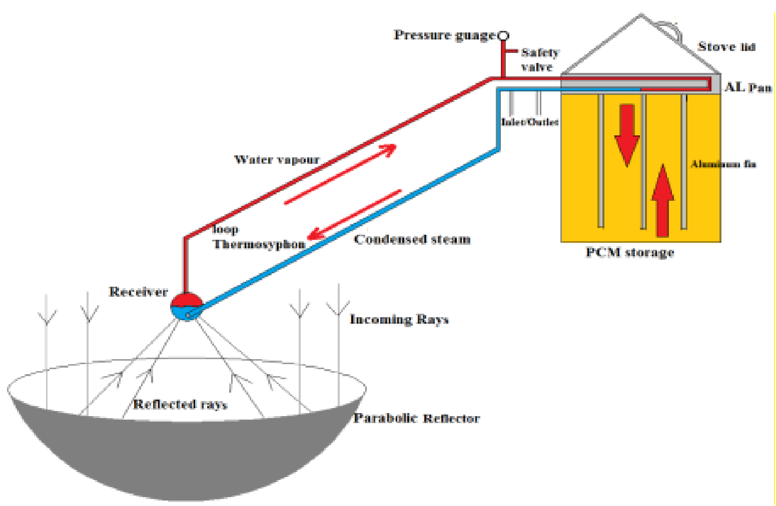

Figure 2.6: Concentrator type SC with PCM thermal storage

2.3 Thermal storage

TES is a device which stores thermal energy by raising or lowering the temperature of a medium that stores the thermal energy later for the purpose of cooling, heating, and power production. Because of the erratic nature (intermittent) of solar radiation, TES has received a lot of interest in thermodynamic systems. By saving energy, TES not only minimizes the connection between solar radiation supply mismatch with demand but also increases system performance and thermal dependability (Sarbu & Sebarchievici, 2018).

To satisfy the requirements of TES, thermal energy storage materials must have particular physical, chemical, and economic qualities (Zheng, 2015), (Sharma et al., 2009). Furthermore, thermal energy storage system features are stated in accordance of capacity, power, efficiency, storage period, charging-discharging interval, and cost. The needed parameters of solar thermal energy storage materials are given in Table 2.1.

Table 2.1: Required properties of solar TES materials (Sharma et al., 2009).

NO	Property	Requirement
1	Density	High
2	Latent heat of fusion	High
3	Specific heat	High
4	Melting point	Relative
5	Thermal conductivity	High
6	Vapor pressure	Low
7	Thermal stability	High
8	Chemical stability	High
9	Volume change	Minimal
10	Availability	Abundant and available
11	Toxicity	Non toxic
12	Corrosiveness	Non corrosive
13	Non flammability	Non flammable
14	Cost	Cheap

2.3.1 Classification and characteristics of heat storage materials

As seen in Figure 2.7, the two significant kinds of thermal energy-storing materials for solar cooking applications SHTES and LHTES. SHTES material holds Sensible heat generated by either raising or reducing the temperature of the medium of storage, which is the most basic way of storing thermal energy (Karthick & Sivalakshmi, 2019). LHTES materials, on the other hand, or phase-changing materials (PCM), keep thermal energy by absorbing the latent heat necessary to change the phase of the storage medium from the thermal energy source. As the medium converts phase from solid to liquid or liquid to gas while storing energy, the chemical linkages within the storage medium break down. Phase changing is heat-absorbing, endothermic way, and the temperature remains constant upon the phase change process; the heat stored while the phase transition process occurred is referred to as latent heat (Republic, 2010).

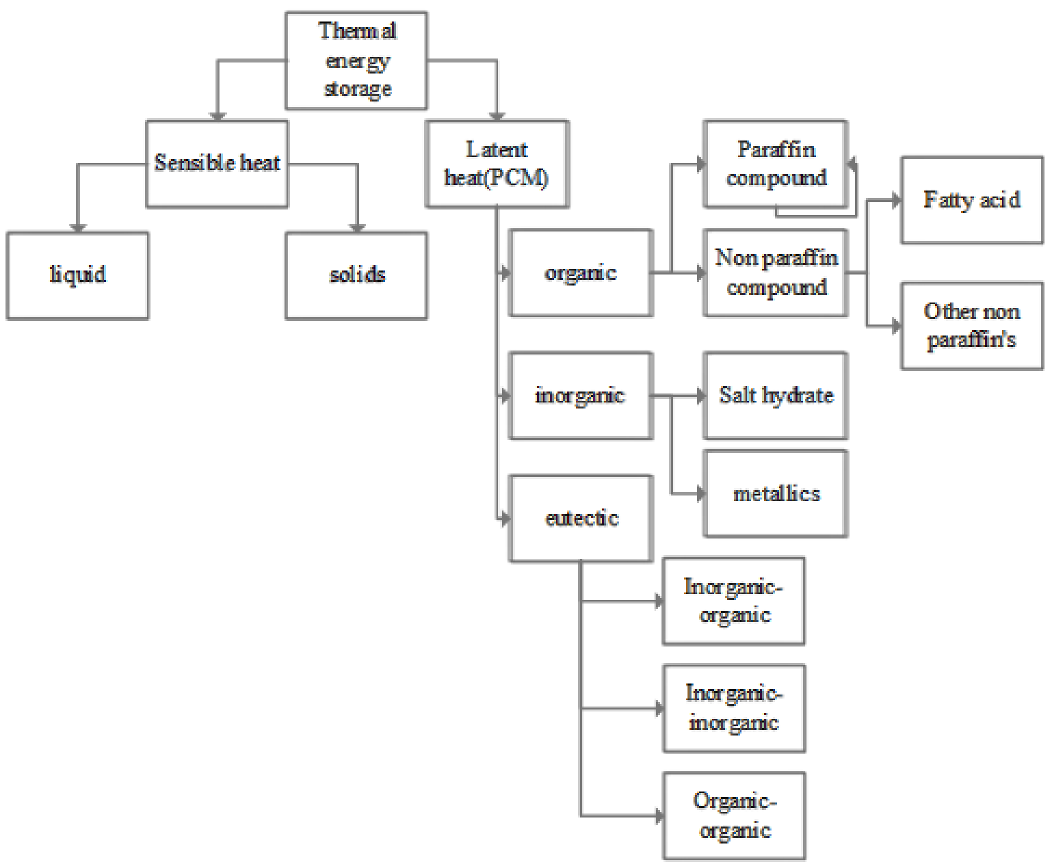

Figure 2.7: Categories of thermal storage material

2.3.2 Latent heat thermal energy storage (LHTES)

PCMs are mediums that store latent heat. LHS may be employed at a wide variety of temperatures. Unlike SHTES material, LHTES based on PCM offers a higher energy storage capacity and behaves isothermally throughout phase transition. (Mawire, 2019). Several research studies on this topic have recently been conducted.

A solar concentric parabolic cooker with the genuine layout of a PCM storage is used. Heat transmission oil fills the space between the receiver's two layers. The receiver's exterior-outermost surface is made up of upright cylindrical PCM pipes with a diameter of 0.025 m. The performance metrics of the solar cooker, including cooking power, optical efficiency factor, and, heat loss factor were determined with and without PCM. The heat loss values are 7.74 W m^2 and 2.46 W m^2, respectively, and the optical efficiency factors are 0.098 and 0.22 for the SC without and having PCM in the receiver. The SC with a PCM receiver has a cooking power of 125.3 W, which is 65.6 W greater than the cooking power without the PCM (Santhi Rekha & Sukchai, 2018).

Kajumba et al. (2020) Examined and studied the thermal capability of a cooking device integrated with TES system appropriate for solar thermal usage. Sunflower oil was employed for heat storage and heat transmission fluid. A hand-operated valve mounted on the line that connected to the cooking appliance was used to control the flow of oil. Boiling fixed amount of water and food items at varied flow rate were used to conduct cooking experiments. The results determined that as the flow rate rises, so did the heating rate, and the cooking unit's efficiencies were 40%, 43%, and 52% for flow rate settings of 4 ml/s, 6 ml/s, and 12 ml/s, respectively, and at the maximum possible flow rate value of 12 ml/s, the system could boil 2 liters of water in around 19 minutes.

A solar cook stove that holds LH in solar salt (PCM) was invented and examined, allowing it to be stored in a container with insulation and utilized to cook in the shadow kitchens when necessary. Within 110 minutes of charging, it efficiently stored heat around the melting point of 220 °C (Bhave & Kale, 2020).

A numerical investigation of shell and tube-kind TES device for solar food preparation using KNO_3-$NaNO_3$ was presented by Abreha et al. (2019). The optimization method is used to choose 19 HTF tubes. Every tube is equipped with four longitudinal fins that increase the heat transfer rate of the PCM. LHESS was simulated using COMSOL Multiphysics, which allowed for the testing of alternative configurations as well as the optimization of the geometry employed. The results show that the PCM is fully charged after 60 minutes; with 5.88 MJ, 4.29 MJ, and 10.17 MJ of stored latent, sensible, and total energy in the LHS system at that time.

The design and experimental examination of a compound parabolic solar collector for cooking with oil and rock as heat storage is given. An absorber with TES is put on the focal point of the two dishes until the absorber stores enough thermal energy for cooking. The system is sized to cook 1 kilogram of rice in 45 minutes using 421 W of stored solar energy. Finally, the authors discussed that the energy transfer to the water is lowered because of losses, and its temperature is 355k (Wollele & Hassen, 2019).

Bhave and Thakare (2018) A concentrating-type solar cooker for boiling cooking was developed, employing magnesium chloride hexahydrate serving as PCM. The authors proposed that the heat stored for boiling cooking be greater than 100 °C, Heat is stored in the lower part of the vessel using a HTF (thermic oil) and closed aluminum tubes holding a PCM. The planned storage could hold an amount of heat for roughly 50 minutes and cook 140 grams of rice in 30 minutes.

Kumaresan et al. (2016) Experimentally investigated the capability of an indirect SC coupled with PCM. Therminol 55 was used as HTF, whereas D-Mannitol was utilized as the PCM. The highest temperature reached 152 °C in 15 minutes during testing, which is roughly half the period required by a standard LPG stove in cooking mode. A thermal balance for the intended cooking system was created to record the heat intake and distribution design. They discovered that the storage mechanism could continuously deliver thermal energy to the pan for cooking for an extended period of time.

2.3.3 Sensible Heat Thermal energy Storage (SHTES)

SHTES materials such as liquids, solids, and solid-liquid mixes were employed in the TES unit of solar cookers. The liquid state SHM utilized included coconut oil (Hararsingh et al., 1996), Mobiltherm 605 (Esen, 2004), cast iron, granite (rock) (Nyahoro et al., 1997), and used motor oil (N M Nahar, 2003). Furthermore, sunflower oil, Shell Thermia C, and Shell Thermia B were evaluated as SHM oils for solar cookers. Sunflower oil, on the other hand, performed better (Mawire et al., 2014).

2.4 LHS system performance enhancement

With its enormous thermal storage intensity and virtually isothermal process, the LHS system is a preferable alternative for heat storage. However, the limited heat transmission and low thermo-physical stable state of PCMs significantly impact LHS system effectiveness during melting and solidification cycles. As a consequence, the widespread practical application of the LHS system needs to be more efficient. Thus, several performance enhancement strategies must be used to address the inadequacies of the LHS system (Khan et al., 2016). Several publications on thermal performance enhancement of LHS systems have been published in recent years (Huang et al., 2021), (Amagour et al., 2021).. According to one of these articles (Tao & He, 2018), performance enhancement strategies may be grouped into three categories: increasing the thermal conductivity PCM, expanding heat transfer surface, and enhancing heat transfer process uniformity, as illustrated in Fig. 2.8. However, this article suggests encapsulating PCMs enhance thermal conductivity and thermo-physical stability.

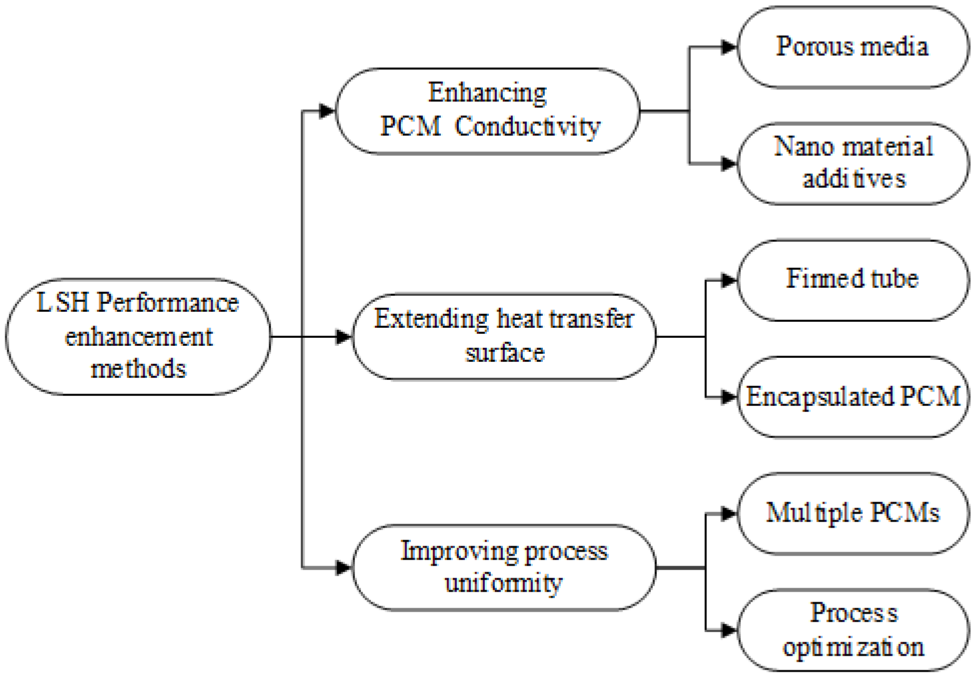

Figure 2.8: Classification of performance enhancement methods for LHS system

2.4.1 PCM encapsulation

Encapsulation of PCM is the way of encasing a PCM in a proper covering material to hold it separated with an environment. Encapsulation guarantees the long-term viability of the PCM's true formulation, which can be influenced by association with the outside environment, minimizes the potential of surrounding response with the PCM, enhances thermal and mechanical durability, increases rate of heat transfer, and integration with unsafe PCMs that are unsuitable for exposure to the surroundings (Khan et al., 2016). PCM encapsulation may be divided as nano (0-1000 nm), micro (0-1000 m), and a macro (above 1 mm), encapsulated PCM, as well as container geometries such as spherical, cylindrical, tubular, or rectangular (Salunkhe & Shembekar, 2012).

For thermal energy storage applications, macro encapsulation is a typical method of coating the PCM. The container might be rectangular, cylindrical, tubular, or spherical in form. High-temperature PCMs are often packaged in macro capsules using ceramic, metal, rocks, polymer, and polymer (Tao & He, 2018). Another study by Liu et al. (2016) showed that due to their greater heat transmission surface area than other forms, spherical and cylindrical capsules were shown to be the most advantageous for commercial uses. Again according to (Agyenim et al., 2010), the typical container forms for improved transmission of heat between the PCM and HTF are cylindrical and rectangular.

A LHS system's thermal performance is capable of being improved by shrinking the capsule's size. The dynamical nature of a packed bed TESS with encapsulated PCMs was examined by (Nithyanandam et al., 2013). It investigated how the design configuration and operational factors affected the system's dynamic storage and delivery performance. According to the data smaller radius capsules produce higher latent utilization, according to the data.

Chandrasekaran et al. (2015) Explored how the size of spherical capsules affected the PCM (water)'s ability to solidify. The capsule size was demonstrated to have an enormous effect on cooling down at lower working temperatures potential, whereas it was abolished greater operating temperatures. Furthermore, the covering materials characteristics have a direct impact on the thermal performance of encapsulated PCMs.

Bellan et al. (2014) and Bellan et al. (2015) examined the capability of the LHSS with an encased PCM numerically as well as experimentally. The findings indicate that a smaller capsule can greatly increase charging and discharging speeds. Additionally, the capsule's shell characteristics greatly impact how well the system conducts heat; this influence grows as the shell's thermal conductivity decreases.

Mol et al. (2020) Developed a computer model to investigate the phase shift in irregularly filled PCM for LHTES. The effect of bed structure employing a variety of sizes of particles and combining a wide range of particle configurations on the process of melt and solidifying of PCM bed was investigated in this work. The particles are all believed to be spherical, and made of paraffin wax. Water was employed as HTF having an input temperature of 343.15 K for charging and 293.15 K for discharging. In all circumstances, the flow rate at the entrance is always 2 L/m and moves from bottom to top. Finally, it was discovered that employing smaller particles causes the bed to charge and discharge more quickly.

Hawlader et al. (2002) The physical and chemical rigidity, as well as the thermal performance, of bigger capsules using paraffin as storage material was investigated. The enclosed paraffin demonstrated great thermal and structural rigidity, as well as a consistent thermal storage capacity, after 1000 heat cycles.

Analytical research was carried out to investigate the impact of size of encapsulation on the process of melt and solidifying rates. When capsule diameter grew out of 4 cm towards 12 cm, the time of melt of $CaCl_2.6H_2O$ inside the capsule went up from 26 minutes to 192 minutes. Similarly, enlarging the capsule diameter lowers the solidification rate, thus the enclosed PCM takes longer to solidify when compared with a small diameter (Veerappan et al., 2009).

Zhang et al. (2014) Conducted a computational and experimental investigation to estimate the rise in the rate of solidifying of a mixture of KNO3 (40 wt%) and NaNO3 (60 wt%) with in-cylindrical enclosure(encapsulation). AISI 321 was used to make a capsule. The height and outer diameter of the capsule were 77 mm and 75 mm, respectively. The metallic foam has been utilized to enhance heat transmission. To assess the duration of the solidification, the cylindrical shells were warmed in an electric furnace to melt the PCM before being exposed to water and air. When air conditioning was used, the period of solidification was lowered from about 60 min to 47 min for PCM without any enhancer to PCM with metallic foam. However, when the PCM composite with metallic foam was cooled with water, the solidification time was lowered to 700 s.

Wei et al. (2005) Investigated the influence of capsule coating thickness, diameter, and shape on the thermal capacity of enclosed PCM. In that sequence, thermal performance reduced from sphere to cylinder, plate, and tube. When the PCM diameter increased from 0.2 cm to 0.5 cm, the heat release rate reduced. However, when the thickness of the coating increased from 0.02 cm to 0.04 cm, the amount of PCM in the capsule decreased affecting the thermal storage capacity.

Numerical simulations were used to investigate stresses in cylindrical and spherical capsules, with the materials for the cylinder and the sphere considered to be stainless steel (316L) and nickel, respectively, and zinc as PCM. The cylinder has been identified as the best encapsulation shape (Blaney et al., 2013).

(Siva et al., 2010) investigated configurations containing the same amount of PCM and discovered that a cylinder gives a greater encapsulation than a spherical one. The cylinder has 38% greater area compared to the sphere, resulting in a 47% reduction in overall solidification time. The sizes of the chosen cylinder had been chosen so as to ensure the radius won't be too big since this would increase the time required for solidification. As a result, configuration selection is critical in TES systems.

2.5 Institutional cooking

2.5.1 Solar powered institution cooking

When looking at institutional preparation of foods, a bunch of individuals should eat in a shared kitchen. Refugee camps, religious institutions, canteens, Hostels, hotels, jails, orphanages, and educational institutions, are among other places that may employ community cookers. The population of a community is classified as minimal (all the way up to 50 individuals), moderate (50-100 people) or prominent (above 100 people) based on the number of individuals (Indora & Kandpal, 2018c). As a result, a significant quantity of energy is frequently required daily. People in many impoverished nations count on firewood as their major source of energy, which has serious wellness and ecological repercussions. Solar cooking provides a solution to these issues. As a result, it is particularly desired to encourage solar cooking at commercial entities, community groups, and institutions that serve a big number of people.

Solar cooker promotion has grown in popularity over the years, with a wide range of groups promoting numerous kinds of solar cookers across the globe. Despite the multiple benefits provided by solar cookers and substantial attempts undertaken by various groups and government agencies to encourage their usage, all of their potentials is still untapped.

The available research on institutional solar cookers is rare, with much of the work focusing on home solar cookers and ignoring solar cookers for institutional uses. (Piroschka, 2014) In his study of warming up to solar cooking, he mentioned that many motivating variables significantly influence adopting this type of solar cooker. According to the study, motivational variables were classified as economic, health, and environmental.

Despite several efforts made to implement larger box stoves in public kitchens, they are favored on a lesser scale (Lizaso, 2020). Over time, designs based on parabolic concentrators have shown to be more effective. Parabolic dishes and Scheffler dish cookers are two popular designs. The pot is situated at the reflector's focal point in the former example. Sun rays are still reflected onto a secondary reflector in the latter, and the pot is situated in its focal point, allowing for inside cooking.

In Indian universities, MNRE is now supporting three types of concentrator cookers: manually controlled parabolic dish stoves (SK, PRINCE), the fixed focal automatically monitored (East-West) Scheffler dishes, and completely monitored Fresnel dishes (Lizaso, 2020).

(Indora & Kandpal, 2018a) Investigated the economic acceptability of the Scheffler dish to solar steam cooking at the level of institutions. Small (200 people), medium (500 people), and giant (1000 people) are the three sizes of institutional kitchens. Scheffler dishes with 16 m^2 (a gross aperture area) were investigated for solar steam cooking (SSC) systems. According to the study, the projected discounted payback period for large-sized, medium, and small, institutional kitchens is 6, 7, and 9 years, respectively. This demonstrates that due to economies associated with scale in the system's investment cost, large-scale ones are economically appealing.

Nahar et al. (1993) Compared the performance and evaluation of a hotbox solar cooker having one reflector to that of an enhanced solar community-size cooker. Because the cooker can serve up to 80 people, they recommend it for hostels, temples, canteens, restaurants, and other similar establishments. Furthermore, an economic study of the cooker was performed, taking into account yearly interest, repair costs, fuel price and maintenance costs. Finally, depending on the fuel it replaces, the time frame for payback lasts around 1.16 and 3.85 years. Furthermore, the projected lifespan is 15 years. As a result, using a community-sized solar cooker is cost-effective.

Sekhon and Sethi (2019) Provide thermal modeling as well as an evaluation of a unique twin-chamber communal solar stove as an alternative for biomass-based food preparation. Overall, the results imply TCCS cooker is able to be modified for community-scale preparing dishes and has an immense capacity for substituting biomass-based preparation in numerous nations in the future. In India, Aggarwal (2020) investigated institutional solar steam culinary systems. A solar steam cooking system, according to the study, can prepare meals for 50 to 50,000 people while minimizing the need for traditional fuels. It is also capable of heating water.

2.5.2 Institutional cooking with other source of energy

Limited solar cooking devices for institutional cooking have been built in India, there still needs to be more certainty about their performance, operating aspects, and the number of advantages obtained. However, relevant works and commercially accessible institutional solar-powered cookstoves are described in section 2.5.1, and this section surveys available Institutional cooking using alternative energy sources.

As illustrated in Figure 2.9 biomass based corporate cook stove having a 200-liter capacity was developed using CFD simulation and experimental testing. The WBT was used for stove's performance test. In addition, the CFD model was verified by contrasting it with data from experiments. The stove requires 41.25 grams of SFC / liter and takes 129.5 minutes to cook 200 liters (Desisa et al., 2016).

Figure 2.9: Experiment setup (Desisa et al., 2016)

Commeh et al. (2017) Assessed the efficiency of improved institutional cookstoves in their use in Ghana's agro and food processing industries. The WBT was utilized to measure the efficiency and power of three institutional cook stoves, as illustrated in Figure 2.10. Round bottom pot cook stove had the greatest efficiency of 59.70% and the highest power of 8.8 kW, followed by the flat bottom pot cook stove at 47.40% and 11.5 kW, and finally the mobile cook stove at 33.40% and 11.3 kW.

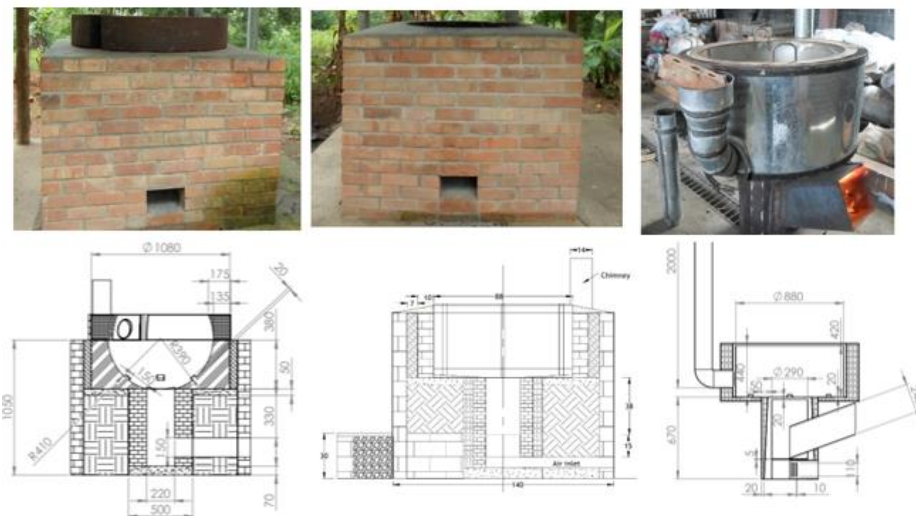

Figure 2.10: Round bottom pot, flat bottom pot and mobile cook stove

The design and performance study of an institutional cooking stove for a high-hill rural community in Nepal was explored by (Adhikaria et al., 2020). The research focuses on designing and constructing a long-lasting stove employing the optimal orientation of insulating bricks while considering technical, social, and economic factors. The stove was built with 12 bricks, a 3mm mild steel top plate, and a well-insulated chimney. WBT was carried out by the national stove testing procedure. The capability of the stove is determined by parameters including thermal efficiency, fuel consumption rate, burning rate, firepower, and turn-down ratio. Finally, the thermal efficiency of Alnus nepalensis, a fuel with an average moisture content of 13% on a wet basis, was 31%.

Research on enhanced institutional biomass stoves employing biomass briquettes as fuel and took three distinct designs of stoves as illustrated in figure 2.11 (i) a gasifier stove, ii) a charcoal-producing stove, and iii) a two-stage top burning stove) performed (Bhattacharya et al., 1998).

Figure 2.11: (i) gasifier stove, (ii) charcoal making stove, (iii) two-stage top burning

According to the results of the investigation, the Gasifier Stove combustion was practically smokeless under certain conditions, with the maximum efficiency seen being around 16% for sawdust briquettes. A two-stage top-down combustion burner with whole or tiny bits of briquettes and an efficiency of around 27% for rice husk was recommended for extended-term use. The Charcoal manufacturing stove was determined to be small, with intermittent smoke. The charcoal created in one process was sufficient to light the stove for the next operation. The highest efficiency was determined to be around 15% for both rice husk and sawdust.

To investigate both the power and efficiency of a “Flat bottom Institutional Cookstove”, a water boiling examination was carried out, followed by CFD using ANSYS Fluent simulations (Commeh et al., 2022). The findings of the practical and computational simulations on water temperature have been compared. The stove produced 11.5 kW and had a 47.4% efficiency.

According to a GIZ report, Ethiopia is a huge nation with abundant renewable energy resources. It is, nonetheless, one of the world's least energy-consuming countries. Only 14% of its 85 million people have access to energy. Because inexpensive electricity sources are few, particularly in rural regions, people continue to rely on traditional types of energy, such as firewood - they cook on three stone stoves and use kerosene lamps to light their homes. This leads to increasing deforestation, soil erosion, and health issues. Therefore, the growth and application of renewable and ecologically friendly sources of energy is unavoidable. As a result, GIZ/EPE and other energy development organizations are pushing ICS and clean cooking technology. Among those the institutional cook stoves promoted by GIZ is given in Table 2.2.

Table 2.2: Institutional biomass cook stove promoted by GIZ

Institutional biomass cook stoves promoted by GIZ			
Types	**Description**	**Schematic**	**Source**
Institutional Mirt stove (IMS) with chimney	• Made from sand and cement • 50% fuel saving • Applicable for baking for productive use, Universities, Prisons, Hotels, restaurants, Hospitals, Army camps, Schools • Produced by trained Mirt stove producers and local artisans		GIZ
Institutional Mirt stove (IMS) with chimney	• Made of clay, pumice,cement liners,shet metals.round bar ,square pipe • Emission reduction significantly reduce CO& PM • Fuell saving more than 50%	 	GIZ
Institutional rocket stove(IRS)	• Made entirely from clay liner, 53% fuel saving • Optimized for baking and cooking	 	GIZ

Table 2.3: Summary of literature review

						Main finding						
					Quantitative						Qualitative	Reference
No	Tittle	storage media	Cooking power	Storage temperature	Discharging time/efficiency	Efficiency of cooker	Charging time	Figure merit		Thermal efficiency		
								F1	F2			
1	Cooking during off-sunshine hours using PCM as storage media	stearic acid	-	78-84°C,	-	-	-	-	-	-	Cooker performance is heavily influenced by sun intensity, cooking medium mass, and the thermophysical parameters of the PCM.	(Domanski et al., 1995)
2	A natural convection flat-plate collector solar cooker with short term storage.	Coconut oil	-	150°C	2 & ½ hr.	-	-	-	-	-	An electric heating unit may be inserted into the chamber used for cooking to allow the stove to be utilized on days with poor insolation.	(Hararsingh et al., 1996)
3	Solar cooker with latent heat storage: design and experimental testing	stearic acid	-	-	-	-	-	-	-	-	Night cooking is feasible with a solar stove that stores latent heat. It also keeps the plate temperature roughly steady in the late evening.	(Sahoo & Buddhi, 1997)

												Main finding	
					Quantitative						Qualitative	Reference
No	Tittle	storage media	Cooking power	Storage temperature	Discharging time/efficiency	Efficiency of cooker	Charging time	Figure merit		Thermal efficiency		
								F1	F2			
4	Design, development and performance evaluation of a latent heat storage unit for evening cooking in a solar cooker	acetamide	-	-	-	-	-	0.14	0.34	-	It was discovered that night cooking was achievable provided excellent storage was utilized.	(Sharma et al., 2000)
5	Performance and testing of a hot box storage solar cooker	used engine oil	-	-	-	27.5%	-	-	-	-	A box cooker with heat storage performed better than an SBC without heat storage	(N.M. Nahar, 2003)
6	Thermal performance evaluation of a latent heat storage unit for late evening cooking in a solar cooker having three reflectors	Acetanilid e	-	-	-	-	-	-	-	-	late evening cooking is possible in a solar cooker having three reflectors to enhance the incident solar radiation with the PCM storage unit	(Buddhi et al., 2003)

Main finding												
Quantitative											Qualitative	Reference
No	Tittle	storage media	Cooking power	Storage temperature	Discharging time/efficiency	Efficiency of cooker	Charging time	Figure merit		Thermal efficiency		
								F1	F2			
7	Thermal performance of a solar cooker based on an evacuated tube solar collector with a PCM storage unit	erythritol	-	130°C	-	-	-	-	-	-	The PCM storage unit can store enough heat for lunch and evening meals and can also sustain the PCM temperature around (75°C) till the following morning.	(S.D. Sharma et al., 2005)
8	Thermal Performance Evaluation of Box Type Solar Cooker using Stone Pebbles for Thermal Energy Storage	Stone pebbles	-	65°C	-	-	-	not black coated 0.21 black coated 0.23	not black coated 0.23 black coated 0.27	-	The period for cooking meals can be postponed by roughly two hours after midday, ensuring the stove is acceptable for a nighttime meal.	(Shrestha & Byanjankar, 2007)
9	Experimental investigation of novel indirect solar cooker with indoor PCM thermal Storage and cooking unit.	magnesium nitrate hexahydrate	-	-	-	-	-	-	-	-	Solar cookers can successfully prepare many types of meals during lunchtime, afternoon, and late.	(Hussein et al., 2008)

		Main finding											
		Quantitative										Qualitative	Reference
No	Tittle	storage media	Cooking power	Storage temperature	Discharging time/efficiency	Efficiency of cooker	Charging time	Figure merit		Thermal efficiency			
								F1	F2				
10	Experimental testing and performance evaluation of SK14 solar cooker	-	375.8 W	-	-	-	-	0.22	0.625	46.4%		The cooker's cooking power and temperature may undoubtedly be modified for Ethiopian home meals.	(Mekonnen et al., 2020)
11	Enhancement of productivity of parabolic dish solar cooker using integrated phase change material	paraffin wax	-	90°C	-	-	120min	-	-	-		PCM increases the productivity of the cook throughout the off-season.	(Senthil, 2021)
12	Experimental and numerical investigation of solar flat plate cooking unit for domestic application	D Mannitol	-	-	-	41%	-	-	-	-		There is a lot of room for improvement by putting all parts near to the cooking device and also by properly insulating all components.	(Kumaresan et al., 2018)

											Main finding	
				Quantitative							Qualitative	Reference
No	Tittle	storage media	Cooking power	Storage/ cooking unit temperature	Discharging time/efficiency	Efficiency of cooker	Charging time	Figure merit		Thermal efficiency		
								F1	F2			
13	Experimental investigation of a solar cooker based on evacuated tube collector with phase change thermal storage unit in Indian climatic conditions	acetanilid e	-	99.3°C	-	-	-	-	-	-	Evening cooking with a PCM heat storge unit is found quicker than daytime cooking at low load, and the possibilty of solar cooker based on an evacuated collector with water as HTF and PCM as TES unit is investigated	(Kumar et al., 2018)
14	Solar cookers with latent heat storage for intensive cooking application	mixture of 40% KNO3 and 60% NaKO3	-	(110-150)°C	-	-	-	-	-	-	If the surface is sufficiently smooth, injera can be baked at a lower temperature on an aluminum surface.	(Tesfay et al., 2016)
15	Design of Phase Change Material Based Domestic Solar Cooking System for Both Indoor and Outdoor Cooking Applications	Not mentioned	125.3 W	-	-	-	-	-	-	-	Instead of employing fossil fuel-based cooking system, the PCM solar cooking system can broaden the usability of solar cookers as a suitable cooking option for cooking uses.	(Santhi Rekha & Sukchai, 2018)

						Main finding						
						Quantitative					Qualitative	Reference
No	Tittle	storage media	Cooking power	Storage/ cooking unit temperature	Discharging time/efficiency	Efficiency of cooker	Charging time	Figure merit		Thermal efficiency		
								F1	F2			
16	Experimental investigation of a cooking unit integrated with thermal energy storage system	Sun flower oil	-	-	-	40%, 43% and 52% for flow rates settings of 4 ml/s, 6 ml/s and 12 ml/s respectively	-	-	-	-	The heating rate rose as the flow rate increased.	(Kajumba et al., 2020)
17	Development of a thermal storage type solar cooker for high temperature cooking using solar salt	solar salt	-	170 – 180°C	-	-	110 min	-	-	-	-	(Bhave & Kale, 2020)
18	Numerical Modeling and Simulation of Thermal Energy Storage for Solar Cooking Using Comsol Multiphysics Software	potassium sodium nitrate salts	-	-	-	-	60 min	-	-	-	-	(Abreha et al., 2019)

					Main finding							
					Quantitative						Qualitative	Reference
No	Tittle	storage media	Cooking power	Storage/ cooking unit temperature	Discharging time/efficiency	Efficiency of cooker	Charging time	Figure merit		Thermal efficiency		
								F1	F2			
19	Design and experimental investigation of solar cooker with thermal energy storage	rock and used engine oil	-	82°C	-	-	-	-	-	-		(Wollele & Hassen, 2019)
20	Performance evaluation of solar box cooker assisted with latent heat energy storage system for cooking application	Oxalic acid dihydrate	-	121°C	57%	-	-	-	-	-	Asolar box cooker built with phase change material might be used to prepare meals during off-peak hours of solar radiation.	(Vigneswaran et al., 2017)
21	Performance Evaluation of a Solar Cooker with Low Cost Heat Storage Material	mixture of sand and granular carbon	44.81 W					0.13 $m^2{}^\circ C/W$	0.44 $m^2{}^\circ C/W$	37.1%		(Saxena, 2017)

						Main finding						
				Quantitative							Qualitative	Reference
No	Tittle	storage media	Cooking power	Storage/ cooking unit temperature	Discharging time/efficiency	Efficiency of cooker	Charging time	Figure merit		Thermal efficiency		
								F1	F2			
22	Performance assessment of solar domestic cooking unit integrated with thermal energy storage system	D-Mannitol	-	152°C	-	73.5%	15min	-	-	-		(Kumaresan et al., 2016)
23	Development of a solar thermal storage cum cooking device using salt hydrate	magnesium chloride hexahydrate	-	-	-	-	50 min	-	-	-		(Bhave & Thakare, 2018)
24	Charging of heat storage coupled with a low cost small scale solar parabolic trough for cooking purpose	Potassium nitrate and sodium nitrate	-	200°C	-	-	-	-	-	-		(Mussard & Nydal, 2013)
25	Thermal performance of a solar pressure cooker based on evacuated tube solar collector	Water	-	120°C	-	-	-	-	-	-	It is believed to have a high potential for community use in sunny areas.	(Kumar Rakesh et al., 2001)

2.6 Research Gap

Solar cooker promotion has grown in popularity over the years, with a wide range of groups throughout the globe advocating a variety of solar cookers. Despite the multiple benefits provided by solar cookers and the substantial attempts undertaken by various groups and government agencies to promote their use, their full capabilities remain untapped. Many developing nations continue to depend on firewood as their primary energy source, which has serious health and ecological consequences. However, most developing nations (including Ethiopia) have enough sun radiation to replace traditional cooking fuels.

Because of the high cost at the beginning, the necessity for storing, and the difficulties in preparing various sorts of meals, the utilization of the sun's energy for institutional food preparation is currently restricted. Furthermore, the lack of performance data and the substantial upfront expenses for such systems raises the financial threats associated with this kind of investment. As a result, potential users must be shown the dependability of such systems.

There has been relatively little study on institutional-type cookers, specifically institutional solar-powered cookstoves with thermal storage devices. Aside from significant efforts invested in research and development in solar cookers integrated with energy storage for household and institutional cooking, most institutional cooking is still done by traditional cooking methods with an efficiency range of 5-20%, with a few with improved cookstoves having an efficiency of around 47%, leading to a major influence on the surroundings and wellness. While power from solar photovoltaic (PV) systems may also be utilized to cover cooking energy needs. Finally, there exists a desire to raise awareness among potential customers on the feasibility of solar based cooking at institutions.

CHAPTER 3: MATERIALS AND METHODS

3.1 Methods

The fundamental goal of this work is to design and simulate the utilization of solar energy (PV system) for institutional cooking by integrating thermal storage materials using CFD. The ANSYS program simulates the institutional standard solar cooker in conjunction with the thermal storage system. Using an existing institutional cook stove, the simulation result was confirmed. This chapter outlines the strategies used to achieve the goal of the research effort, and the following methodology was used.

Background Information

Background information on solar cookers, particularly SCs integrated with thermal storage, is discussed in detail in this topic, and it is concluded from the discussion that solar cookers with thermal storage for household applications are done by several researchers, but the application is limited to the household level. When it comes to institutional cooking, conventional fuel is still used the majority of the time. As a result, the practicality of solar energy at the institutional level of cooking is seen as an interesting problem.

Identifying the existing problems

The current difficulties and measures explored in the area of emphasis are recognized and discussed in the problem statement based on the background information conducted previously on the subjects of interest.

Setting objectives

Since the history and current issues in the area of interest have been recognized, the next step was to determine the objectives of the work, which are supplied as general and specific objectives in chapter one, and this assisted us to identify what to do and what not to do list.

Literature Review

The literature on solar cookers is examined, particularly those integrated with TES. Furthermore, thermal storage for solar cooking applications, thermal energy storage improvement, and institutional cook stoves are assessed.

Data Gathering

Data collected from surveyed study and sources.

- Addis Ababa solar radiation data and ambient temperatures
- The energy required for cooking at the institutional level, especially for boiling water.
- Material selection for the proposed system, sizing of thermal storage, and PV system are carried out.
- properties of materials(Specifically storages) from reliable references

Two major choices for material have been made: storage materials (PCM and HTF) and insulating materials. Materials for heat storage can be chosen based on their operating temperature range, thermal conductivity, latent heat of fusion, and local availability, among other factors. Low heat conductivity and local availability was used to pick insulation materials.

Physical Concept

The physical idea offered a schematic portrayal of the system connection after estimating every component depending on the amount of energy demand needed to be stored. The charging and discharging processes' system flow procedure and functioning concept were addressed.

Mathematical Model

The system's energy conversion equations that incorporate PV as well as thermal storage developed for the HTF and PCM. Two distinct zones are developed to use the proper models to replicate the HTF and PCM. The commonly employed single-phase Navier-Stokes equations were used to simulate the HTF. Furthermore, the PCM behavior was modeled using a melting and solidification model that included a correction component in the Navier-Stokes equations.

Computational Model and Validation of Computational Model

The solar thermal storage system linked with the PV system for cooking was simulated using ANSYS fluent software. The numerical model simulates the unsteady temperature variation of PCM and HTF for charging and discharging situations by enthalpy porosity method. The reliability of the simulation results has been verified by comparing them to other experimental investigations.

Results and Discussions

The computational model's results were given and mentioned in this section. The temperature variation in the storage during solidification and melting were discussed. The thermal storage efficiency, comparison with previous works, and melt fraction of PCM thermal storage were all investigated.

3.1.1 Flow process of Methods of analysis

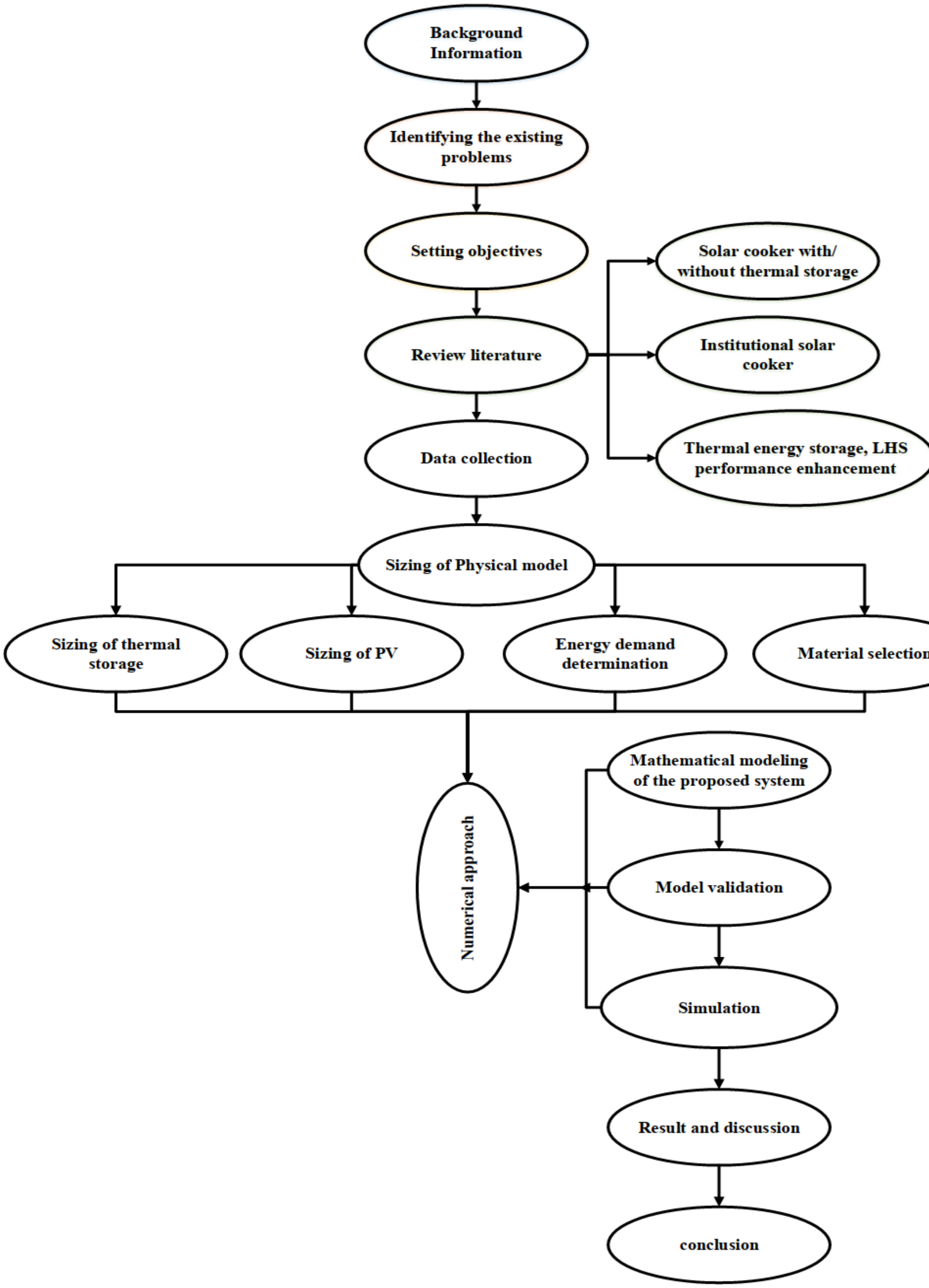

Figure 3.1: Flow process of methods of analysis

3.2 Description of the proposed model

Figure 3.2 depicts the schematic diagram utilized in the investigation. A photovoltaic panel is used to charge a TES system that is linked to an institutional cookstove. The institutional cook stove paired with the thermal energy storage system comprises PCM, HTF, and heater with integrated temperature controller in the storage tank. The PV system powers the heater and warms the HTF, which is stored in a tank to completely submerge the copper tubes holding PCM and the heater itself. Section 4.1 provides a detailed discussion of the systems, including correct sizing.

Item No	Part Name
1	Insulation cover
2	PCM tube
3	Container Support
4	container
5	Inverter
6	Charge controller
7	Cable
8	PV

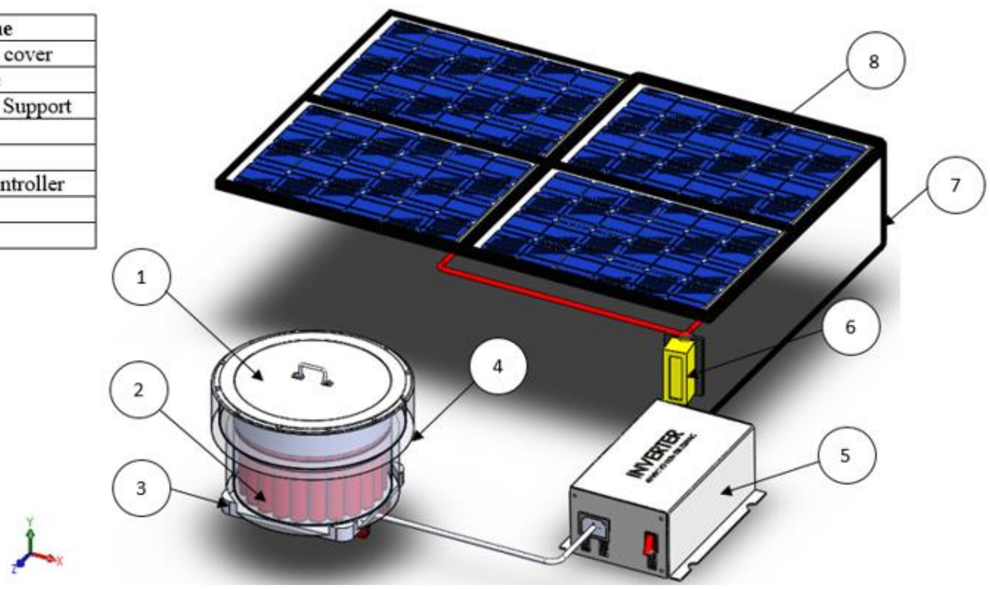

Figure 3.2: Thermal storage combined with photovoltaic system

3.3 Energy Demand Determination

Energy used in cooking is expected as required energy to raise medium temperature from room temperature to the required maximum temperature achieved during cooking and maintaining it for specific amount of time depending on the properties of the meal expanded by system heat loss.

For example, the energy used in boiling water is the energy expected in bringing the water from initial water temperature to the final needed temperature, which is the boiling point temperature of the water, plus the energy lost in the vaporization process, which is known as latent heat. For simplicity, the energy consumption for one cycle boiling of water at the institutional level is chosen in this analysis, which is almost the same temperature necessary to cook most Ethiopian meals according to Yishak (2019), and Alemu (2020). However, the system permits consistent heat transmission to the different kinds of cooking like baking, frying and roasting, which happens at a temperature between 150-190 °C (Bhave & Kale, 2020), in addition to boiling type cooking, which requires heat held above 100 °C (Bhave & Thakare, 2018).

Table 3.1: Design considerations

Parameters	**value**	**Reference**
Specific heat capacity of water at 23°C (J/ kg K)	4185.5	Steam table
The density of water (kg/m^3)	1000	Stem table
Initial temperature of water (°c)	23	(kebede, 2020)
Water loss by evaporation during solar cooking process (%)	10	(Biadgelegn, 2018), (Bhave & Thakare, 2018)
Water's latent heat of vaporization at 92°C (KJ/Kg)	2277.34.4	Steam table
Boiling temperature of Water (°C) estimated by $\mathbf{T_b = \left(100 - \frac{h}{300}\right) °C}$ Where h is $\mathbf{2349.69m}$ altitude.	92	

As shown in figure 3.3 using the exterior diameter of the cooking pot as 580mm and the thickness and height of the pot as 4mm and 0.4m, respectively, the volume of the cooking unit (V) may be computed as follows:

$$V = \pi r^2 h \qquad 3\text{-}1$$

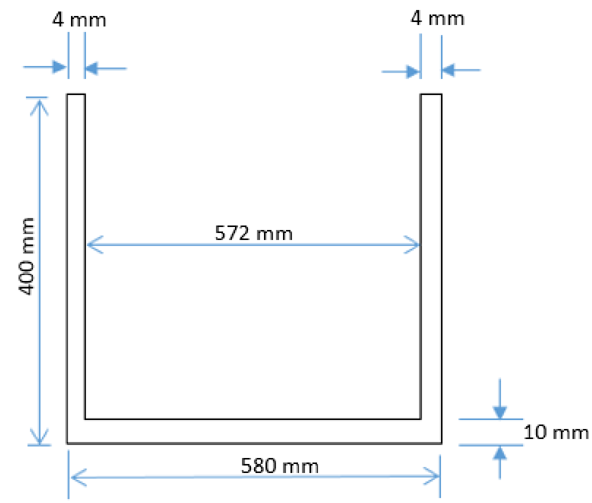

Figure 3.3: Representation of the cooking pot

According to Equation 3 1, the cooking unit can contain a volume of about 100 lit; however, when boiling, the pot is not filled to its maximum capacity; thus, 10% of the height of the pot is left vacant; as a consequence, the volume considered for the design of this research is 90 lit.

Therefore, the energy required is calculated as;

$$E_{utilized} = mc_p\Delta T + (m_i - m_f)h_{vaporization} \qquad 3\text{-}2$$

Where, m is calculated as:

$$m = \rho V \qquad 3\text{-}3$$

For the purpose of determining the energy loss of the system, we assume that there is negligible loss from the device during charging since, the cooking device is entirely insulated. However, 10% heat loss is calculated during discharge, which is heat loss vaporization. As a result of this:

$$mc_p\Delta T = 26\mathrm{MJ}$$

$$(m_i - m_f)h_{vaporization} = 20\mathrm{MJ}$$

$$E_{utilized} = 46\mathrm{MJ}$$

3.4 Material selection

3.4.1 PCM Heat storage material selection

The selection of heat storage materials (PCMs) is critical to attaining the highest efficiency for any particular application. “PCM is typically classed as organic (including paraffin and fatty acids), inorganic (including hydrated salts), and eutectic (including eutectic fatty acid mixtures and hydrate salts)”. Each form of PCM has benefits and disadvantages, which have been examined in many prior research in the literature survey and further investigated by (Milián et al., 2017), (Ramirez et al., 2020).

In general, organic PCMs possess an elevated latent heat of fusion, are chemically and thermally stable, non-corrosive, and are recyclable. Their flammable properties, lower phase transition enthalpy, poor conductivity, sub cooling, and material issues caused by their doubtful interaction with polymer vessel media are the disadvantages. Inorganic PCMs are less expensive, have higher thermal conductivity, and have a high phase transition enthalpy. Their corrosive character, inadequate levels of thermal stability, sub-cooling, and phase segregation are all disadvantages. On the other hand, eutectic mixtures can be expensive, require perfect mixing, and still have a number of the negative characteristics of metallic salts, salt hydrates, and salts. (Elias & Stathopoulos, 2019), making it difficult to choose the best one for a given application (Rastogi et al., 2015). The eutectic PCM combination, on the other hand, can produce new PCM with superior characteristics and a new phase transition temperature.

Prior research has revealed that an appropriate PCM for TES operations needs to satisfy the parameters stated in Table 2.1. In reality, however, satisfying all selection requirements concurrently with a single material is difficult, if not impossible. Furthermore, some concerns arising from the usage of PCM systems, such as phase splitting or super-freezing effects, should play a larger role in the selection of specific systems (Liu et al., 2018).

PCMs serve a purpose based on their operating temperature tolerances (-20° C to +200° C or higher). A total of four distinct temp ranges are considered depending on the use,: "small-temperature range" (-20° C to +5° C) for both residential and commercial refrigeration;

medium low-temperature range (+5° C to +40° C) for heating and cooling applications in buildings; medium temperature range (+40° C to +80° C) for solar-based heating, hot water, and electronic applications; and high-temperature range (+80° C to +200° C or above) for absorption cooling, waste heat recovery, and electricity" (Du et al., 2018).

When it comes to institutional and communal food preparation, the majority of the energy is frequently required daily. As a result, it is extremely desirable to choose a PCM with a greater Latent heat of fusion for keeping extra heat energy capable of compensating for the required energy consumption in addition to the acceptable temperature range required and availability.

Table 3.2: PCM candidates for the thermal storage

PCM NAME	TYPE	MELTING POINT[^{O}C]	HEAT OF FUSION [KJ/KG]	THERMAL CONDUCTIVITY [W/m K]	DENSITY [Kg/m3]	HEAT CAPACITY [KJ/Kg k]	REFRENCE
$MgCl_2 \cdot 6H_2O$	SALT HYDRATE	118	167	0.57	1560	1.72(sol) 2.82(liq)	(Bhave & Thakare, 2018)
ERYTHRITOL	SUGAR ALCOHOL	118	339.8	2.64	1480	1.38	(S.D. Sharma et al., 2005)
PARAFFIN WAX	PARAFFIN	106	80	0.63	1200	NA	(Senthil, 2021)
SOLAR SALT	SALT HYDRATE	210-220	108.67	0.8	1800/ 1700	1.59498	(Bhave & Kale, 2020)
ACETANILIDE	NA	118.9	222	NA	1210	2	(Saini & Kumar, 2017)
D-Mannitol	SUGAR ALCOHOL	167-169	326.8	NA	1490	NA	(Kumaresan et al., 2016)

As a result, after considering several options, as indicated in Table 3.2, solar salt (a combination of 60% NaNO3 and 40% KNO3) was chosen for further exploration as a phase transition material. Because of their desirable melting point range of 210-220°C and the Latent heat fusion 108.67 KJ/Kg, they were chosen as storage (PCM) contenders for the cooking model. Thermo-physical parameters of the PCM storage in use are described in Table 3.3.

Table 3.3: Thermo-physical parameters of solar salt (Bhave & Kale, 2020)

Property	**Value**
Thermal conductivity (W/m K)	0.8
Density (Kg/m^3)	1800(below 220°c) 1700(above 220°c)
Enthalpy of fusion (KJ/Kg)	108.67
Melting point (^{O}C)	phase transition 210-220°c
Phase transition enthalpy (KJ/Kg)	31.91

3.4.2 Container for the PCM (encapsulation of PCM) geometry selection

Following the selection of the PCM, the configuration of the PCM container is critical to the thermal performance of the LHS system. The PCM container has a geometric configuration that directly influences the type of heat transmission and, as a result, the pace of phase transition (Khan et al., 2016).

Many studies on LHS have been produced throughout the years on the benefits of different PCM setups. An investigation of ways for advancing the heat transfer rate of the LHS was a critical concern in the design of the LHS. To address the low performance of heat exchange, many configurations have been devised, and Table 3.4 highlights some of the most commonly utilized designs.

Encapsulated phase change materials (EPCMs) were investigated in this work because Encapsulation can enhance the heat transport surface and lower the resistance to heating associated with conduction in a PCM storage system. As a result, encapsulation can dramatically reduce the period of heat transfer for PCMs, especially when the storage media has poor conductivity of heat. Furthermore, some PCMs have practical issues, such as most salt hydrates or some eutectic salts having subfreezing and separation issues during thermal cycling. Nonetheless, encapsulation has the potential to alleviate such issues. Furthermore, encapsulation can shield the PCM from heat transfer fluid (HTF) exposure and subsequent corrosion (Zhao et al., 2013).

According to the results of the literature review, encapsulated PCM improves LHS performance, and as the capsule size decreases, thermal performance improves even more. As a result, microcapsule is viable solution for improving LHS performance. Because of the manufacturing issue, however, the microcapsule are often employed for minimal-temperature PCM. As a consequence, the cylindrical PCM Macro capsule container (shell and tube arrangement) is employed in this study to achieve the optimum Heat movement between the PCM and the external heat transfer medium. Furthermore, the cooking unit's layout is more directly integrated with the cylindrical form container.

Table 3.4: Overview of configurations containing PCM as a storage material

Capsule configuration	Common arrangement	findings	Schematic	Reference
Spherical	Constrained melting, Unconstrained melting	The heat transmission rate was significantly improved. However, the initial cost is large and it is only employed for low-temperature applications.	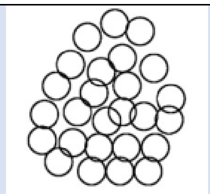	(Ehms et al., 2018) (Maheswari & Reddy, 2013)
Cylindrical	Pipe model	has a reduced rate of heat loss to the environment since almost all of the heat given from the center ends up melting the PCM	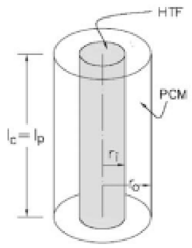	(Zayed et al., 2020) (Punniakodi & Senthil, 2021)
	Cylinder model	aid to smooth melting by eliminating impediments to convection currents, potentially as a result of its progressive surface area fluctuation	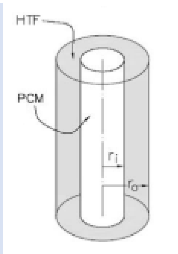	(Narasimhan, 2019) (Zayed et al., 2020)
	Shell and tube model	Enhanced heat transmission in PCMs The PCM melting rate increases as the spiral diameter of HTF in STHE grows.	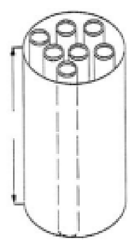	(Han et al., 2017) (Mahfuz et al., 2014) (Hosseini et al., 2014)
Rectangular	-	The easiest boundary conditions, which are also the easiest to construct, will melt more when inclined at a 60° angle.	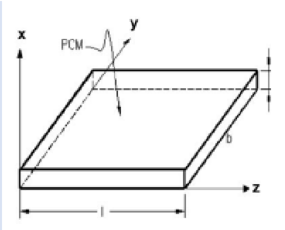	(Jellouli et al., 2007) (Zhao et al., 2018) (Yadav & Samir, 2019)

3.4.3 Encapsulation shell materials selection

The covering material is equally significant and is determined by an assortment of criteria, including the target application temperature, conductivity, wrapping technique, permeability, harmful effects, and interaction with the inner core (PCM) and the environment around it will be included. As a result, appropriate materials must be carefully chosen (Ramirez et al., 2020). According to Jacob and Bruno (2015) and Regin et al. (2008), desirable features of encapsulation material are vital to consider while building a TES system that uses encapsulated PCMs.

As a result, PCM encapsulation material should:

- ✓ Meet the strength, flexibility, corrosion resistance, and thermal stability criteria;
- ✓ Safeguard the PCM from damaging connections with the outside world by serving as a barrier.
- ✓ Provide a large enough surface area for heat transmission;
- ✓ Ensure that structure is stable and ease of use;

Table 3.5: Different encapsulation materials

MATERIAL	THERMAL CONDUCTIVITY [W/m ^{O}C]
Aluminum	202
Brass (70 Cu-30Zn)	99
Carbon steel	45
copper	386
Stainless steel, type 304 (18Cr-8 Ni)	16
Titanium	19

Considering the encapsulation shell material (Table 3.5) selection criteria, Copper will be the encapsulation material of the PCM for this study, due to its greater conductivity of heat and mechanical strength (Parrado et al., 2015), (Alemu, 2020).

3.4.4 Thermal Heat Storage Insulation Material

Thermal insulating materials must be used around thermal energy storage systems to reduce heat losses. The primary goal of insulation is to lower the rate of heat passage in order to avoid or restrict variations in temperature in the region. Table 3.6 outlines some of the insulation materials available on the market with varying insulating characteristics. It is mandatory to pick a suitable kind of insulating material in accordance with the system temperature and the manner of heat transfer implicated. An ideal insulating material should meet various characteristics, including low thermal conductivity, non-corrosiveness, nontoxicity, nonflammability, and little or no decomposition over time (Deshmukh et al., 2017). Thermal parameters, such as thermal conductivity, specific heat capacity, and thermal diffusivity, should be considered when selecting an insulating material (Ayugi et al., 2011).

By examining the insulating materials listed in Table 3.6. In this study, fiberglass is employed as an insulating medium since it is moderately dense and comes in a variety of thicknesses. With a service temperature of up to 350°C, the thermal conductivity varies from 0.033–0.04W/m K.

Table 3.6: Summary of thermal insulation materials

Types	Available Structures	Thermal conductivity	The density	Temperature range	The compressive strength	Water vapour transmission	Reference
Glass mineral wool	flexible rolls, rigid slabs and preformed pipe sections	0.031 - 0.042 W/ mK	ranges from 10 to 80 kg/m^3	-200°C to 450°C	1 to 8 kN/m^2	346 to 417 μgm/Nh	(Ilkka Valovirta, 2004)
Cellulose glass	40 to 160 mm thickness	0.034 - 0.081 W/mK	available with relatively high density	-260°C to 430°C	700 kN/m^2	Zero	(MP Westman SG Laddha et al., 2010)
Calcium silicate	25 to 100 mm thickness	0.054 W/mK	240 kg/ m^3	1000°C maximum	600 kN/m^2	no water vapour penetration	(Deshmukh et al., 2017) (Papadopoulos, 2005)
Ceramic fiber	6 to 50 mm thickness	0.030 - 0.079 W/mK	64 to 192 kg/m^3	up to 1400°C	2.5 kN/m^2	zero	(Papadopoulos, 2005)
Melamine foam	10 to 50 mm thickness	0.034 W/mK	11 kg/ m^3	10°C to 150°C	5 to 20 kN/m^2	350 μgm/Nh	(Deshmukh et al., 2017) (Hung Anh & Pásztory, 2021)
Perlite expanded	25 to 300 mm thickness	0.057 W/mK	80 kg/m^3	-250°C to 1000ºC		zero	(Deshmukh et al., 2017)
Rock mineral wool	20 to 120 mm thickness	0.033 W/ mK	80 kg/m^3	-200°C to 900°C	7.5 to 10.5 kN/m^2	385-400 μgm/Nh	(Papadopoulos, 2005)
Vermiculate	according to the use	0.066 - 0.083 W/mK	50 to 150 kg/m^3	0°C to 1300ºC		350 μgm/Nh	(Hung Anh & Pásztory, 2021)
Fiberglass	according to the use	0.033–0.04 W/mK	24–112 kg/m^3	- 4–350 °C	-	-	(Hung Anh & Pásztory, 2021)

3.4.5 Heat transfer fluid selection

The HTF selection criteria are depends on the fluid's viscosity, boiling point, decomposition point, specific heat density , and availability (Malik et al., 2020). However, HTF must be aligned with the enclosure materials and storage medium, as well as be able to function within the specified temperature range (Kuravi et al., 2013). The commercial oil SHELL TERIMA OIL B was chosen as a HTF for this investigation among the various heat transfer fluids investigated and listed in Table 3.7. The SHELL THERMIA OIL B was selected for its greater effectiveness in indirect closed systems running at higher temperatures. SHELL THERMIA OIL B offers remarkable thermal stability for maximum temperatures up to 320^{o}C and to 340^{o}C film temperatures, according to the shell safety data sheet. The shell data sheet given in Appendix A1 contains typical design data for THERMIA OIL B.

Table 3.7: HTF candidates for thermal storage

NAME OF HTF	HEAT CAPACITY [KJ/KG K]	THERMAL CONDUCTIVITY [W/M K]	DENSITY [KG/M^3]	OPPERATING TEMPERATURE [^{O}C]	NORMAL BOILING POINT [^{O}C]	REF
Taurus Therm 500	3.22	0.110	840	-		(Bhave & Thakare, 2018)
THERMINOL VP-1	1.546	0.1363	1068	12-400	257	(Rongrong et al., 2013),(Benoit et al., 2016)
Duratherm XLT-50	2.065	0.136	809.68	-45-121	NA	(Kantole, 2012)
WATER	4.185	NA	1000	0-100	100	(Kumar Rakesh et al., 2001)
SHELL TERIMA OIL B	1.882	0.134	873	-10-320	365	(Getenet, 2011)

3.5 Theoretical storing capacity of the system

Since the thermal storage of the proposed system is achieved by combination of PCM and HTF to calculate the theoretical storing capacity of the system, one has to calculate the energy storing capacity in the oil, and PCM for the system.

$$Q_{total} = Q_{PCM} + Q_{oil} \tag{3-4}$$

Where the energy stored in the Oil is given by:

$$Q_{oil} = m\, C_{P\, oil}\, \Delta T \tag{3-5}$$

Where, m is mass of Oil given by equation 3-6, C_p specific heat capacity of Oil, ΔT is the change in temperature.

$$m = \rho V \tag{3-6}$$

The energy stored in the PCM capsule is given by Equation 3-7 as mentioned by (Tesfay et al., 2014):

$$Q_{PCM} = \int_{T_i}^{T_m} mC_P dT + ma_m \Delta h_m + \int_{T_m}^{T_f} mC_P dT \tag{3-7}$$

Where, m is mass of PCM, C_p specific heat capacity of PCM, Δh_m enthalpy of phase fusion and a_m is the fraction melted.

Temperature dependent Heat capacity of PCM (C_P):

$$C_p = \begin{cases} 0.75\ if\ \ T < 110\ °C \\ 4.2\ if\ 110°C \le T \le 120°C \\ 1.4\ if\ 120°C < T < 210°C \\ 12\ if\ 210°C \le T \le 220°C \\ 1.6\ if\ T > 220°C \end{cases} \tag{3-8}$$

3.5.1 Quantifying the Amount of PCM AND HTF

By taking into consideration the melting point of PCM which is in the temperature range of 210-220 °C (Bhave & Kale, 2020) and the remarkable thermal stablity of HTF for maximum temperature up to 320 °C (Getenet, 2011) the final temperature of the HTF is considered to achive 300 °C. Therefore, taking the volume of the oil in the tank to be 41 l, initial oil temperature 23°C and final oil temperature of 300°C the energy stored in the oil can be obtained as follows:

$$Q_{oil} = m\, C_{P\, oil}\, \Delta T = 18509.58KJ$$

Where 861.05 [*Kg/m*^{3}] is the density, and 1.8928 [*KJ/Kg K*] specific heat of SHELL TERIMA OIL B, at 23 °C collected from Appendix A1.

The quantity of PCM is decided by how much energy is required to boil the specified amount of water (90 L) which is Q=46MJ, however the thermal storage is achieved by a combination of PCM and HTF, from prior calculations and assumptions considered $18509.58KJ$ of energy is stored in HTF while the rest is required to be stored in the PCM for that it was assumed that for the PCM to store the energy it must be completely melted as a result the final temperature of PCM is assumed to be 220 ^{o}C, therefore the mass of PCM required can be determined based on the equation 3-4.

$$46000KJ = Q_{PCM} + 18509.58KJ$$

$$Q_{PCM} = 27490.42KJ$$

$$Q_{PCM} = \int_{23}^{109} \mathrm{mC_p\,dT} + \mathrm{ma_m \Delta h_m} + \int_{110}^{120} \mathrm{m\,C_P dT} + \int_{121}^{209} \mathrm{m\,C_P dT} + \int_{210}^{220} \mathrm{m\,C_P dT}$$

$$27490.42KJ = \mathrm{m_{pcm}}[0.75(109-23) + 4.2(120-110) + 1.4(209-121) + 12(220-210) + 108.67]$$

$$\mathrm{m_{pcm}} = 60\mathrm{kg}$$

$$\mathrm{V_{pcm}} = \frac{\mathrm{m_{pcm}}}{\rho_{\mathrm{pcm}}} = 0.03529\mathrm{m^3} \sim 35\mathrm{lit}$$

Where, $\mathrm{m_{pcm}}$ is mass of PCM, ρ_{pcm} is density of PCM collected from *Table 3.3* and $\mathrm{V_{pcm}}$ is volume of PCM.

However, a ten percent volume was left vacant for expansion during melting (Tesfay et al., 2014). As result, whole volume of PCM by considering 10% clearance volume is given by:

$$\mathrm{V_{pcm\,total}} = (\mathrm{V_{pcm}})0.1 + (\mathrm{V_{pcm}}) = 0.038819\mathrm{m^3}$$

3.5.2 Size of encapsulation tube

For 2 1/2 inch Nominal or standard size inch copper tube; Di = 62.611 mm, Do = 66.675 mm and thickness 2 mm shown in *Figure 3.4* taking the height of 300 mm volume of the copper tube is calculated as:

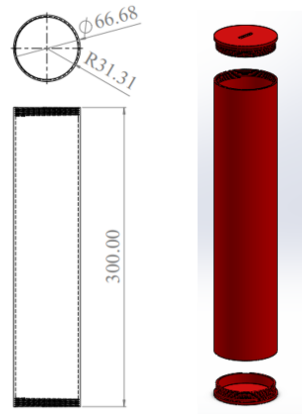

Figure 3.4: Encapsulation tube

$$V_{encapsulated\ tube} = \frac{\pi D_i{}^2}{4} * L \qquad \textit{3-9}$$

$$\mathrm{V_{encapsulated\ tube}} = 0.000924\mathrm{m}^3$$

To calculate the amount of tubes required to encapsulate the total amount of PCM in the storage total volume of PCM is given as:

$$V_{pcm\ total} = n * V_{encapsulated\ tube} \qquad \textit{3-10}$$

Therefore,

Number of cylindrical tube (n);

$$\mathrm{n} = \frac{\mathrm{V_{pcm\ total}}}{\mathrm{V_{encapsulated\ tube}}} = 42$$

To calculate the total volume of tank

Total volume of the encapsulated tubes by using the external diameter of the PCM tube will be calculated by;

$$\mathrm{V_{encapsulated\ tube(D_o)}} = \frac{\pi \mathrm{D_o}^2}{4} * \mathrm{L} = 0.001047$$

$$\mathrm{V_{encapsulated\ tube(total)}} = \mathrm{n} * \mathrm{V_{encapsulated\ tube(D_o)}} = 0.043974\mathrm{m}^3$$

$$\mathrm{V_{tank,total}} = \mathrm{V_{encapsulated\ tube(total)}} + \mathrm{V_{Oil}}$$

$$\mathrm{V_{tank,total}} = 0.084974\ \mathrm{m}^3$$

3.6 PV sizing

Sizing of the PV array for independent PV system is a vital aspect of system design. This section demands solar radiation statistics for the in- tended geographical position, demand for power and manufacturing data for PV modules.

3.6.1 Panel Inclination and Site Meteorological Data

Addis Ababa is situated at 9.0403° latitude and 38.7631° longitude. The geographical latitude determines the angle at which a solar panel should be installed to produce the greatest energy in a particular year. However, for best yearly production, fix the solar panel tilt angle to the geographical latitude. Therefore, the panel inclination will be 9.0403 degree facing south. To forecast the capability of a photovoltaic (PV) system in a specified location, weather information must be gathered. Table 3.8 displays the monthly average daily solar radiation information striking on both equator-facing inclined by the site's latitude angle and horizontal photovoltaic (PV) panels.

Table 3.8: NASA Monthly Solar radiation data

20-year Meteorological and Solar Monthly & Annual Climatologies (January 2001 - December 2020)		
Location: Latitude 9.0398 Longitude 38.7627		
Month	Solar Irradiance for Equator Facing Horizontal Surface (kW-hr/m^2/day)	Solar Irradiance for Equator Facing Latitude Tilt (kW-hr/m^2/day)
JAN	6.08	6.5
FEB	6.46	6.73
MAR	6.39	6.46
APR	6.2	6.11
MAY	6.13	5.92
JUN	5.59	5.38
JUL	4.72	4.59
AUG	4.59	4.51
SEP	5.37	5.36
OCT	6.15	6.31
NOV	6.03	6.38
DEC	5.96	6.43

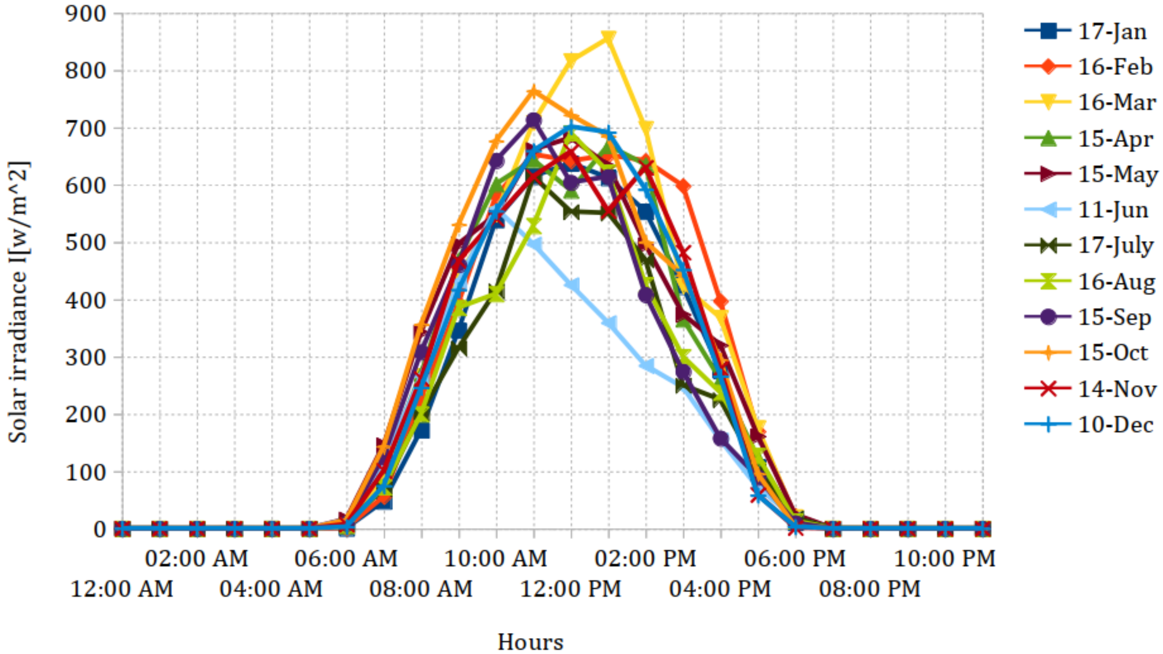

Figure 3.5: Hourly total solar radiation of Addis Ababa for recommended days in months

3.6.2 Energy Requirement

The sizing of PV array are made on the basis of the energy demand, solar energy available and efficiencies of the system. The system sizing is done in the worst operating condition which is august as shown in *Table 3.8.*

The load demand is 46MJ which needs to be supplied for one cycle boiling. However considering 23% system losses (Bruce, 2021) the load demand corresponds to 56.58MJ.

$$E_{demand} = 56.58MJ \; = 56580KJ = 15.7KWh$$

As a result, the dimension of the photovoltaic array utilized in the present investigation can be determined through the equation below (Gont, 2019):

$$PV_{area} = \frac{E_{demand}(KWh/day)}{H\left(\frac{\frac{KWh}{m^2}}{day}\right) * \eta_{PV} * PR} \qquad \textit{3-11}$$

Where H is solar radiation on tilted plane, η_{PV} is PV efficiency which is 18.44% obtained from manufacturing data (of selected PV) and PR is performance ratio, coefficient for losses (default value = 0.75) (Skunpong & Plangklang, 2011).

Thus, using equation 3-11 the PV area is 25m^2. PV modules of various sizes provide differing amounts of power. The total peak wattage generated is necessary to estimate the size of the PV module. The peak watt (We) produced is governed by the PV module size and the climate of the site location. At a peak solar radiation (PSI) of 1000 W/m^2, the PV peak power is thus (El Shenawy et al., 2017),

$$PV_{peak\ power} = PV_{area} * PSI * \eta_{pv} \qquad \textit{3-12}$$

$$PV_{peak\ power} = 4610W$$

However, Theoretical output energy of the system in [KWh] given by (Skunpong & Plangklang, 2011):

$$E_{th} = \eta_{PV} E_{global} A_{array} \qquad \textit{3-13}$$

$$= 20.7911KWh = 74847.96\ KJ$$

Where, PV efficiency which is 18.44%, global radiation (E_{global}) 4.51 KWh/m^2 and 25m^2 PV area (A_{array}) is used.

Considering the peak sun hour of the design month which is 4.59h, the theoretical output power of the PV system is given as follows:

$$\frac{74847.96\ KJ}{4.59 * 3600s} = 4.52965KW = 4529.65W$$

Thus, taking into consideration the availability and the number of panels going to be used the chosen modules are 300 Watt Monocrystalline Solar with specifications given in *Table 3.9* (PEIMAR, 2022). When viewed alongside polycrystalline or thin-film panels, monocrystalline silicon PV panels are extremely efficient and take up the least amount of area.

Table 3.9: SG300M (BF) solar panel technical data sheet

Electrical characteristics (STC)	**SG300M (BF)**
Nominal output (Pmax)	300W
Flash test power tolerance	0/+5W
Voltage at Pmax (Vmp)	32V
Current at Pmax (Imp)	9.4A
Open circuit voltage (Voc)	40.2V
Short circuit current (Isc)	9.71A
Maximum system voltage	1500V
Maximum series fuse rating	15A
Module efficiency	18.44%

Therefore,

$$Number\ of\ Modules = \frac{4530W}{300W} = 15.1$$

Thus, 16 Panels are employed to provide the desired energy.

Series and parallel combinations of the final PV array could be arranged to meet the needed voltage and current. For this study the required voltage output of the PV module which is going to be supplied to the chosen heater is 220V (AC).

Thus, solar modules linked in series are determined by:

$$Number\ of\ modules_{series} = \frac{voltage\ required}{operating\ voltage\ of\ a\ single\ module} \qquad \textit{3-14}$$

DC current needs to be maintained as low as feasible to mitigate system losses. As suggested, a 48 V DC voltage bus is preferable (El Shenawy et al., 2017).

$$= \frac{48\ V}{32V} = 1.5{\sim}2 modules$$

Solar modules linked in parallel can be determined as:

$$Number\ of\ modules_{parallel} = \frac{Number\ of\ modules}{Number\ of\ modules_{series}} \qquad \textit{3-15}$$

$$Number\ of\ modules_{parallel} = \frac{16}{2} = 8$$

As a consequence, the array was setup with eight parallel strings of two series connected modules, yielding a rated output of 4812.8 watts.

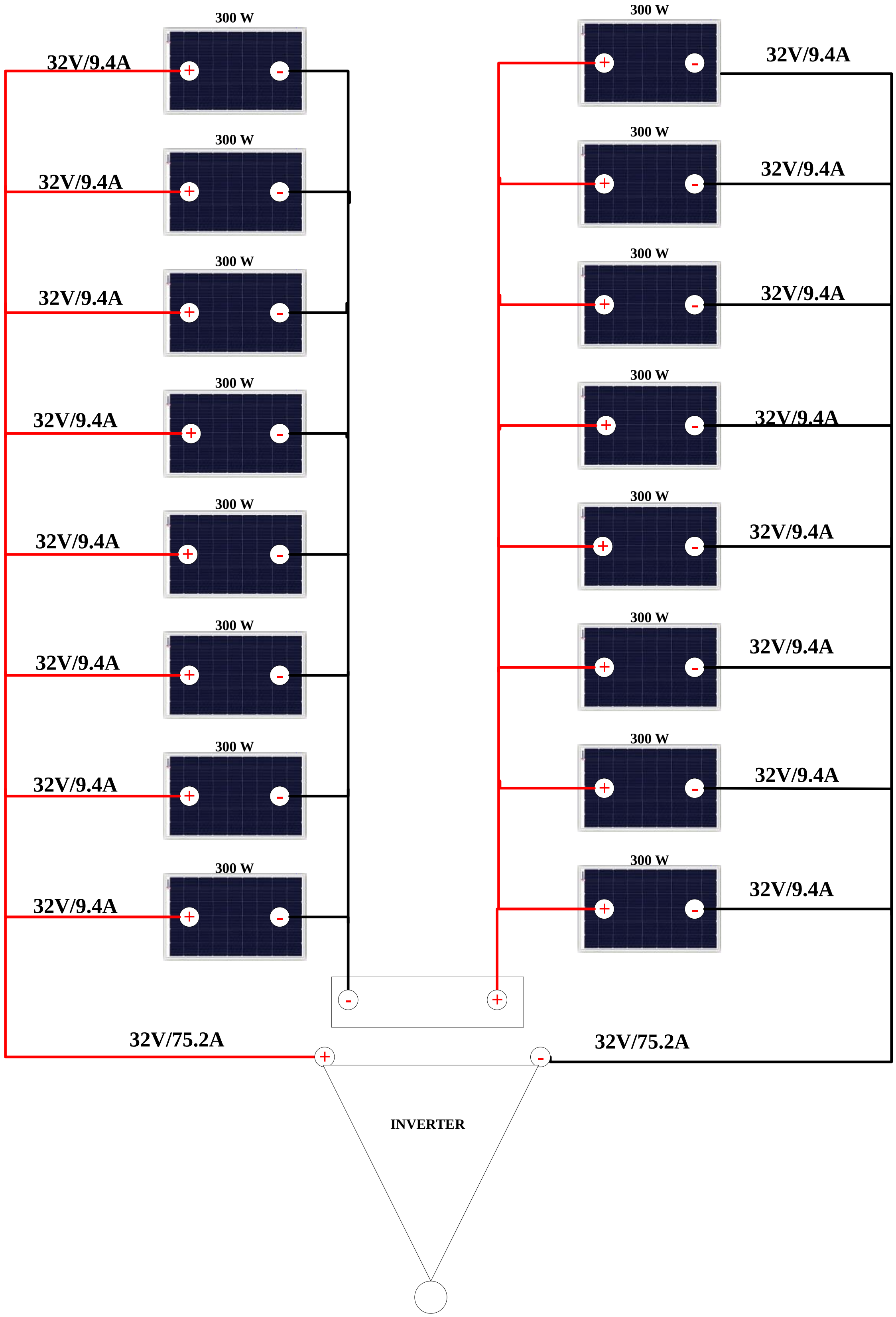

Figure 3.6: PV array configuration

3.6.3 Sizing Charge Controller

Charge controller is essential to charge the storage or inverter in the system securely and to extend their lifetime. In addition it smooths down the fluctuation, allowing the inverter to receive power at a consistent and safe rate. For that, It must be capable of handling the PV array short-circuit current (Gont, 2019). The charge controller current input rating is equal to the product of the PV module's short circuit current, the number of PV modules connected in parallel, and the safety factor, where the safety factor is 1.25 (HASSEN, 2020)

$$I_{Rated} = (N_{PV\ Parallel} * I_{SC}) * 1.25 \qquad 3\text{-}16$$

Where:

- ✓ I_{Rated} = Solar charge controller rating
- ✓ I_{SC} = Short circuit current
- ✓ $N_{PV\ Parallel}$ = Number of PV modules in parallel
- ✓ 1.25 is safety factor

In our case, it may be selected to withstand 97.1A while keeping the DC bus voltage around 48V. As a consequence, an MPPT solar charge controller with the model number SCCM10048 was chosen. Appendix A4 contains the electrical specifications of the selected solar charge controller.

3.6.4 Inverter selection

The inverter (a power conditioning device) is the heart of a standalone PV system. A PV system generates DC voltage. As a result, an inverter that transforms DC power into AC power is required (Pal et al., 2015).So the inverter needs to be chosen based on its DC input voltage (VDC) and output power (PKVA). On the other hand the inverter is selected in a way that it can manage the maximum predicted power of AC loads. As a result, it should be at least 10% more than the total rated power of the needed AC loads (Agarwal et al., 2013).

Considering the system's AC load which is 4529.65 watts, the rated power of the inverter is 4982.615 W. As a result, the inverter parameters will be 5000 W, 48 VDC, and 220 VAC as listed in Appendix A3. For that case the LS SERIES (LS 5048) Inverter was chosen.

3.6.5 Cable Sizing

PV system design is not complete unless the right dimension and kind of cable are chosen for connecting all of the parts. Cable size is critical for stand-alone solar systems since they link the different PV system parts with the electrical load. Their size is generally dictated by the greatest current-carrying capabilities and should be sufficient to prevent voltage drops and resistive wastage. Furthermore, they must be UV and water-resistant, as well as ideal for outdoor use. The two types DC cables: battery to inverter and SPV to inverter. In our situation, however, an SPV to inverter DC wire is necessary. The amount of cable is established on-site by physically measuring the distance between the components of the solar system. Cable size should be chosen to reduce voltage drop or cable loss (Pal et al., 2015).

3.7 Heating element selection

Heating element (Immersion electric oil heater) having features of high watt density stainless steel which provides 4500w 220v of power with integrated temperature control device aimed at maintaining the temperature inside the storage at $300^{O}C$ is chosen for this study depending on the power and voltage output of the PV system and inverter to supply the load demand.

CHAPTER 4: MATHEMATICAL MODELING AND NUMERICAL APPROACH OF LHTES

4.1 Physical model

PV panels were employed to power an institutional cook stove equipped with thermal energy storage devices. The cook stove comprises a heating element, HTF, and PCM inside a container, as seen in Figure 4.1. The thermal storage device container was constructed using an aluminum cylindrical vessel, as illustrated in Figure 4.2 A. A mixture of 41L of commercial SHELL THERMIA OIL B (HTF) and sealed copper tubes carrying a total of 60 kg of PCM is used to store heat.

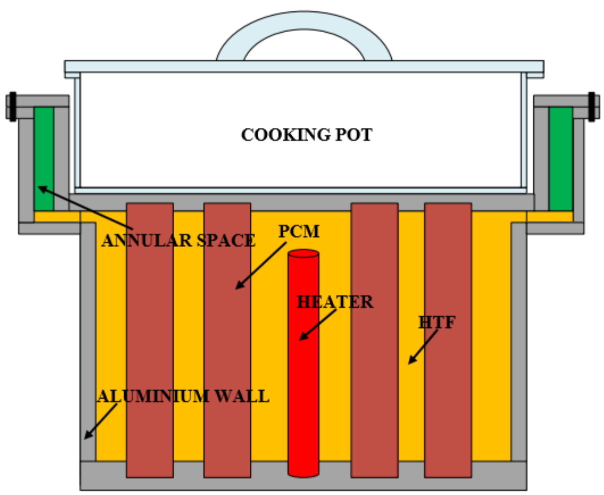

Figure 4.1: Configuration of a thermal storage cooking gadget

The PCM is housed within 42 cylindrical copper tubes measuring 300mm long, 2mm thick, and 62.611mm internal diameter (Figure 4.2 C). Both ends were internally threaded, and a copper plate with outside threads was used to seal the tube. The HTF (SHELL THERMIA OIL B) was filled in the storage compartment to cover the copper tubes and also operate as a heat transfer medium. A heater having 4500 W and 220 V is immersed inside storage as a power source during the charging phase.

The upper part of the thermal storage tank was placed from the top into the storage container, and the two pieces were joined at the flanges. Figure 4.2 B, with a 3mm thick gasket in between to prevent oil leakage. The cylinder walls, the top section of the cook stove, and thermal storage compartments would be insulated against heat loss while charging.

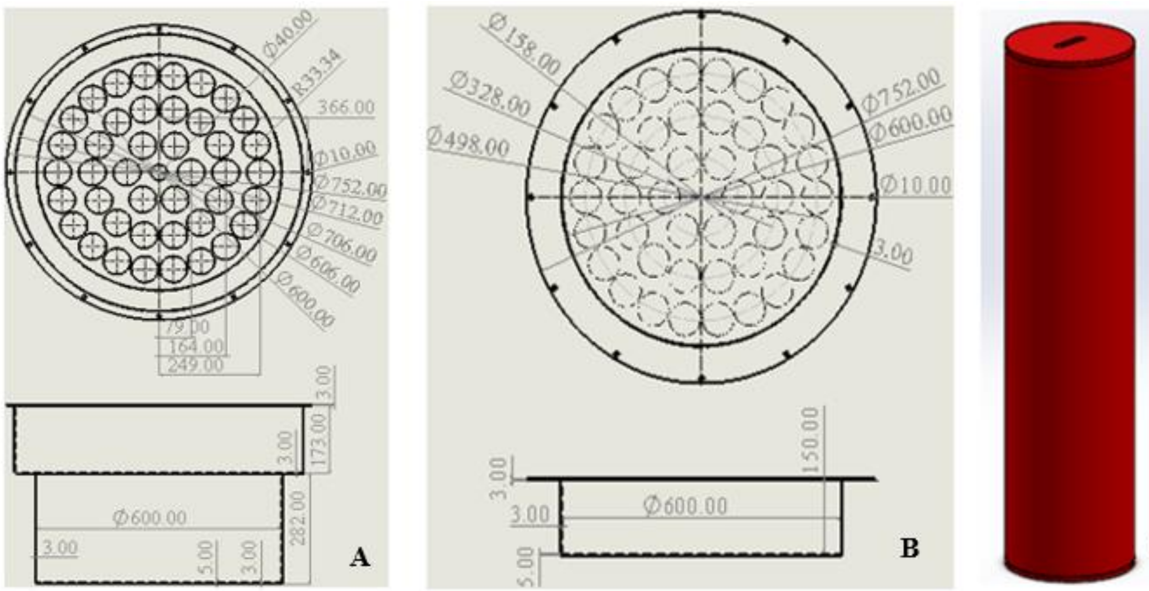

Figure 4.2: (A) Container base (B) container top (C) PCM tube

When cooking begins, the insulating cover on the top of the device is removed, and the cooking pot is inserted with the appropriate food with it. Gradually the temperature increases, and cooking begins. Which results in reduction of HTF temperature following that The PCM-contained in cylindrical tubes will release its heat via coupled boundary conditions to the HTF, Thus, natural convection heats the whole underside of the cooking pot and the food is cooked. Farther Design Specifications of the cook stove with TES is given in Table 4.1 and Figure 4.3 B and C shows the configuration of the cooking unit assembly.

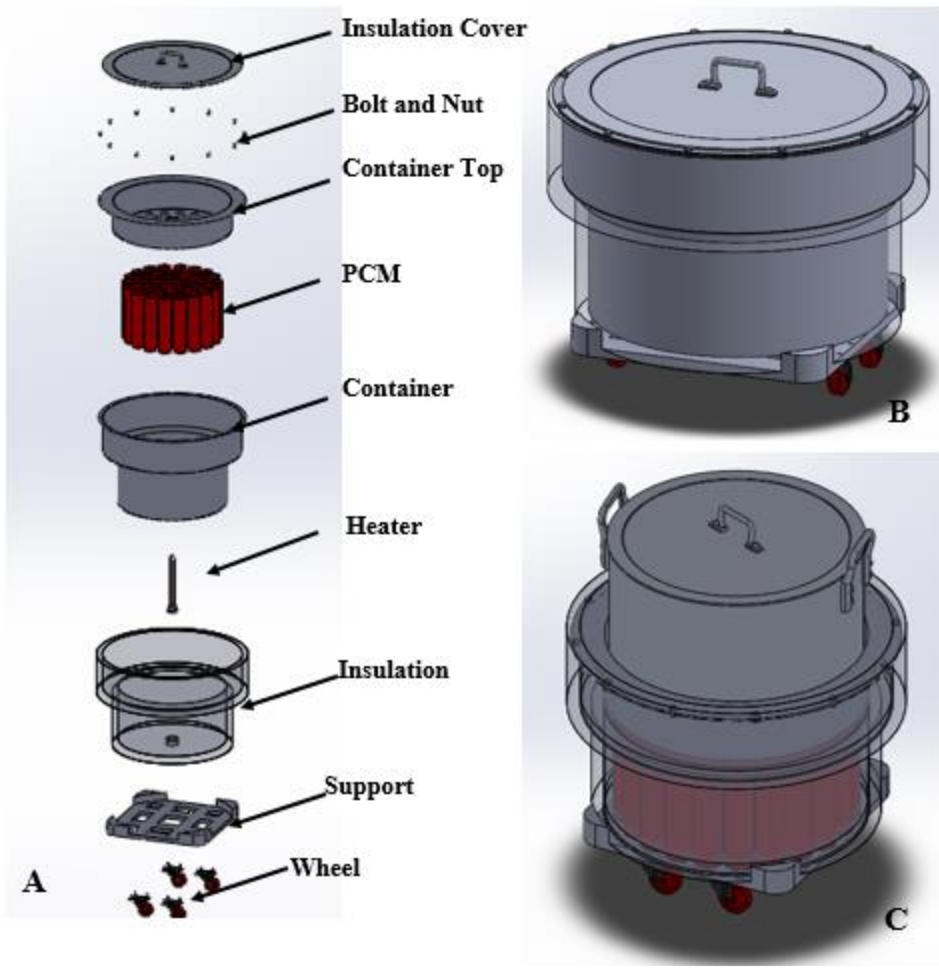

Figure 4.3: (A) Exploded view (B) charging condition assembly (C) discharging assembly

Table 4.1: Cooking unit Design specifications

Component	**Specifications**
Heater	Power = 4500 W, 220 V
Cooking unit	outer diameter = 580 mm, thickness = 4 mm
PCM vessel outer diameter	66.675mm
PCM vessel inner diameter	62.611 mm
Number of PCM tubes/capsules	42
Height of PCM capsule	300 mm
Mass of PCM total	60 kg
Amount of HTF used in storage	41L

4.2 Numerical Approach

Over the past few years, there seems to be plenty of problems involving phase changes.' The shifting interface (or interfaces) at which (or between which) the phase change happens is the key aspect of such situations. It is made more difficult by the fact that the solid-liquid border shifts according to the rate at which this latent heat is taken in or released. In principle phase transition happens at a single temperature, while it really occurs throughout a temperature range, resulting in the two-phase zone. (Soibam, 2017).

The literature divides numerical phase change models into two categories: Table 4.2 describes detailed classification obtained from literature. From the performed literature review, fixed grid models are found to be easier to develop than variable grid and the outcomes are always correct. (Ma & Zhang, 2006).

Table 4.2: Numerical phase change models in the literature

Numerical phase change models in the literature	**Description**	**Latent heat modeling**	**Velocity transition modeling**	**Reference**
Fixed grid or continuum models	There is just one computing domain and one set of equations.	Source term (E-STM), enthalpy (E-EM), or temperature (temperature-transforming models)	Switch–off (SOM), source term (STM), and variable viscosity (VVM)	(Hu & Argyropoulos, 1996), (Nazzi Ehms et al., 2019), (Karthikeyan et al., 2021) (Regin et al., 2006)
Variable grid or two-phase models	Solid and liquid computational domains are distinct.	-	-	(Ismail et al., 2014), (Ismail & Henríquez, 2000)

Since phase changing contains transition of both velocity and latent heat, an appropriate computational approach employs a combined effort of the approaches outlined in the preceding sections. As a result, the combination of the enthalpy technique E-EM with the Darcy STM (smoother variations of the SOM and STM groups), named "enthalpy-porosity," has proven to be the most often used in the literature.

Numerous market software packages are available for the numerical study of charging and discharging process of PCM. Nonetheless, as reported by Al-abidi et al. (2013), ANSYS Fluent is the greatest commonly used program. As a result, the created model was numerically studied using ANSYS Fluent 19.2. ANSYS Fluent employs the enthalpy-porosity technique, in which the mushy zone is modeled as a porous medium whose porosity is determined by the liquid percentage.

4.2.1 Computational domain

Simplifying conditions are commonly used in numerical models to accelerate convergence and allow for a solution in an acceptable amount of time. Geometry, material qualities, physical events related to the issue, and boundary conditions can all be taken to constitute simplifying conditions. The application of a smaller domain and the adoption of symmetry criteria are two geometrical simplifications: the first one requires some equations to be dealt with, while the other decreases the area of the computational space.

In our situation, numerical simulations were performed utilizing a finite volume numerical code and a 2Daxisymmetric approximation based on the problem features. The model assumes that the HTF enclosing the cylinders is located in cylinder jackets around the tubes. Of course, the total volume of all these cylinder jackets is the same as the total volume of fluid in the actual storage container.

As indicated in Figure 4.4, two distinct zones are specified or implementing the necessary model to the HTF and PCM. The well-known single-phase Navier-Stokes equations were used to simulate the HTF. The PCM behavior, on the contrary, was studied using a solidification and melting model with a correction component in the Navier-Stokes equations. This can simulate the phase change of the mass within the closed shell in which the PCM is contained. Figure 4.5 depicts a 2D axisymmetric region that has been taken for simulation.

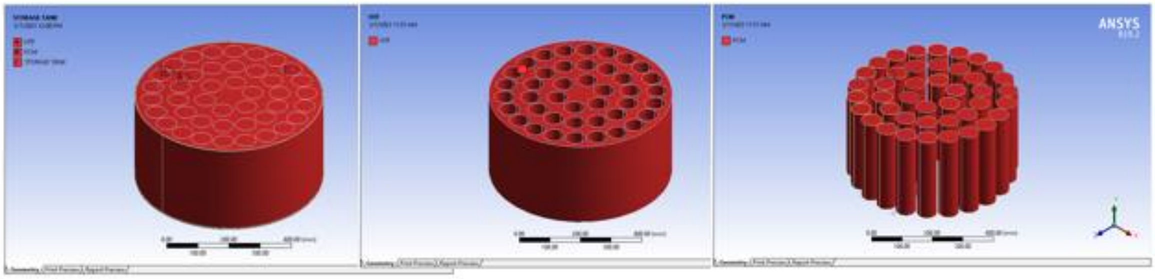

Figure 4.4: Over all geometry of thermal storage model

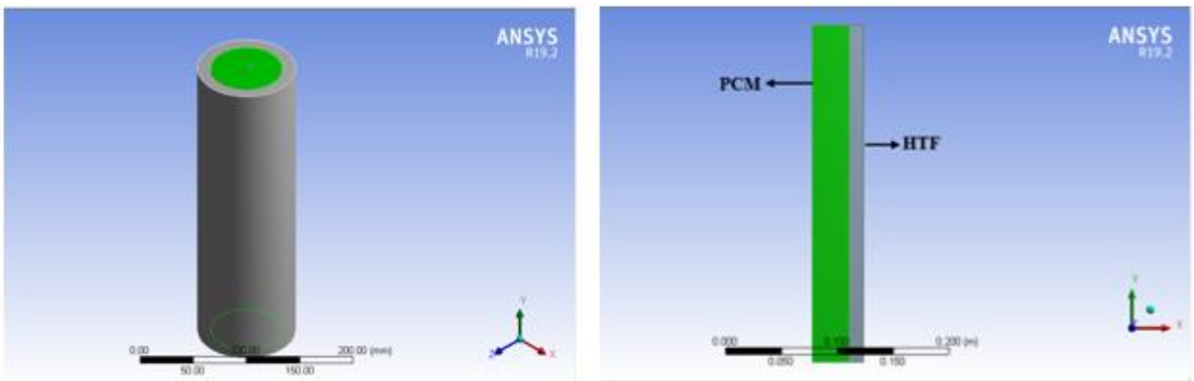

Figure 4.5: Computational domain considered for simulation

4.2.2 Grid generation

The quality of the mesh is critical when solving a numerical solution since it significantly influences the precision and security of the calculations. As a result, a deeper examination was performed to ensure adequate mesh quality. First, the skewness of the entire geometry mesh was checked to ensure that it was near zero. Examining the mesh's orthogonal quality, which should be near 1 is also critical. In our situation, mesh cell size is critical since there is a phase shift from solid to liquid or vice versa during the simulation, resulting in a severe gradient locally. After all of these parameters were considered and applied, the total number of mesh nodes and elements were discovered to be 56494 and 55800, respectively. Figure 4.6 depicts the mesh geometry.

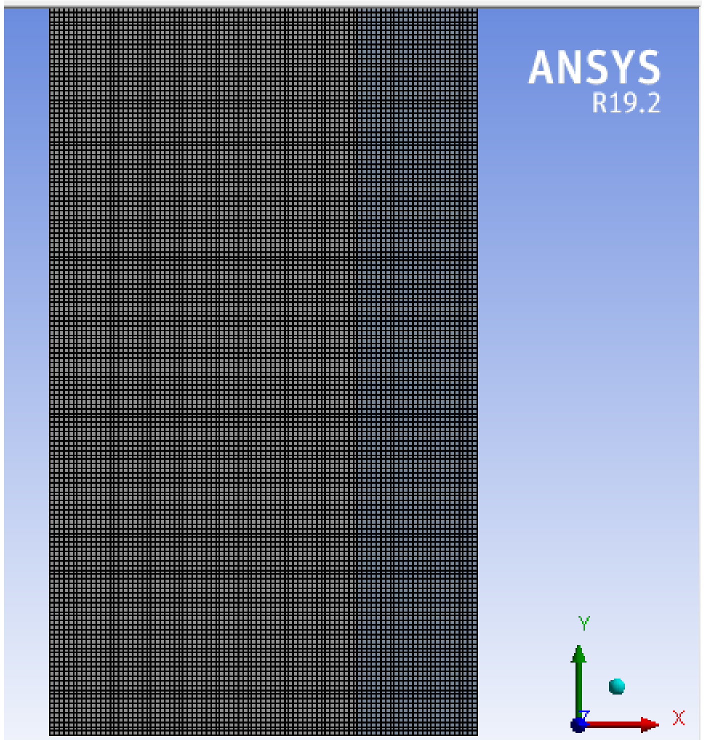

Figure 4.6: 2D axisymmetric mesh geometry

4.3 Mathematical modeling

As indicated in Figure 4.4, two distinct zones are specified to apply the necessary models to simulate the HTF and PCM. Furthermore, when a liquid phase occurs in the PCM, the so-called Boussinesq approximation is used to approximate natural convection. In the governing equations, density is treated as a constant number, except in one of the components of the momentum equation, where density(ρ) fluctuates with temperature and is estimated using a thermal expansion coefficient(β), provided (Fornarelli et al., 2016):

$$\rho = \rho_o(1 - \beta \Delta T)$$

Where ΔT is the difference between the actual temperature and reference temperatureT_o, at which the reference density, ρ_o is measured.

4.3.1 Assumptions employed:

- ✓ The melting process is represented mathematically using the enthalpy-porosity method.
- ✓ The liquid PCM flow was modeled as a laminar, incompressible Newtonian fluid.
- ✓ Molten PCM has been defined as a Newtonian and Boussinesq fluid.
- ✓ Except for the density, which was estimated using the Boussinesq approximation to account for buoyancy effects, the PCM was assumed to have phase-wise constant thermophysical characteristics.
- ✓ Initially, the HTF and PCM temperatures in the storage tank are said to be uniform.
- ✓ Radiant heat transport is disregarded.
- ✓ Because the tank is entirely insulated, there is no heat leakage from the tank surface to the surrounding environment.
- ✓ The fluctuation in the liquid fraction was thought to be linear with temperature.
- ✓ The heat-transfer fluid is incompressible and is referred to as a Newtonian fluid.

4.3.2 Governing equation

Finite difference, finite element, and finite volume methodologies are available for solving mathematical models (Soibam, 2017). Because the CFD simulation is done with FLUENT 19.2, the finite volume technique is the most applicable for the current case study. FLUENT offers the Solidification and Melting model, which is based on the enthalpy approach and is extensively used in the analysis of phase transition problems.

Furthermore, the liquid-solid front is not explicitly monitored in this model; instead, it employs an enthalpy-porosity formulation that treats the solidified zone as a porous medium. Based on the enthalpy balance, the porosity in that element is set equal to the liquid fraction in this formulation, and the liquid fraction is determined for each iteration. The mushy zone is defined as the region where the liquid percentage is between 0 and 1. As a result, when a material is solidified in an element, its porosity is zero. The finite volume approach is used in CFD modeling to solve the common continuity, momentum, and energy equations in specific domains. These equations are known as the Navier-Stokes equations, and they are presented in Equations 4-1 – 4-10.

Continuity Equation:

$$\frac{\partial \rho}{\partial t} + \frac{1}{r}\frac{\partial}{\partial r}(\rho r v_r) + \frac{1}{r}\frac{\partial}{\partial \Theta}(\rho v_\Theta) = 0 \qquad 4\text{-}1$$

Energy Balance:

Energy balance in terms of enthalpy variations is:

$$\frac{\partial(\rho h)}{\partial t} + \frac{1}{r}\frac{\partial(\rho r v_r h)}{\partial r} + \frac{1}{r}\frac{\partial(\rho v_\Theta h)}{\partial \Theta} = \frac{k}{c_p}\left[\frac{1}{r}\frac{\partial}{\partial r}\left(r\frac{\partial h}{\partial r}\right) + \frac{1}{r^2}\frac{\partial^2 h}{\partial \Theta^2}\right] - S_h \qquad 4\text{-}2$$

Where the source term is:

$$S_h = \frac{\partial(\rho \Delta H)}{\partial t} + \frac{1}{r}\frac{\partial(\rho r v_r \Delta H)}{\partial r} + \frac{1}{r}\frac{\partial(\rho v_\Theta \Delta H)}{\partial \Theta} \qquad 4\text{-}3$$

In this equation, h and ΔH accounts for sensible and latent heat respectively.

On the other hand, H is the total volumetric enthalpy, which is the sum of sensible and latent heats:

$$H = h + \Delta H \qquad 4\text{-}4$$

$$H(T) = h(T) + \rho_1 g(T) L \qquad 4\text{-}5$$

And where,

$$h = \int_{T_m}^{T} \rho_k c_k dT \qquad 4\text{-}6$$

In the case of isothermal phase change, the liquid fraction g is given by:

$$g = \begin{cases} 0 & T < T_m \quad solid, \\ ]0,1[& T = T_m \quad mushy, \\ 1 & T > T_m \quad liquid \end{cases} \qquad 4\text{-}7$$

Momentum equation:

Radial momentum along (r) direction:

$$\frac{\partial(\rho v_r)}{\partial t} + \frac{1}{r}\frac{\partial(\rho r v_r)}{\partial r} + \frac{1}{r}\frac{\partial(\rho v_r r)}{\partial \Theta} = -\frac{\partial \rho}{\partial r} + \mu\left[\frac{\partial}{\partial r}\left(\frac{1}{r}\frac{\partial(r v_r)}{\partial r}\right) + \frac{1}{r^2}\frac{\partial^2 v_r}{\partial \Theta^2} + \frac{2}{r^2}\frac{\partial v_\Theta}{\partial \Theta}\right] + \rho g - s_i \qquad 4\text{-}8$$

Axial momentum along (Θ) direction:

$$\frac{\partial(\rho v_\Theta)}{\partial t} + \frac{1}{r}\frac{\partial(\rho r v_\Theta)}{\partial r} + \frac{1}{r}\frac{\partial(\rho v_\Theta)}{\partial \Theta} = -\frac{1}{r}\frac{\partial \rho}{\partial \Theta} + \mu\left[\frac{\partial}{\partial r}\left(\frac{1}{r}\frac{\partial(r v_\Theta)}{\partial r}\right) + \frac{1}{r^2}\frac{\partial^2 v_\Theta}{\partial \Theta^2} + \frac{2}{r^2}\frac{\partial v_\Theta}{\partial \Theta}\right] - \rho g - s_i \qquad 4\text{-}9$$

Where the source term in the momentum equation is defined as;

$$s_i = \frac{(1-g)^2}{g^3 + \varepsilon} c v_i \qquad \text{4-10}$$

Where g is the liquid portion of the melted PCM. To avoid division by zero, 0.001(ε) is added to the denominator (Voller & Prakash, 1987). The mushy zone characteristics c quantify the steepness of achieving zero velocity during solidification. For most modeling applications, values between 10^4 and 10^7 are recommended (Joybari et al., 2017),(Al-abidi et al., 2013); hence, 10^5 Kg $m^{-3}s^{-1}$ was used in this work.

4.3.3 Computational methodology

To model the procedure, ANSYS Workbench was used in a step-by-step fashion. First, the 2D axisymmetric half of the simplified model was drawn in the Design Modeler environment, as illustrated in Figure 4.5. The mesh was then created via ANSYS Meshing. The simulation was then built up in the ANSYS Fluent environment. Because it is the only choice in the program for solving melting/solidification processes, a pressure-based solver was utilized to solve the equations. The semi-implicit pressure-linked equation (SIMPLE) approach was employed for pressure-velocity coupling. The PRESTO (pressure staggering option) and QUICK systems were used for spatial discretization of pressure and momentum, respectively. To enable FLUENT to distinguish the two distinct fluid materials employed in the HTF and PCM domains, the simulation was conducted with the settings provided in Table 4.3. In addition, the Standard technique was used for pressure interpolation at the cell faces. Under relaxation values of 0.7, 0.3, and 0.9 were evaluated for the momentum, pressure, and liquid fraction, respectively, to increase convergence stability. For the continuity, momentum (x and y velocities), and energy equations, respectively, convergence residual values of 10^6 10^6 and 10^8 were set.

Table 4.3: Fluent simulation setup

Description	Type
Solver	Pressure based
Velocity formulation	Absolute
Time	Transient
Gravity	On
Energy	On
viscous	Laminar /K-epsilon model
Solidification and melting	On

4.3.4 Initial and boundary conditions

The entire system is initially at ambient temperature (Ta = 296 K), and the charging mode begins at t = 0 s by supplying a continuous power of 4500 W to the heat transfer fluid as the heat flux wall boundary. During the charging phase, the system is referred to as adiabatic. Figure 4.7 shows the boundary conditions properly.

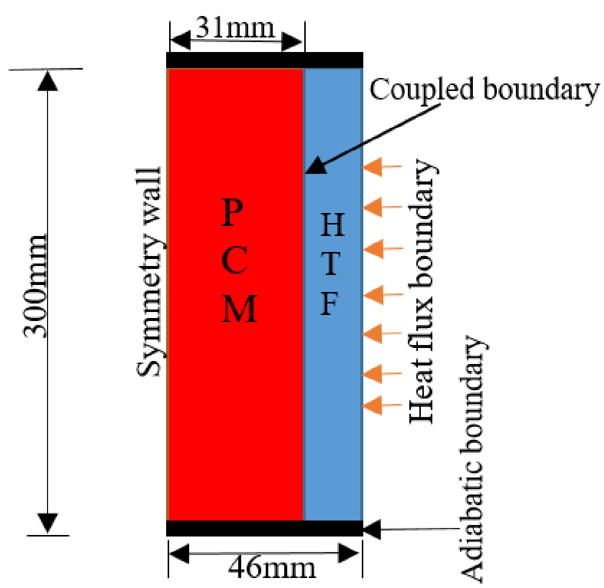

Figure 4.7: Charging boundary condition

It was assumed that PCM was melted in the solidification case; this was accomplished by patching the temperature of PCM based on the temperature obtained during the melting case

(300^oC). Furthermore, the heat transfer fluid is patched in the same manner as PCM. However, in this scenario, heat is lost from the top section of the storage (where the stored heat is needed for cooking) through convection. The adiabatic boundary condition specified during system charging stays unchanged, however, the top section is assumed to have the following boundary conditions:

Neglecting the thickness of storage cover heat transfer from storage (heated oil in vertical cylindrical) to the ambient takes place using a convection heat transfer coefficient as follows:

$$h_c = \frac{Nu\, k}{L} \qquad 4\text{-}11$$

Where,

h_c = Convection heat transfer coefficient (W/m^2 K),

Nu = Nusselt number,

k = thermal conductivity of the fluid (W/m K), and

L = characteristic length (m).

Considering characteristic length is the length of the cylinder the thermal property is evaluated at the film temperature from Appendix A1:

$$T = \frac{23 + 300}{2} = 161.5\ °C$$

$$\beta = \frac{1}{T(K)} = 0.0008$$

$$K = 0.123$$

$$\gamma = 2.85\ X\ 10^{-6}\ {m^2}/{s}$$

$$P_r = 29$$

$$g = 9.81\ {m}/{s^2}$$

The dimensionless numbers are:

$$G_r = \frac{g\beta L^3 \Delta T}{\gamma^2} = \frac{9.81 * 0.0008 * 0.3^2 * (300 - 23)}{(2.85 * 10^{-6})^2} = 7.226 * 10^9$$

$$R_a = G_r * P_r = 7.226 * 10^9 * 29 = 209{,}561{,}165{,}650.96$$

$$R_a = 2.09 * 10^{11}$$

$$Nu = 0.1 {R_a}^{1/3}, \quad 10^9 < R_a < 10^{13}$$

$$Nu = 593.9778$$

$$h_c = \frac{593.9778 * 0.123}{0.3} = 244 \; {}^{W}\!/_{m^2K}$$

4.4 Grid independency test

Grid independence analysis is performed to discover the appropriate grid size with the best solution and the least amount of computing work. A mesh independence analysis was performed at a period of 8000 seconds using four different grid sizes. The model's meshing is accomplished through the use of multi-zone approaches. The initial system temperature, boundary conditions, and time step sizes are all fixed in all four scenarios studied. Table 4.5 and Figure 4.8 show the average surface vertex value temperature for the position inside PCM generated from the numerical model for the four distinct grids. In addition, Table 4.4 shows the outline of all the parameters considered for the grid independency test.

Table 4.4: Outlines of all parameters considered for grid independency test

Outline of All Parameters

	A	B	C	D
1	ID	Parameter Name	Value	Unit
2	Input Parameters			
3	new charging (A1)			
4	P4	Mesh Element Size	1	mm
*	New input parameter	New name	New expression	
6	Output Parameters			
7	new charging (A1)			
8	P2	Mesh Nodes	14448	
9	P3	Mesh Elements	14100	
10	P5	temp pcm	435.93	K

Table 4.5: Grid independency test

Table of Design Points

	A	B	C	D	E
1	Name	P4 - Mesh Element Size	P2 - Mesh Nodes	P3 - Mesh Elements	P5 - temp pcm
2	Units	mm			K
3	DP 0 (Current)	1	14448	14100	435.93
4	DP 1	0.75	25664	25200	490.55
5	DP 2	0.5	56494	55800	489.96
6	DP 3	0.375	1.0013E+05	99200	492.39

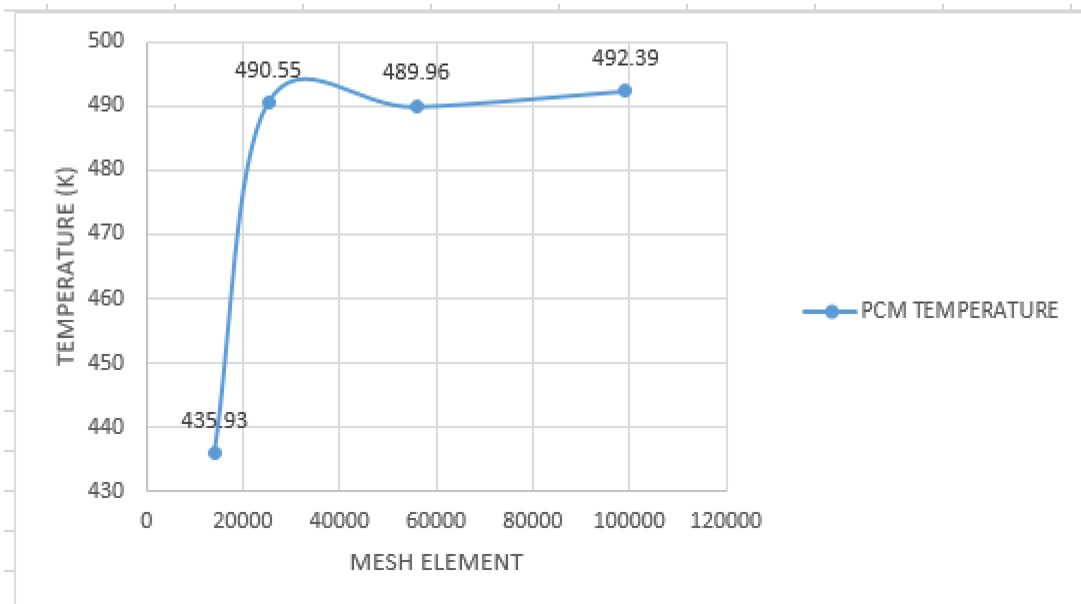

Figure 4.8: Graphical representation of grid independency test

4.5 Model validation

The charging and discharging behavior of a PCM and HTF is explored in this work; hence, the results were compared with experimental data from previous studies to verify the model. Charging model validation was performed using experimental data from (Bhave & Thakare, 2018).

4.5.1 Charging process

The charging process of thermal storage is validated by modeling it with magnesium chloride hexahydrate (MgCl26H2O) phase change material and Taurus Therm 500 heat transfer fluid.

The thermal storage consisted of 21 tubes, each holding 0.48 kilogram PCM (10 cm in length and 1.6 cm in diameter) and 660 ml of heat transfer fluid. When it comes to validation, several researchers have reported on the various strategies used to match observed data to model-calculated values, yet practically all of the offered methods have shortcomings. It is strongly advised to employ a combination of multiple procedures rather than a single strategy (Commeh et al., 2022). In this work, for example, a graphical technique and percentage error are used to validate the model. Figure 4.9 depicts a comparison of numerical and experimental average temperature values for the PCM and HTF, with the result indicating a percentage error of 8% for the HTF and 7% for the PCM. Hence there is an acceptable agreement with experimental data the model can be used to numerically study the charging simulation of the institutional thermal storage-based cook stove.

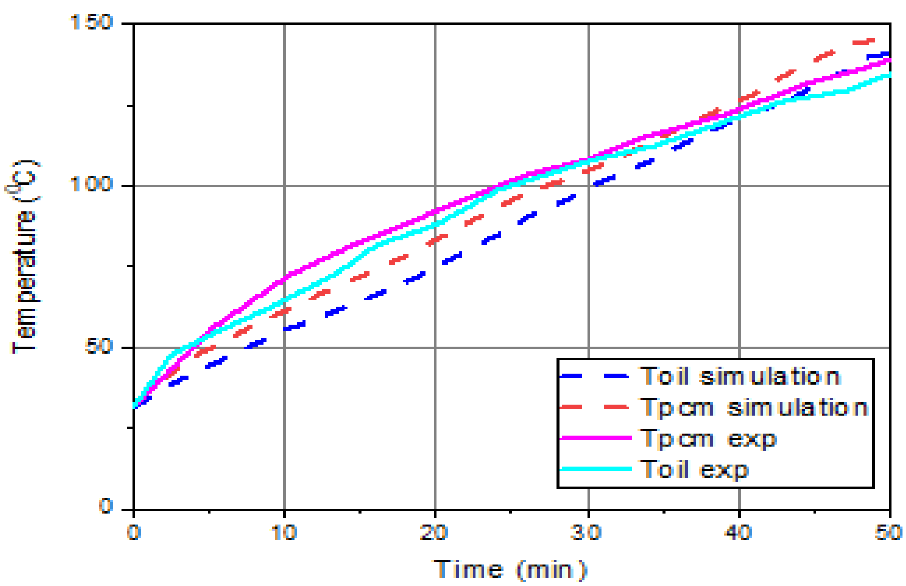

Figure 4.9: Comparison of the numerical and experimental results

CHAPTER 5: RESULTS AND DISCUSSION

5.1 Charging Conditions

Using a constant PV output of 4500W, the time-dependent variability in temperatures inside the PCM thermal storage was examined. This section also covers PCM's molten fraction as well as performance analysis. The following findings show the temperature variations and melt fractions beneath the storage. Storage temperature (PCM) rose to the point where the solid PCM began to melt and maintain constant temperature phase change. When the PCM completely melts, the temperature of the liquefied zone rises. Following the charging for 3.889 hours, all PCM capsules in storage are liquefied. Figure 5.1 and Figure 5.2 shows the temperature distribution inside PCM, the phase transition or liquid fraction fluctuation of PCM total volume while charging respectively.

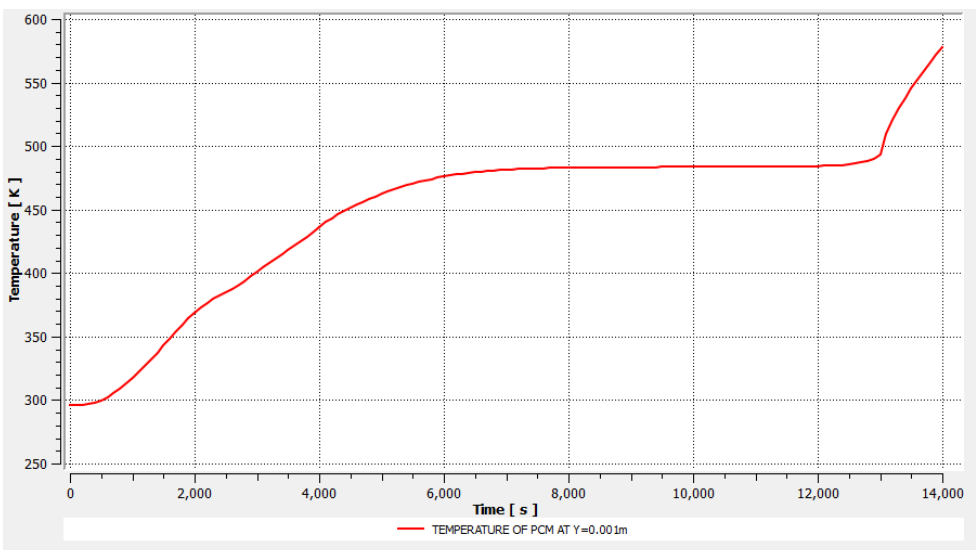

Figure 5.1: PCM temperature fluctuation while charging for 3.889 hours.

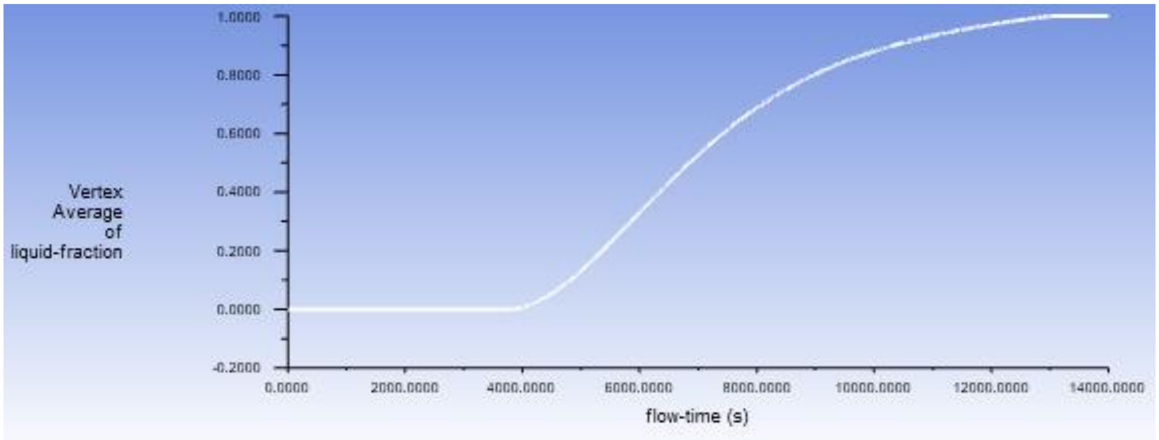

Figure 5.2: PCM melt percentage against charging time

On the other hand, the temperature fluctuation of HTF and PCM inside thermal storage tank, the liquid fraction at different points during charging inside PCM and the molten fraction contours of charging process are depicted in Figures 5.3, 5.4, 5.5 and 5.6 respectively.

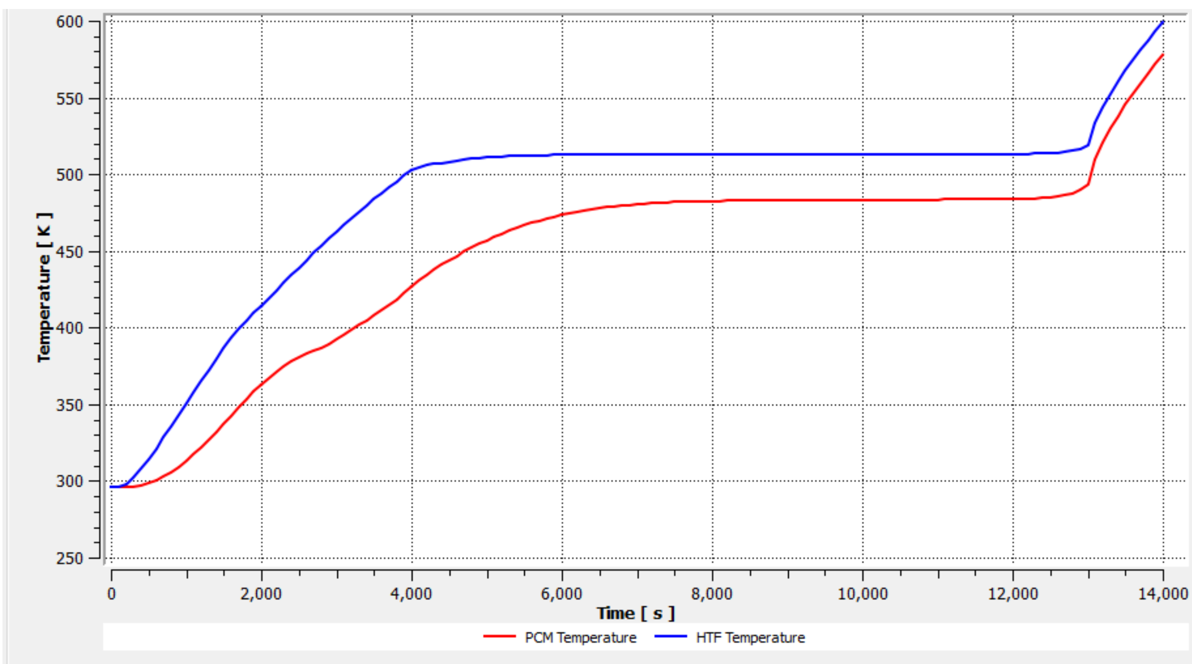

Figure 5.3: Temperature variation of HTF and PCM during charging for 3.889 hours

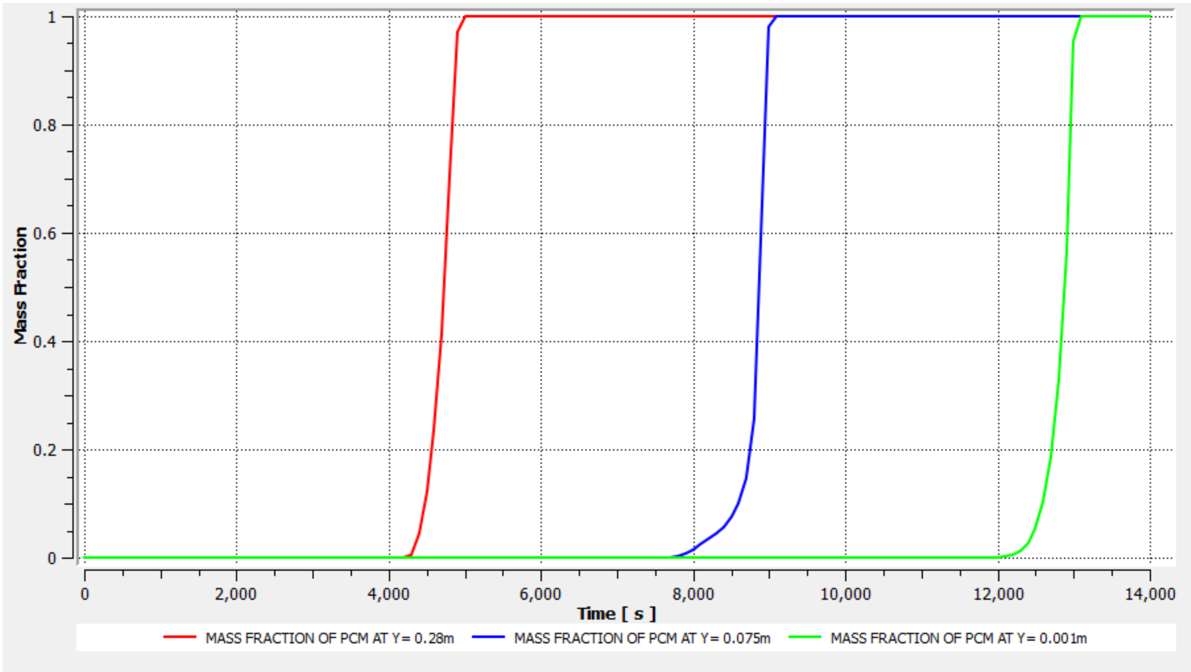

Figure 5.4: The mass fraction at various point inside PCM during charging

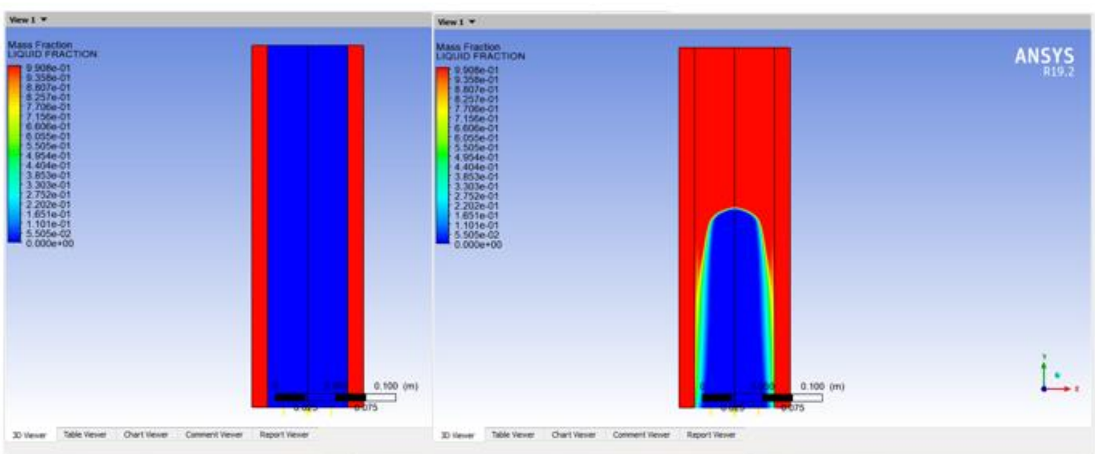

Figure 5.5: Mass fraction contour of PCM at 3600s and 7200s respectively

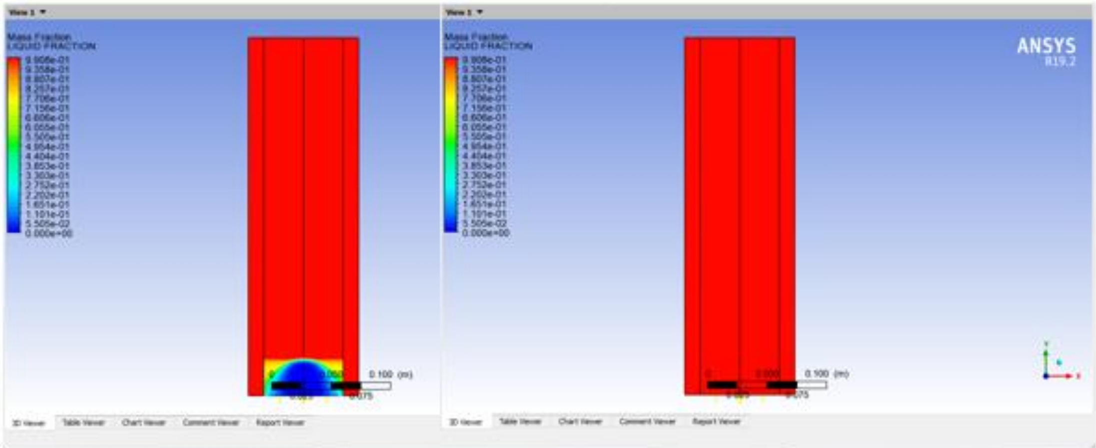

Figure 5.6: Mass fraction contour of PCM at 10800s and 14000s respectively

5.2 Discharging condition

Since the PCM capsules are fully immersed inside the HTF, during discharging the PCM will release its stored heat to the heat transfer medium by coupled boundary condition integrated inside ANSYS fluent solver. Following that neglecting the thickness of storage cover heat transfer from storage to the ambient takes place using a convection heat transfer coefficient of 244 (W/m^{2}K) and a free stream temperature of 373K. Figure 5.7 depicts the thermal storage (PCM) temperature fluctuation over time while discharging. Figure 5.8 displays the solidification of the entire volume of PCM by melt fraction.

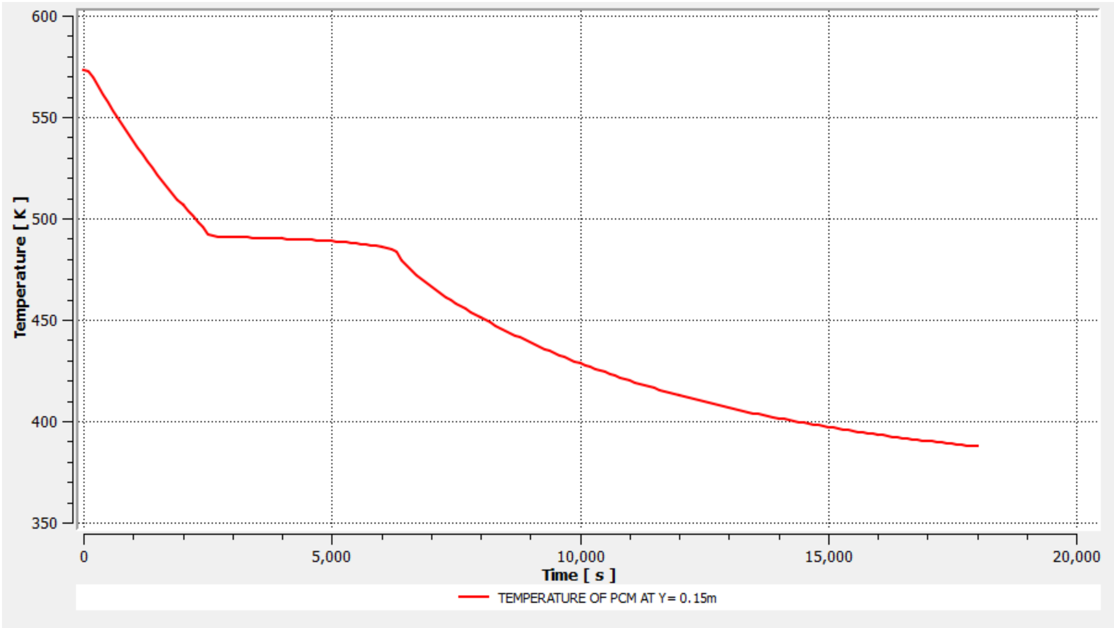

Figure 5.7: Temperature variation of PCM at y = 0.15m during discharging for 5 hours.

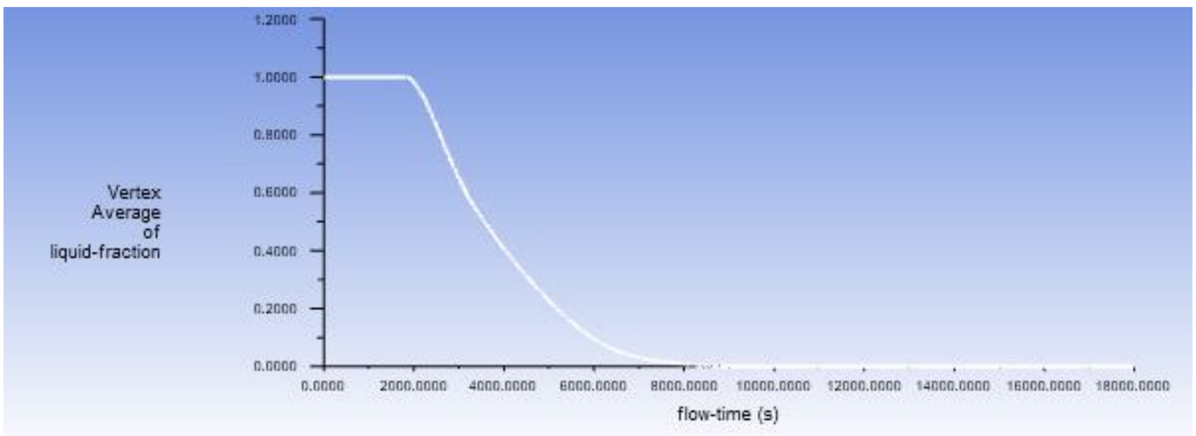

Figure 5.8: The volume of PCM that has melted over time while being discharged

The temperature of HTF and PCM at y=0.25m inside thermal storage tank, the liquid fraction at different points during discharging and discharging molten fraction counters are depicted in consecutive Figures 5.9, 5.10, and 5.11. Furthermore, 5.12 demonstrate the temperature fluctuation of PCM at different heights of storage during discharge.

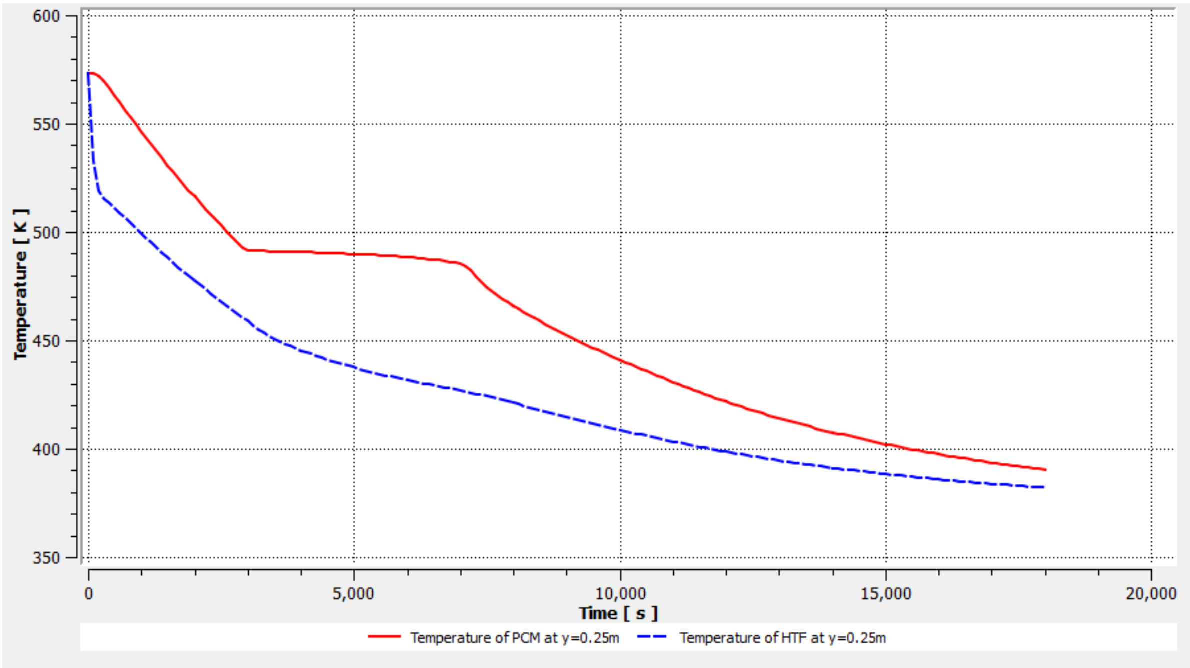

Figure 5.9: Temperature variation of HTF and PCM at y=0.25m during discharging.

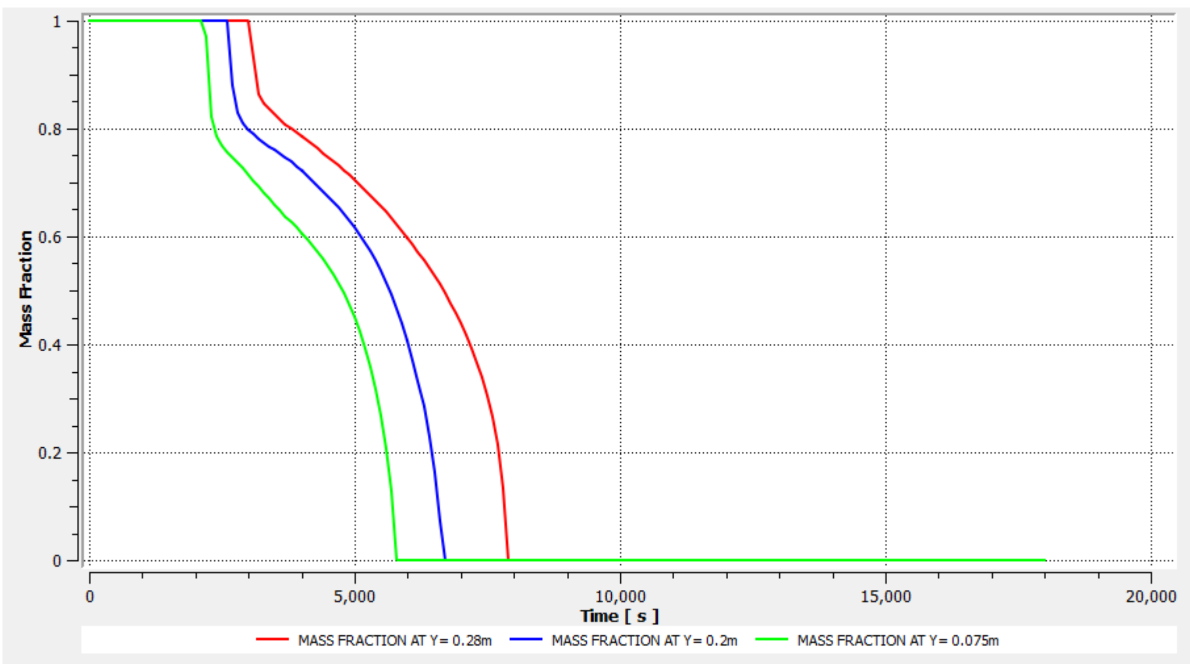

Figure 5.10: The mass fraction at various point inside PCM during discharging

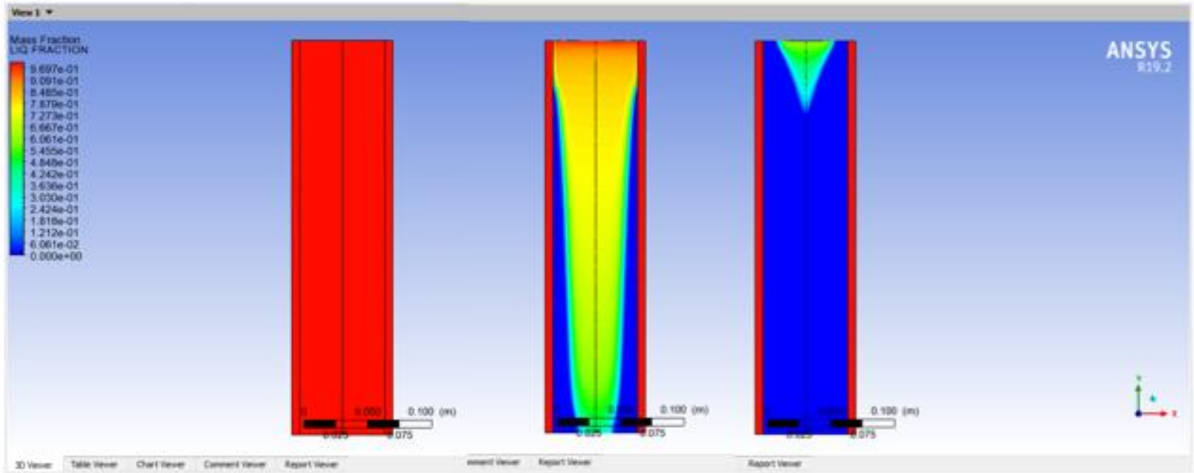

Figure 5.11: Mass fraction contour of PCM discharging at 0s, 3600s and 7200s

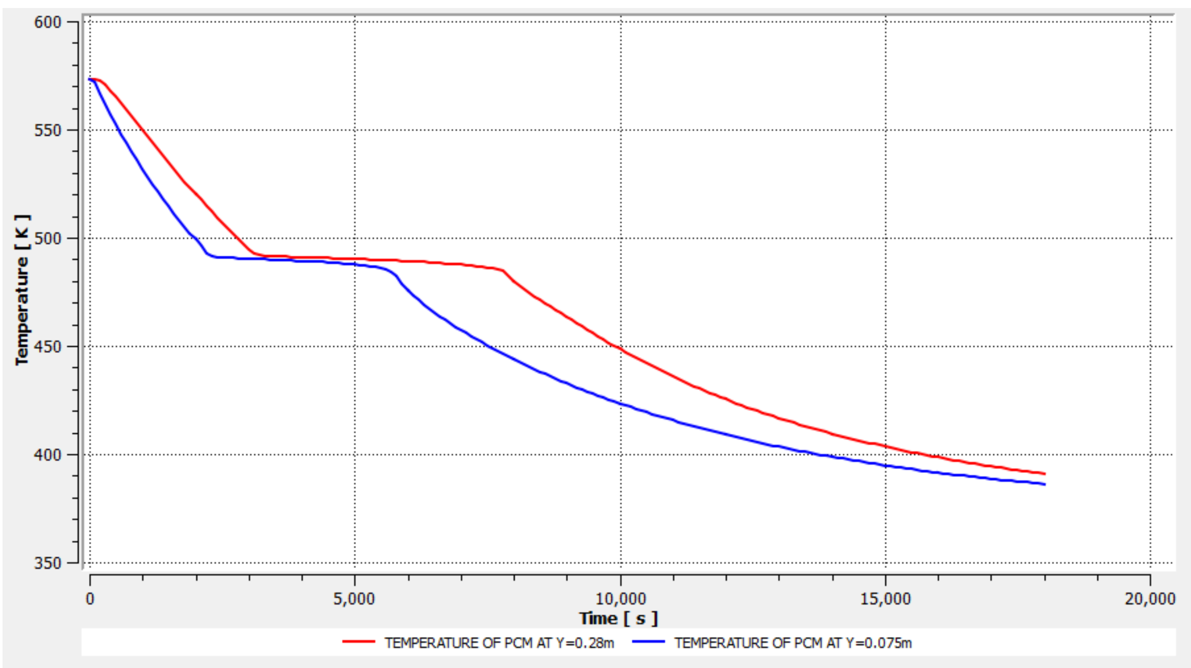

Figure 5.12: Temperature fluctuation of PCM at various storage heights during discharge.

5.3 Energy balance and efficiency

The simulation results are used to calculate energy balance and efficiency as follows:

5.3.1 Energy balance

Oil, PCM and ambient temperatures considered at the start were:

$$T_{oil} = T_{PCM} = T_{ambient} = 23°C$$

$$m_{PCM} = 60\ kg$$

$$m_{HTF} = 35.303\ kg$$

Since the theoretical output energy of the system is calculated according to Equation 3-13 which is:

$$E_{th} = 20.7911 KWh = 74847.96\ KJ$$

The amount of energy stored in the thermal storage while charging is estimated using simulated temperature data of the PCM and HTF, as shown in Equation 3-4.

Total stored energy:

$$Q_{stored} = m_{oil} C_{p\ oil} \left(T_{oil\ f} - T_{oil\ i} \right) + m_{PCM} C_{p\ PCM} (T_{PCM\ F} - T_{PCM\ I}) + m_{PCM} H_L$$

$$Q_{stored,oil} = 35.303 * 1.8928 * 277 = 18509.58\ KJ$$

$$Q_{stored,PCM} = 60 * 0.75(109 - 23) + 60 * 4.2(120 - 110) + 60 * 1.4(209 - 121) + 60 * 12(220 - 210) + 60 * 108.67 + 60 * 1.6(300 - 221) = 35086\ KJ$$

$$Q_{stored} = Q_{stored,oil} + Q_{stored,PCM} = 53595.58 KJ$$

Useful stored energy for cooking is calculated by using heat stored above 92 °C, assuming that stored heat below the 92 °C is not sufficient for boiling. As a result, Q_{US} >92 °C is obtained by;

$$(Q_{Stored}) > 92°C = 35.303 * 1.8928 * 208 + 60 * 0.75(109 - 92) + 60 * 4.2(120 - 110) + 60 * 1.4(209 - 121) + 60 * 12(220 - 210) + 60 * 108.67 + 60 * 1.6(300 - 221) = 45880.075\ KJ$$

The energy needed to boil 90 liters of water Q_{US-req} is approximated as the rise in sensible heat of the water to the highest temperature achieved during boiling, increased by 10% evaporation losses.

$$Q_{US-req} = m_w C_{pW}(92 - T_a) + 0.1 m_W H_{fg\,W} = 46MJ \qquad 5\text{-}1$$

5.3.2 Efficiency

$$\eta_{overall} = \frac{Q_{US-req}}{E_{th}} = 0.6146 = 61.46\%$$

$$\eta_{charging} = \frac{Q_{stored}}{E_{th}} = 0.7161 = 71.61\%$$

$$\eta_{storage} = \frac{(Q_{Stored}) > 92°\mathrm{C}}{E_{th}} = 0.6129 = 61.29\%$$

Energy usage efficiency of stored energy over 92 °C (discharging efficiency), for cooking:

$$\eta_{uti>92°\mathrm{C}} = \frac{(Q_{Stored}) > 92°\mathrm{C}}{Q_{stored}} = 0.8560 = 85.6\%$$

The total boiling time of 90 l water for one cycle obtained from simulation result is 300 min (18000sec). Therefore, the useful power is

46000kJ/18000seconds = 2.5556 KW= 2555Watts

5.4 Comparison with other research

The performance of institutional biomass (wood) flat-bottom cookstoves was studied by (Commeh et al., 2022). Their analysis of the water temperature results revealed that the efficiency of the stove was 47.4%, and they suggested that adopting the recommended Stove might also improve the ecology of the earth and the health of its inhabitants by reducing the consumption of wood fuel for cooking and carbon emissions. However, in our situation, the proposed model's efficiency is 61% and is also ecologically healthy, making it a preferable option for replacing biomass stoves.

Desisa et al. (2016) Conducted an extensive study of a 200-liter institutional cook stove, including design, modeling, and field testing. The water boiling test was used for the new stove, and parametric calculations were performed using WBT (Water Boiling Test) version 4.2.2. The average fuel consumption (wet) was 12.63 kg for 200 liters of water, and the average thermal efficiency was 47%. However, the complete combustion of 1 kilogram of wood creates 2 kg of CO_2 (Sekhon & Sethi, 2019); hence, by conserving 12.63 kg of wood combustion for one cycle of cooking, 25.26 kg of CO_2 emissions into the environment may be avoided by employing green energy-based cookstoves. As a result, the suggested community solar cooker is attractive in terms of GHG emissions and system efficiency.

Several biomass cooker designs have been presented in the past. The development goal has been to enhance energy efficiency and lower the fuel used in cooking systems. Conventional cooking techniques have thermal efficiencies ranging from 5 to 20% (Commeh et al., 2022). When compared to the three-stone open-fire method, the enhanced biomass cookstoves developed by GIZ save 50%, 53%, and more than 50% of the fuel. As with replacing three-stone open fires with upgraded cookstoves, replacing these stoves with solar-powered clean stoves would favor cost savings, environmental advantages, and energy efficiency.

CHAPTER 6: CONCLUSION AND RECOMMENDATION

6.1 Conclusion

For intermittent behavior of the solar radiation thermal energy storage is an excellent option. In developing nations such as Ethiopia, where biomass accounts for 89% of the total final energy supply, massive volumes of greenhouse gas emissions and deforestation occur.

The viability of a solar-powered institutional cook stove with heat storage employing shell thermia B as the heat transfer media and PCM (solar salt) for institutional cooking has been proven satisfactorily. The thermal storage model illustrates the effective analysis of both latent and sensible thermal storage combined with photovoltaic systems. The performance of the thermal storage was evaluated using constant heat flux. The proposed storage numerical model for charging was validated against experimental work by (Bhave & Thakare, 2018) and the results were found to be compatible.

A performance study was carried out based on the simulation findings. The thermal storage can hold $53595.58KJ$ of energy, and the total cooking, charging, and discharging efficiencies were 61.46%, 71.61%, and 85.6%, respectively.

In this study, the energy demand for one cycle boiling of water at the institutional level is considered for simplicity which almost is the closer temperature required to cook most of Ethiopian meals according to Yishak (2019), and Alemu (2020). However, the system permits uniform heat transfer to roasting, baking, and frying cooking types performed at temperatures ranges from 150 to 190 °C (Bhave & Kale, 2020) in addition to the boiling type cooking which requires heat stored above 100 °C (Bhave & Thakare, 2018).

6.2 Recommendation

For intermittent behavior of the solar radiation thermal energy storage appears to be an excellent option and is also employed in indoor cooking applications. This study creates a numerical model and thermal storage performance analysis coupled with a solar photovoltaic system for institutional level cooking. It is advised that the simulation be supplemented with experiments as well as the efficiencies be evaluated under actual sunshine conditions.

The photovoltaic system is sized for the lowest sun radiation month, resulting in lower output power; nevertheless, the PV system may produce more electricity during the peak solar radiation months. For this, I propose including extra storage, such as batteries, in the system so that the excess power generated by the PV system may be used for other appliances.

The quantity of energy required to boil 90 liters of water is evaluated in this study since the majority of the time the performance test is done by a water boiling test. However, I propose expanding the application area to include additional sorts of meals. Finally, I advocate conducting a cost analysis of the system with its payback period to provide institutions with a more accurate feasibility of the system is much more attractive.

Furthermore in this study the thermal performance capability of PCM storage for institutional cooking is performed. However I recommend the comparison of the thermal storage system with systems without storage and again performance compassion with other existing institutional cooking technologies will accurately show the feasibility of the system.

REFERENCES

Abreha, B. G., Mahanta, P., & Trivedi, G. (2019). Numerical modeling and simulation of thermal energy storage for solar cooking using Comsol multiphysics software. *AIP Conference Proceedings, 2091*(April).

Adhikaria, P., Adhikaria, A., Dhitala, S. K., Shrestha, B., & Durab, H. B. (2020). Design and performance analysis of institutional cooking stove for high hill rural community of Nepal. *Kathmandu University Journal of Science, Engineering and Technology, 14*(1).

Agarwal, N., Kumar, A., & Varun. (2013). Optimization of grid independent hybrid PV–diesel–battery system for power generation in remote villages of Uttar Pradesh, India. *Energy for Sustainable Development, 17*(3), 210-219. doi: 10.1016/j.esd.2013.02.002

Aggarwal, R. (2020). Institution based solar steam cooking systems in India. *Current World Environment, 15*(2), 204.

Agyenim, F., Hewitt, N., Eames, P., & Smyth, M. (2010). A review of materials, heat transfer and phase change problem formulation for latent heat thermal energy storage systems (LHTESS). *Renewable and Sustainable Energy Reviews, 14*(2), 615-628.

Al-abidi, A. A., Bin Mat, S., Sopian, K., Sulaiman, M. Y., & Mohammed, A. T. (2013). CFD applications for latent heat thermal energy storage: a review. *Renewable and Sustainable Energy Reviews, 20*, 353-363. doi: 10.1016/j.rser.2012.11.079

Alemu, M. (2020). *Design and cfd analysis of thermal energy storage using pcm for cooking application.* (Degree of Master of Science in Mechanical Engineering (Thermal Engineering Stream)), Addis Ababa University.

Amagour, M. E. H., Bennajah, M., & Rachek, A. (2021). Numerical investigation and experimental validation of the thermal performance enhancement of a compact finned-tube heat exchanger for efficient latent heat thermal energy storage. *Journal of Cleaner Production, 280*, 124238. doi: 10.1016/j.jclepro.2020.124238

Aramesh, M., Ghalebani, M., Kasaeian, A., Zamani, H., Lorenzini, G., Mahian, O., & Wongwises, S. (2019). A review of recent advances in solar cooking technology. *Renewable Energy, 140*, 419-435. doi: 10.1016/j.renene.2019.03.021

Ayugi, G., Banda, E., & D'Ujanga, F. (2011). Local thermal insulating materials for thermal energy storage. *Rwanda Journal, 23*.

Badran, A. A., Yousef, I. A., Joudeh, N. K., Hamad, R. A., Halawa, H., & Hassouneh, H. K. (2010). Portable solar cooker and water heater. *Energy Conversion and Management, 51*(8), 1605-1609. doi: 10.1016/j.enconman.2009.09.038

Bellan, gonzalez, Romero, Rahman, goswami, stefanakos, & couling. (2014). numerical analysis of charging and discharging performance of a thermal energy storage system with encapsulated phase change material. doi: 10.1016/j.applthermaleng.2014.07.009

Bellan, S., Alam, T. E., González-Aguilar, J., Romero, M., Rahman, M. M., Goswami, D. Y., & Stefanakos, E. K. (2015). Numerical and experimental studies on heat transfer characteristics of thermal energy storage system packed with molten salt PCM capsules. *Applied Thermal Engineering, 90*, 970-979. doi: 10.1016/j.applthermaleng.2015.07.056

Benoit, H., Spreafico, L., Gauthier, D., & Flamant, G. (2016). Review of heat transfer fluids in tube-receivers used in concentrating solar thermal systems: Properties and heat transfer coefficients. *Renewable and Sustainable Energy Reviews, 55*, 298-315. doi: 10.1016/j.rser.2015.10.059

Bhattacharya, S., Siddique, A. M. M., Leon, M. A., Pham, H., & Mahandari, C. (1998). A study on improved institutional biomass stoves. *A report of the renewable energy technologies in Asia: RET's in Asia. Energy program, Asian Technology of Technology, Bangkok*.

Bhave, A. G., & Kale, C. K. (2020). Development of a thermal storage type solar cooker for high temperature cooking using solar salt. *Solar Energy Materials and Solar Cells, 208*, 110394. doi: 10.1016/j.solmat.2020.110394

Bhave, A. G., & Thakare, K. A. (2018). Development of a solar thermal storage cum cooking device using salt hydrate. *Solar Energy, 171*, 784-789. doi: 10.1016/j.solener.2018.07.018

Biadgelegn, M. (2018). *DESIGN AND EXPERIMENTAL INVESTIGATION OF SOLAR COOKER WITH THERMAL ENERGY STORAGE.* (Mastres degree), Addis Ababa.

Blaney, J. J., Neti, S., Misiolek, W. Z., & Oztekin, A. (2013). Containment capsule stresses for encapsulated phase change materials. *Applied Thermal Engineering, 50*(1), 555-561. doi: 10.1016/j.applthermaleng.2012.07.014

Bruce, J. (2021). Solar Panel Sizing – How To Calculate Home Solar System Size. *Solar Energy Website - DIY Solar Projects*.

Buddhi, D., Sharma, S. D., & Sharma, A. (2003). Thermal performance evaluation of a latent heat storage unit for late evening cooking in a solar cooker having three reflectors.

Chandrasekaran, P., Cheralathan, M., & Velraj, R. (2015). Influence of the size of spherical capsule on solidification characteristics of DI (deionized water) water for a cool thermal energy storage system – An experimental study. *Energy, 90*, 807-813. doi: 10.1016/j.energy.2015.07.113

Commeh, M. K., Agyei-Agyemang, A., Tawiah, P. O., & Asaaga, B. A. (2022). CFD analysis of a flat bottom institutional cookstove. *Scientific African, 16*, e01117.

Commeh, M. K., Einzinger, F., Heijndermans, E., Tabi, R., Agyei-Agyemang, A., & Kwarteng, E. (2017). Improved Institutional Cookstoves: An Assessment of the Efficiency in its Application in the agro and food processing industry in Ghana.

Craig, O. O., & Dobson, R. T. (2015). <Stand-Alone CSP Parabolic Solar Cookers...l Industrialisation in Southern Africa.pdf>.

Cuce, E., & Cuce, P. M. (2013). A comprehensive review on solar cookers. *Applied Energy, 102*, 1399-1421. doi: 10.1016/j.apenergy.2012.09.002

Deshmukh, G., Birwal, P., Datir, R., & Patel, S. (2017). Thermal Insulation Materials: A Tool for Energy Conservation. *Journal of Food Processing & Technology, 08*(04). doi: 10.4172/2157-7110.1000670

Desisa, D. G., Venkata Ramayya, A., & Tiba, G. S. (2016). PRODUCT DEVELOPMENT THROUGH CFD SIMULATION AND EXPERIMENTAL TESTING OF A 200 LITER BIOMASS FIRED INSTITUTIONAL COOK STOVE.

Domanski, el-sebaii, a. a., & jaworski, m. (1995). Cooking during off-sunshine hours using pcms as storage media. *20*(7).

Du, K., Calautit, J., Wang, Z., Wu, Y., & Liu, H. (2018). A review of the applications of phase change materials in cooling, heating and power generation in different temperature ranges. *Applied Energy, 220*, 242-273. doi: 10.1016/j.apenergy.2018.03.005

Ehms, J. N., Oliveski, R. D. C., Rocha, L. O., & Biserni, C. (2018). Theoretical and numerical analysis on phase change materials (PCM): A case study of the solidification process of erythritol in spheres. *International Journal of Heat and Mass Transfer, 119*, 523-532.

El Shenawy, E., Hegazy, A., & Abdellatef, M. (2017). Design and optimization of stand-alone PV system for Egyptian rural communities. *International Journal of Applied Engineering Research, 12*(20), 10433-10446.

Elias, C. N., & Stathopoulos, V. N. (2019). A comprehensive review of recent advances in materials aspects of phase change materials in thermal energy storage.

Esen, M. (2004). Thermal performance of a solar cooker integrated vacuum-tube collector with heat pipes containing different refrigerants. *76*.

Fornarelli, F., Camporeale, S. M., Fortunato, B., Torresi, M., Oresta, P., Magliocchetti, L., Miliozzi, A., & Santo, G. (2016). CFD analysis of melting process in a shell-and-tube latent heat storage for concentrated solar power plants. *Applied Energy, 164*, 711-722.

Getenet, G. (2011). *HEAT TRANSFER ANALYSIS DURING THE PROCESS OF INJERA BAKING BY FINITE ELEMENT METHOD.* (masters), Addis Ababa Univeristy

Gont, S. D. (2019). Design of a standalone photovoltaic system for a typical household around Dessie City-Ethiopia. *American Journal of Electrical and Electronic Engineering, 7*(1), 1-7.

Han, G.-S., Ding, H.-S., Huang, Y., Tong, L.-G., & Ding, Y.-L. (2017). A comparative study on the performances of different shell-and-tube type latent heat thermal energy storage units including the effects of natural convection. *International Communications in Heat and Mass Transfer, 88*, 228-235.

Hararsingh, d., mco.st, l., & headley, c. (1996). A natural convecion flat plate collector solar cooker with short term storage.

HASSEN, R. (2020). *DESIGN OF SOLAR PHOTOVOLTAIC SYSTEM TO POWER AIR CONDITIONING UNIT FOR A LIGHT CITY TRAIN.* (Maters), Addis Ababa university.

Hawlader, M. N. A., Uddin, M. S., & Zhu, H. J. (2002). Encapsulated phase change materials for thermal energy storage: Experiments and simulation. *International Journal of Energy Research, 26*(2), 159-171. doi: 10.1002/er.773

Hosseini, M., Rahimi, M., & Bahrampoury, R. (2014). Experimental and computational evolution of a shell and tube heat exchanger as a PCM thermal storage system. *International Communications in Heat and Mass Transfer, 50*, 128-136.

Hu, H., & Argyropoulos, S. A. (1996). Mathematical modelling of solidification and melting: a review. *Modelling and Simulation in Materials Science and Engineering, 4*(4), 371.

Huang, Y., Han, Q., & Liu, X. (2021). Experimental investigation on the melting and solidification performance enhancement of a fractal latent heat storage unit. *International Journal of Heat and Mass Transfer, 179*, 121640. doi: 10.1016/j.ijheatmasstransfer.2021.121640

Hung Anh, L. D., & Pásztory, Z. (2021). An overview of factors influencing thermal conductivity of building insulation materials. *Journal of Building Engineering, 44*, 102604. doi: 10.1016/j.jobe.2021.102604

Hussein, H. M. S., El-Ghetany, H. H., & Nada, S. A. (2008). Experimental investigation of novel indirect solar cooker with indoor PCM thermal storage and cooking unit. *Energy Conversion and Management, 49*(8), 2237-2246. doi: 10.1016/j.enconman.2008.01.026

Ilkka Valovirta, J. V. (2004). Water Vapor Permeability and Thermal Conductivity as a Function of Temperature and Relative Humidity.

Indora, S., & Kandpal, T. C. (2018a). Financial Appraisal of Using Scheffler Dish for Steam Based Institutional Solar Cooking in India. *Renewable Energy*. doi: 10.1016/j

Indora, S., & Kandpal, T. C. (2018b). Institutional and community solar cooking in India using SK-23 and Scheffler solar cookers: A financial appraisal. *Renewable Energy, 120*, 501-511. doi: 10.1016/j.renene.2018.01.004

Indora, S., & Kandpal, T. C. (2018c). Institutional cooking with solar energy: A review. *Renewable and Sustainable Energy Reviews, 84*, 131-154. doi: 10.1016/j.rser.2017.12.001

Indora, S., & Kandpal, T. C. (2019a). A framework for analyzing impact of potential financial/fiscal incentives for promoting institutional solar cooking in India. *Renewable Energy, 143*, 1531-1543. doi: 10.1016/j.renene.2019.05.097

Indora, S., & Kandpal, T. C. (2019b). Solar energy for institutional cooking in India: prospects and potential. *Environment, Development and Sustainability, 22*(8), 7153-7175. doi: 10.1007/s10668-019-00471-9

Ismail, K., & Henríquez, J. (2000). Solidification of PCM inside a spherical capsule. *Energy Conversion and Management, 41*(2), 173-187.

Ismail, K. A., Lino, F. A., Da Silva, R. C., De Jesus, A. B., & Paixao, L. C. (2014). Experimentally validated two dimensional numerical model for the solidification of PCM along a horizontal long tube. *International Journal of Thermal Sciences, 75*, 184-193.

Jacob, R., & Bruno, F. (2015). Review on shell materials used in the encapsulation of phase change materials for high temperature thermal energy storage. doi: 10.1016/j.rser.2015.03.038

Jellouli, Y., Chouikh, R., Guizani, A., & Belghith, A. (2007). Numerical study of the moving boundary problem during melting process in a rectangular cavity heated from below. *American Journal of Applied Sciences, 4*(4), 251-256.

Joybari, M. M., Haghighat, F., & Seddegh, S. (2017). Numerical investigation of a triplex tube heat exchanger with phase change material: Simultaneous charging and discharging. *Energy and buildings, 139*, 426-438.

Kajumba, P. K., Okello, D., Nyeinga, K., & Nydal, O. J. (2020). Experimental investigation of a cooking unit integrated with thermal energy storage system. *Journal of Energy Storage, 32*(October).

Kantole, J. B. (2012). *Modelng and Design of a Laten heat thermal storage system with reference to solar absorbation refiregeration* university of johannsburg.

Karthick, & Sivalakshmi, D. S. (2019). A review on thermal energy storage materials for solar cooking 2. *International Journal of Research and Innovation in Engineering Technology, 05*(09).

Karthikeyan, S., Ravikumar, K., Kumaresan, G., & Velraj, R. (2021). Enthalpy based mathematical modelling for thermal energy storage filled with paraffin encapsulated balls as storage material. *Materials Today: Proceedings, 45*, 6006-6010. doi: 10.1016/j.matpr.2020.09.433

kebede, D. (2020). *Computational Modeling and Performance Analysis of Solar Thermal Storage Integrated with Parabolic Solar Concentrator for Cooking Application.* (PhD), Addis Ababa.

Khan, Z., Khan, Z., & Ghafoor, A. (2016). A review of performance enhancement of PCM based latent heat storage system within the context of materials, thermal stability and compatibility. *Energy Conversion and Management, 115*, 132-158. doi: 10.1016/j.enconman.2016.02.045

Kumar Rakesh, R.S. Adhikari, H.P. Garg, & Kumar, A. (2001). Thermal performance of a solar pressure cooker based on evacuated tube solar collector

Kumar, S., Kumar, A., & Yadav, A. (2018). Experimental investigation of a solar cooker based on evacuated tube collector with phase change thermal storage unit in Indian climatic conditions.

Kumaresan, G., Santosh, R., Raju, G., & Velraj, R. (2018). Experimental and numerical investigation of solar flat plate cooking unit for domestic applications. *Energy, 157*, 436-447. doi: 10.1016/j.energy.2018.05.168

Kumaresan, G., Vigneswaran, V. S., Esakkimuthu, S., & Velraj, R. (2016). Performance assessment of a solar domestic cooking unit integrated with thermal energy storage system. *Journal of Energy Storage, 6*, 70-79. doi: 10.1016/j.est.2016.03.002

Kuravi, S., Trahan, J., Goswami, D. Y., Rahman, M. M., & Stefanakos, E. K. (2013). Thermal energy storage technologies and systems for concentrating solar power plants. *Progress in Energy and Combustion Science, 39*(4), 285-319. doi: 10.1016/j.pecs.2013.02.001

Lambert, J. G., Hall, C. A. S., Balogh, S., Gupta, A., & Arnold, M. (2014). Energy, EROI and quality of life. *Energy Policy, 64*, 153-167. doi: 10.1016/j.enpol.2013.07.001

Lentswe, K., Mawire, A., Owusu, P., & Shobo, A. (2021). A review of parabolic solar cookers with thermal energy storage. *Heliyon, 7*(10), e08226. doi: 10.1016/j.heliyon.2021.e08226

Liu, L., Su, D., Tang, Y., & Fang, G. (2016). Thermal conductivity enhancement of phase change materials for thermal energy storage: A review. *Renewable and Sustainable Energy Reviews, 62*, 305-317.

Liu, Z., Yu, Z., Yang, T., Qin, D., Li, S., Zhang, G., Haghighat, F., & Joybari, M. M. (2018). A review on macro-encapsulated phase change material for building envelope applications. *Building and Environment*, *144*, 281-294. doi: 10.1016/j.buildenv.2018.08.030

Lizaso, M. (2020). A review of cooking technology around the world and the potential of solar cooking.

Ma, Z., & Zhang, Y. (2006). Solid velocity correction schemes for a temperature transforming model for convection phase change. *International Journal of Numerical Methods for Heat & Fluid Flow, 16*(2), 204-225.

Maheswari, C. U., & Reddy, R. M. (2013). Thermal analysis of thermal energy storage systemwith phase change material. *Int J Eng Res Appl, 3*, 617-622.

Mahfuz, M., Anisur, M., Kibria, M., Saidur, R., & Metselaar, I. (2014). Performance investigation of thermal energy storage system with Phase Change Material (PCM) for solar water heating application. *International Communications in Heat and Mass Transfer, 57*, 132-139.

Malik, M. S., Iftikhar, N., Wadood, A., Khan, M. O., Asghar, M. U., Khan, S., Khurshaid, T., Kim, K.-C., Rehman, Z., & Rizvi, S. T. u. I. (2020). Design and Fabrication of Solar Thermal Energy Storage System Using Potash Alum as a PCM. *Energies*, *13*(23), 6169. doi: 10.3390/en13236169

Mawire, A. (2019). Solar cookers with thermal energy storage: A sustainable cooking solution for developing countries.

Mawire, A., Phori, A., & Taole, S. (2014). Performance comparison of thermal energy storage oils for solar cookers during charging. *73*(1).

Mekonnen, B. A., Liyew, K. W., & Tigabu, M. T. (2020). Solar cooking in Ethiopia: Experimental testing and performance evaluation of SK14 solar cooker. *Case Studies in Thermal Engineering, 22*, 100766. doi: 10.1016/j.csite.2020.100766

Milián, Y. E., Gutiérrez, A., Grágeda, M., & Ushak, S. (2017). A review on encapsulation techniques for inorganic phase change materials and the influence on their thermophysical properties. *Renewable and Sustainable Energy Reviews, 73*, 983-999. doi: 10.1016/j.rser.2017.01.159

Mol, J., Shahi, M., & Mahmoudi, A. (2020). Numerical Modeling of Thermal Storage Performance of Encapsulated PCM Particles in an Unstructured Packed Bed. *Energies, 13*(23), 6413. doi: 10.3390/en13236413

MP Westman SG Laddha, LS Fifield TA Kafentzis, & Simmons, K. (2010). natural fiber composite: a review *UNITED STATES DEPARTMENT OF ENERGY under Contract DE-AC05-76RL01830*.

Mussard, M., & Nydal, O. J. (2013). Charging of a heat storage coupled with a low-cost small-scale solar parabolic trough for cooking purposes. *Solar Energy, 95*, 144-154. doi: 10.1016/j.solener.2013.06.013

Nahar, Gupta, & Sharma. (1993). Performance and testing of an improved community size solar cooker. *34*(4).

Nahar, N. M. (2003). Performance and testing of a hot box storage solar cooker.

Nahar, N. M. (2003). Performance and testing of a hot box storage solar cooker. *44*.

Narasimhan, L. N. (2019). Assessment of latent heat thermal storage systems operating with multiple phase change materials. *Journal of Energy Storage, 23*, 442-455.

Narayan, S., & Doytch, N. (2017). An investigation of renewable and non-renewable energy consumption and economic growth nexus using industrial and residential energy consumption. *Energy Economics, 68*, 160-176. doi: 10.1016/j.eneco.2017.09.005

Nazzi Ehms, J. H., De Césaro Oliveski, R., Oliveira Rocha, L. A., Biserni, C., & Garai, M. (2019). Fixed Grid Numerical Models for Solidification and Melting of Phase Change Materials (PCMs). *Applied Sciences, 9*(20), 4334. doi: 10.3390/app9204334

Negash, D., Abegaz, A., & Smith, J. U. (2021). Environmental and financial benefits of improved cookstove technologies in the central highlands of Ethiopia. *Biomass and Bioenergy, 150*, 106089. doi: 10.1016/j.biombioe.2021.106089

Nithyanandam, pitchumani, & mathur. (2013). Analysis of a latent thermocline storage system with encapsulated phase change material for concentrating solar power doi: 10.1016/j.apenergy.2013.08.053

Nyahoro, K., Johnson, R. r., & Edwards, J. (1997). Simulated performance of thermal storage in a solar cooker *59*(96).

Pal, A. M., Das, S., & N.B.Raju. (2015). Designing of a Standalone Photovoltaic System for a Residential Building in Gurgaon, India. *Sustainable Energy, 3*. doi: 10.12691/rse-3-1-3

Panwar, N. L., Kaushik, S. C., & Kothari, S. (2012). State of the art of solar cooking: An overview. *Renewable and Sustainable Energy Reviews, 16*(6), 3776-3785. doi: 10.1016/j.rser.2012.03.026

Papadopoulos, A. M. (2005). State of the art in thermal insulation materials and aims for future developments. *Energy and buildings, 37*(1), 77-86. doi: 10.1016/j.enbuild.2004.05.006

Parrado, C., Cáceres, G., Bize, F., Bubnovich, V., Baeyens, J., Degrève, J., & Zhang, H. L. (2015). Thermo-mechanical analysis of copper-encapsulated NaNO3–KNO3. *Chemical Engineering Research and Design, 93*, 224-231. doi: 10.1016/j.cherd.2014.07.007

PEIMAR. (2022). Peimar Full Black 300 Watt, 20V 60-Cell Monocrystalline Solar Panel (SG300M-FB).

Piroschka, O. P. (2014). Warming Up to Solar Cooking – A Comparative Study on Motivations and the Adoption of Institutional Solar Cookers in Developing Countries. *Energy Procedia, 57*, 1632-1641. doi: 10.1016/j.egypro.2014.10.154

Punniakodi, B. M. S., & Senthil, R. (2021). A review on container geometry and orientations of phase change materials for solar thermal systems. *Journal of Energy Storage, 36*, 102452.

Ramirez, Jaramillo, & Gomez. (2020). Systematic review of encapsulation and shape-stabilization of phase change materials. doi: 10.1016/j.est.2020.101495

Rastogi, M., Chauhan, A., Vaish, R., & Kishan, A. (2015). Selection and performance assessment of Phase Change Materials for heating, ventilation and air-conditioning applications. *Energy Conversion and Management, 89*, 260-269. doi: 10.1016/j.enconman.2014.09.077

Regin, A. F., Solanki, S. C., & Saini, J. S. (2006). Latent heat thermal energy storage using cylindrical capsule: Numerical and experimental investigations. *Renewable Energy, 31*(13), 2025-2041. doi: 10.1016/j.renene.2005.10.011

Regin, A. F., Solanki, S. C., & Saini, J. S. (2008). Heat transfer characteristics of thermal energy storage system using PCM capsules: A review. doi: 10.1016/j.rser.2007.06.009

Republic, C. (2010). Latent heat storage systems. *Intensive Programme "Renewable Energy Sources, i*(May).

Rongrong, Z., Yongping, Y., Qin, Y., & Yong, Z. (2013). Modeling and Characteristic Analysis of a Solar Parabolic Trough System: Thermal Oil as the Heat Transfer Fluid. *Journal of Renewable Energy, 2013*, 1-8. doi: 10.1155/2013/389514

S.D. Sharma, Takeshi Iwata, Kitano, H., & Sagara, K. (2005). Thermal performance of a solar cooker based on an evacuated tube solar collector with a PCM storage unit

Sahoo, L. K., & Buddhi, D. (1997). Solar cooker with latent heat storage : Design and experimental testing. *38*(5).

Saini, S., & Kumar, N. (2017). <Thermal Performance of Solar Cooker Based on Evacuated Tube Collector and PCM Storage Unit.pdf>. *Asian Review of Mechanical Engineering, 6*.

Salunkhe, P. B., & Shembekar, P. S. (2012). A review on effect of phase change material encapsulation on the thermal performance of a system. *Renewable and Sustainable Energy Reviews, 16*(8), 5603-5616. doi: 10.1016/j.rser.2012.05.037

Santhi Rekha, S. M., & Sukchai, S. (2018). Design of Phase Change Material Based Domestic Solar Cooking System for Both Indoor and Outdoor Cooking Applications. *Journal of Solar Energy Engineering, 140*(4). doi: 10.1115/1.4039605

Sarbu, I., & Sebarchievici, C. (2018). A Comprehensive Review of Thermal Energy Storage. *Sustainability, 10*(1), 191. doi: 10.3390/su10010191

Sawarn, H., Kumar Shukla, S., & Singh Rathore, P. K. (2021). Development in Solar Cooking Technology in the Last Decade: A Comprehensive Review. *IOP Conference Series: Materials Science and Engineering, 1116*(1), 012046. doi: 10.1088/1757-899x/1116/1/012046

Saxena, A. (2017). Performance Evaluation of a Solar Cooker with Low Cost Heat Storage Material. *International Journal of Sustainable and Green Energy, 6*(4), 57. doi: 10.11648/j.ijrse.20170604.12

Saxena, A., Varun, Pandey, S. P., & Srivastav, G. (2011). A thermodynamic review on solar box type cookers. *Renewable and Sustainable Energy Reviews, 15*(6), 3301-3318. doi: 10.1016/j.rser.2011.04.017

Sekhon, M., & Sethi, V. (2019). Thermal modeling and analysis of novel twin-chamber community solar cooker as a replacement of biomass-based cooking. *International Journal of Green Energy, 16*(2), 167-184.

Senthil, R. (2021). Enhancement of productivity of parabolic dish solar cooker using integrated phase change material. *Materials Today: Proceedings, 34*, 386-388. doi: 10.1016/j.matpr.2020.02.197

Sharma, Buddhi, Sawhney, & Sharma. (2000). Design, development and performance evaluation of a latent heat storage unit for evening cooking in a solar cooker. *Energy Conversion & Management*.

Sharma, A., Tyagi, V. V., Chen, C. R., & Buddhi, D. (2009). Review on thermal energy storage with phase change materials and applications. *Renewable and Sustainable Energy Reviews, 13*(2), 318-345. doi: 10.1016/j.rser.2007.10.005

Sharma, C., Sharma, A. K., Mullick, S. C., & Kandpal, T. C. (2016). Uncertainty in estimating renewable energy utilisation potential: a case of solar thermal power generation in India. *International Journal of Ambient Energy, 38*(8), 765-773. doi: 10.1080/01430750.2016.1222952

Shrestha, J. N., & Byanjankar, M. R. (2007). Thermal Performance Evaluation of Box Type Solar Cooker using Stone Pebbles for Thermal Energy Storage

Singh, H. R., Sharma, D., & Soni, S. L. (2021). Dissemination of Sustainable Cooking: A Detailed Review on Solar Cooking System. *IOP Conference Series: Materials Science and Engineering, 1127*(1), 012011. doi: 10.1088/1757-899x/1127/1/012011

Siva, K., Lawrence, M. X., Kumaresh, G. R., Rajagopalan, P., & Santhanam, H. (2010). Experimental and numerical investigation of phase change materials with finned encapsulation for energy-efficient buildings. *Journal of Building Performance Simulation, 3*(4), 245-254. doi: 10.1080/19401491003624224

Skunpong, R., & Plangklang, B. (2011). A Practical Method for Quickly PV Sizing. *Procedia Engineering, 8*, 120-127. doi: 10.1016/j.proeng.2011.03.022

SNV. (2018). Review of Policies and Strategies Related to the Clean Cooking Sector in Ethiopia.

Soibam, J. (2017). *Numerical Investigation of a Phase Change Materials (PCM) heat exchanger.* Norwegian University of Science and Technology.

Tao, Y. B., & He, Y.-L. (2018). A review of phase change material and performance enhancement method for latent heat storage system. *Renewable and Sustainable Energy Reviews, 93*, 245-259. doi: 10.1016/j.rser.2018.05.028

Tesfay, H, A., Kahsay, M. B., & Nydal, O. J. (2019). Numerical and experimental Analysis of Solar Injera Baking with a PCM Heat Storage. *Momona Ethiopian Journal of Science, 11*(1), 1. doi: 10.4314/mejs.v11i1.1

Tesfay, Kahsay, M. B., & Nydal, O. J. (2016). Solar Cookers with Latent Heat Storage for Intensive Cooking Application. 1-9. doi: 10.18086/swc.2015.10.09

Tesfay, A. H., Kahsay, M. B., & Nydal, O. J. (2014). Solar Powered Heat Storage for Injera Baking in Ethiopia. *Energy Procedia, 57*, 1603-1612. doi: 10.1016/j.egypro.2014.10.152

Veerappan, M., Kalaiselvam, S., Iniyan, S., & Goic, R. (2009). Phase change characteristic study of spherical PCMs in solar energy storage. *Solar Energy, 83*(8), 1245-1252. doi: 10.1016/j.solener.2009.02.006

Vigneswaran, V. S., Kumaresan, G., Sudhakar, P., & Santosh, R. (2017). Performance evaluation of solar box cooker assisted with latent heat energy storage system for cooking application. *IOP Conference Series: Earth and Environmental Science, 67*, 012017. doi: 10.1088/1755-1315/67/1/012017

Voller, & Prakash. (1987). A fixed grid numerical mode~~ing methodology for convection-diffusion mushy region phase-change problems *International jornal of Heat and Mass Transfer, 30*.

Wei, J., Kawaguchi, Y., Hirano, S., & Takeuchi, H. (2005). Study on a PCM heat storage system for rapid heat supply. *Applied Thermal Engineering, 25*(17-18), 2903-2920. doi: 10.1016/j.applthermaleng.2005.02.014

WHO. (2018). Opportunities for transition to clean household energy., 76.

Wollele, & Hassen. (2019). Design and experimental investigation of solar cooker with thermal energy storage. *AIMS Energy, 7*(6), 957-970. doi: 10.3934/energy.2019.6.957

Yadav, A., & Samir, S. (2019). Experimental and numerical investigation of spatiotemporal characteristics of thermal energy storage system in a rectangular enclosure. *Journal of Energy Storage, 21*, 405-417.

Yishak, N. D. (2019). *Experimental Investigation, Selection and Thermal Performance Evaluation of Eutectic Mixture Using PCM for Cooking Application.* (Degree of Master of Science in Thermal Engineering experimetal), Adama Science and Technology University.

Zayed, M. E., Zhao, J., Li, W., Elsheikh, A. H., Elbanna, A. M., Jing, L., & Geweda, A. (2020). Recent progress in phase change materials storage containers: Geometries, design considerations and heat transfer improvement methods. *Journal of Energy Storage, 30*, 101341.

Zhang, H. L., Baeyens, J., Degrève, J., Cáceres, G., Segal, R., & Pitié, F. (2014). Latent heat storage with tubular-encapsulated phase change materials (PCMs). *Energy, 76*, 66-72. doi: 10.1016/j.energy.2014.03.067

Zhao, J., Zhai, J., Lu, Y., & Liu, N. (2018). Theory and experiment of contact melting of phase change materials in a rectangular cavity at different tilt angles. *International Journal of Heat and Mass Transfer, 120*, 241-249.

Zhao, W., Elmozughi, A. F., Oztekin, A., & Neti, S. (2013). Heat transfer analysis of encapsulated phase change material for thermal energy storage. *International Journal of Heat and Mass Transfer, 63*, 323-335. doi: 10.1016/j.ijheatmasstransfer.2013.03.061

Zheng, Y. (2015). Thermal Energy Storage with Encapsulated Phase Change Materials for High Temperature Applications.

APPENDIX

A1 Property design data for Thermia oil b

Temperature (℃)	Density (kg/m^3)	Specific heat $(k\,J/kg.K)$	Thermal conductivity $(W/m.K)$	Kinematic viscosity $(10^{-6}\times m^2/s)$	Prandtle number
0	876	1.809	0.136	230	3375
20	863	1.882	0.134	-	919
40	850	1.954	0.133	25	375
60	837	2.027	0.131	18.2	273
80	824	2.100	0.129	11.5	171
100	811	2.173	0.128	4.7	69
120	797.8	2.246	0.127	-	54
150	778	2.355	0.125	-	32
200	746	2.538	0.121	1.2	20
250	713	2.720	0.118	-	14
300	681	2.902	0.114	0.5	11
320	668	2.975	0.113	-	10
340	655	3.048	0.111	-	9

A2 Peimar full black 300 watt monocrystalline solar panel

ELECTRICAL CHARACTERISTICS (STC)*	SG300M (BF)
Nominal Output (Pmax)	300 W
Flash Test Power Tolerance	0/+5 W
Voltage at Pmax (Vmp)	32 V
Current at Pmax (Imp)	9.4 A
Open Circuit Voltage (Voc)	40.2 V
Short Circuit Current (Isc)	9.71 A
Maximum System Voltage	1500 V
Maximum Series Fuse Rating	15 A
Module Efficiency	18.44%

MECHANICAL CHARACTERISTICS

Solar Cells	60 (6x10) monocrystalline ***PERC***
Solar Cells Size	156x156 mm / 6x6"
Front Cover	3.2 mm / 0.12" thick, low iron tempered glass
Back Cover	TPT (Tedlar-PET-Tedlar)
Encapsulant	EVA (Ethylene vinyl acetate)
Frame	Anodized aluminium alloy, double wall
Frame finishing	Black
Backsheet finishing	White
Diodes	3 Bypass diodes serviceable
Junction Box	IP67 rated
Connector	MC4 or compatible connector
Cables Length	900 mm / 35.4"
Cables Section	4.0 mm² / 0,006 in²
Dimensions	1640x992x40 mm / 64.5x39x1.57"
Weight	18 Kg / 39.7 lbs
Max. Load	Certified to 5400 Pa

TEMPERATURE CHARACTERISTICS

NOCT**	45±2 °C
Temperature Coefficient of Pmax	-0.40 %/°C
Temperature Coefficient of Voc	-0.32 %/°C
Temperature Coefficient of Isc	0.047 %/°C
Operating Temperature	-40 °C ~ +85°C

PACKAGING***

Pallet dimensions	1700x1200x1200 mm / 67x47x47"
Pieces per pallet	27
Weight	516 Kg / 1138 lbs

CERTIFICATIONS

Fire Resistance Rating	1 (UNI 9177)

A3 Inverter specifications

INVERTER MODEL	LS-2012	LS-2324	LS-2548	LS-3024	LS-3548	LS-4024	LS-5048	LS-7048
Nominal DC Voltage	12V	24V	48V	24V	48V	24V	48V	48V
Continuous Power	2000W	2300W	2500W	3000W	3500W	4000W	5000W	7000W
1/2 Hour Rating	2200W	2800W	3000W	3700W	4100W	4500W	6000W	8500W
Surge Rating (5 Secs)	6000W	7000W	7500W	9000W	10500W	12000W	15000W	20000W
Current (Inrush)	25A	29A	31A	37A	43A	50A	62A	83A
Max. Out. Fault Current	25A	29A	31A	37A	43A	50A	62A	83A
Max. Out. Overcurrent protection	26A	30A	32A	38A	44A	51A	63A	84A
Input Voltage Range	10.5-17V	21-34V	42-68V	21-34V	42-68V	21-34V	42-68V	42-68V
Standby Current	75mA	45mA	35mA	50mA	40mA	60mA	55mA	60mA
Inverter ON-no load	1.1A	0.51A	0.30A	0.6A	0.33A	1.1A	0.47A	0.49A
Peak Efficiency	90%	94%	94%	93%	94%	94%	95%	95%
Weight	22Kg	22Kg	22Kg	24Kg	24Kg	30Kg	30Kg	34Kg
Dimensions	370mm(L) x 386 mm(W) x 180 mm(H)					475mm x 458mm x 187mm		
Output Voltage	230Vac +/- 4%							
Output Frequency	50Hz +/- 0.1%							
Output Waveform (THD)	True Sinewave (< 4%)							
Power Factor	All Conditions							
Autostart Sensitivity	0 - 20 W adjustable							
Operating Temperature	-20°C to +50°C							
DC to AC Isolation	3500 V							
Protection Circuitry	Overtemperature, Overload/Short Circuit, Battery Undervoltage/Overvoltage							
Battery Leads	1.5 m long with 10 mm mounting lugs							
AC Output Wiring	3 Terminal Hardwired Junction Box, labelled 'AC Output'							
AC Input Wiring	3 Terminal Hardwired Junction Box, labelled 'AC Input'							
AC Transfer Switch	230VAC, 40 Amps, 50Hz (Inrush 80A 0.5 seconds) (Only with KX option)							
Chassis	Powder Coated 3mm Aluminum					P.C 4mm Aluminum		
Warranty	3 Years Parts and Labour							
Standards	AS2279, AS3000, AS3100, EN55014, & C-TICK							
Ratings	Specifications @ 25° C ambient nominal battery voltage & unity power factor							
Operating Environment	5% - 95% (non-condensing) humidity, up to 2000m above sea level							

Due to constant improvements, specifications are subject to change without prior notice.

18

INVERTER SPECIFICATIONS

A4 Solar charge controller

MODEL	SCCM3024	SCCM4524	SCCM4548	SCCM6048	SCCM8048	SCCM10048	SCCM12048
Maximum Battery Current	30Amps	45Amps	45Amps	60 Amps	80 Amps	100Amps	120 Amps
Nominal System Voltage	12,24VDC(Auto detection)		12V, 24V, 48V DC (Auto detection)				
Maximum Solar Input Voltage	95V		145V			195V	
PV Start-up Voltage	15V						
PV Array MPPT Voltage Range	12VDC/24VDC		12VDC / 24VDC / 48VDC				
	15-80VDC/30-80VDC		15-130VDC / 30-130VDC 60-130VDC			15-170VDC / 30-170VDC 60-170VDC	
Maximum Input Power	12V - 420W	12V - 625W	12V - 625W	12V - 825W	12V - 1100W	12V - 1375W	12V - 1650W
	24V - 830W	24V - 1250W	24V - 1250W	24V - 1650W	24V - 2200W	24V - 2750W	24V - 3300W
	/	/	48V - 2500W	48V - 3300W	48V - 4400W	48V - 5500W	48V - 6600W
PV Array voltage & Battery current	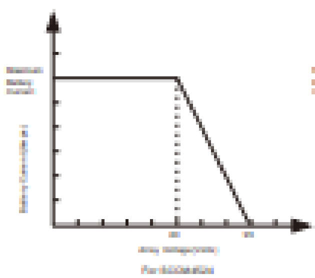 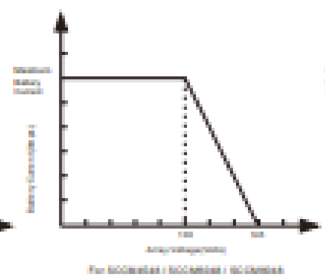 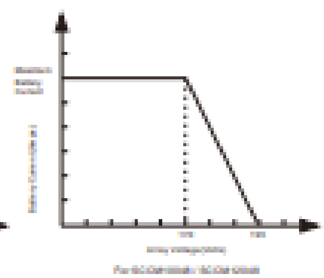						
Heatsink temperature & Battery current	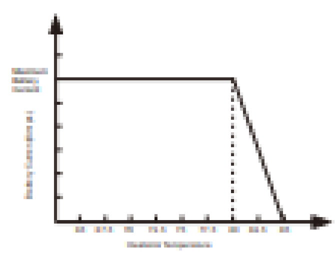						
Transient Surge Protection	4500 Watts / port						
Protections	Solar high voltage disconnect Solar high voltage reconnect Battery high voltage disconnect Battery high voltage reconnect High temperature disconnect High temperature reconnect						

A5 Thermal storage container base drawing

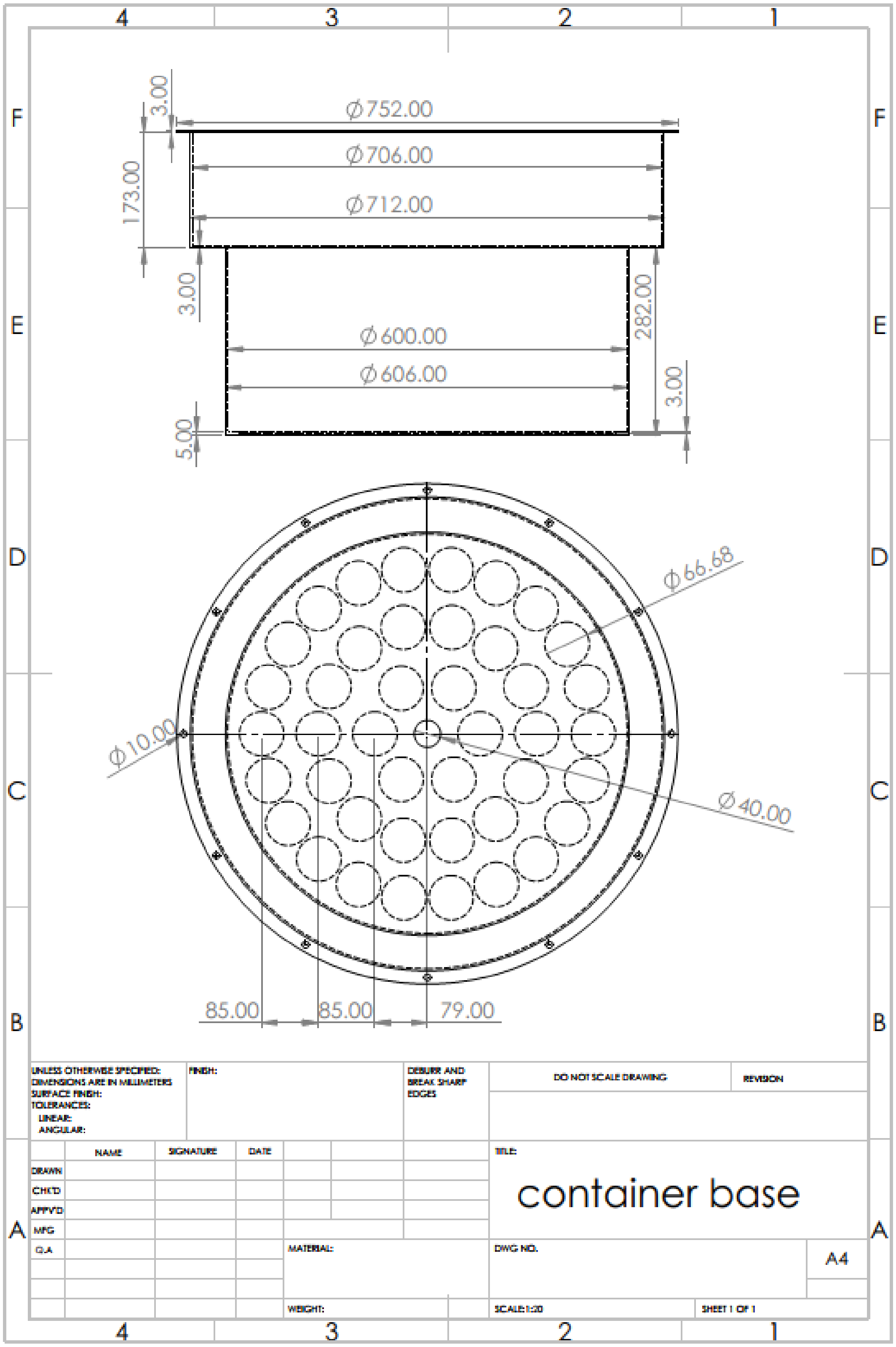

A6 Thermal storage container base cover drawing

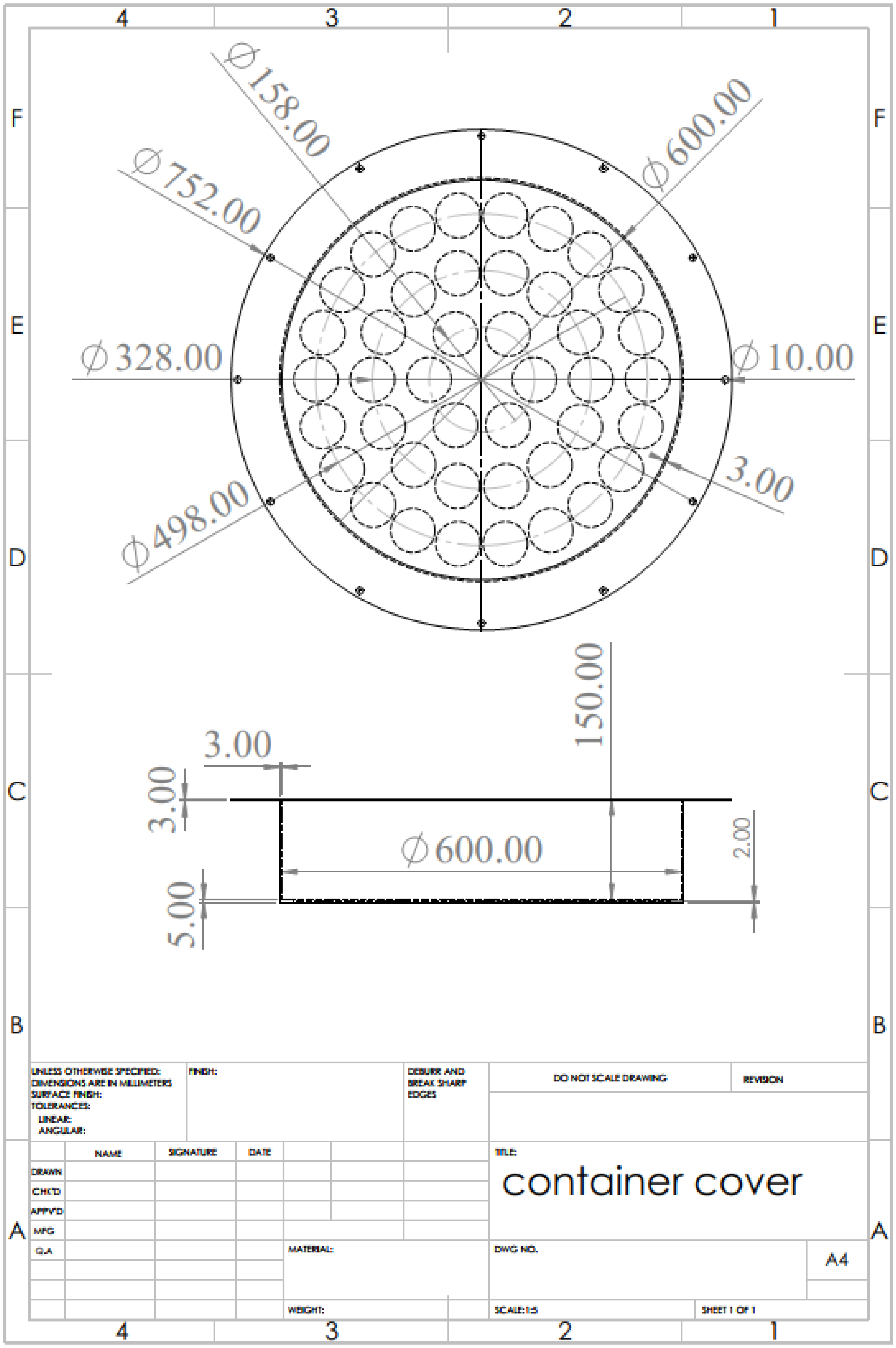

A7 PCM thermal storage container drawing

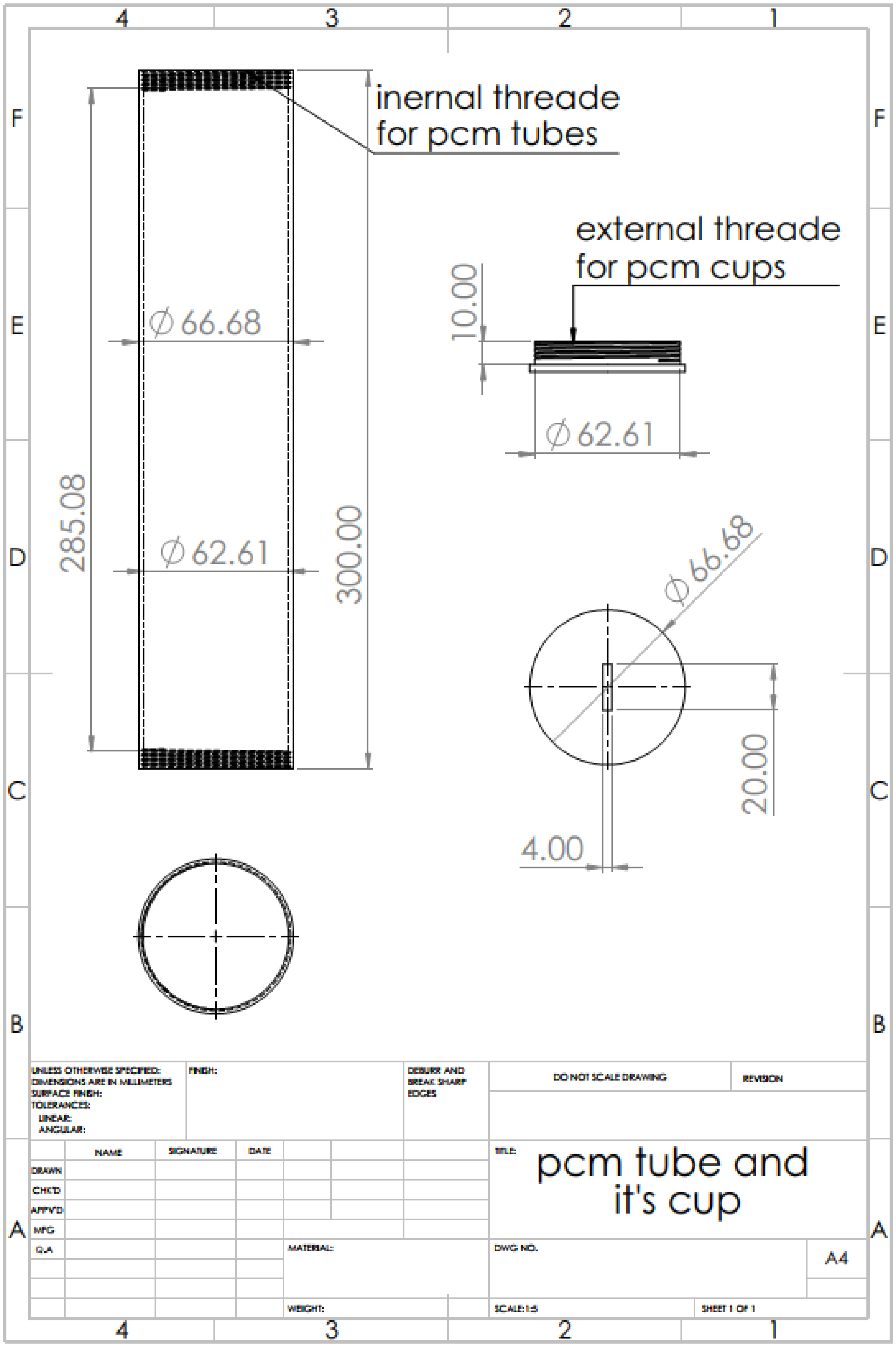

A8 Immersion oil heater drawing

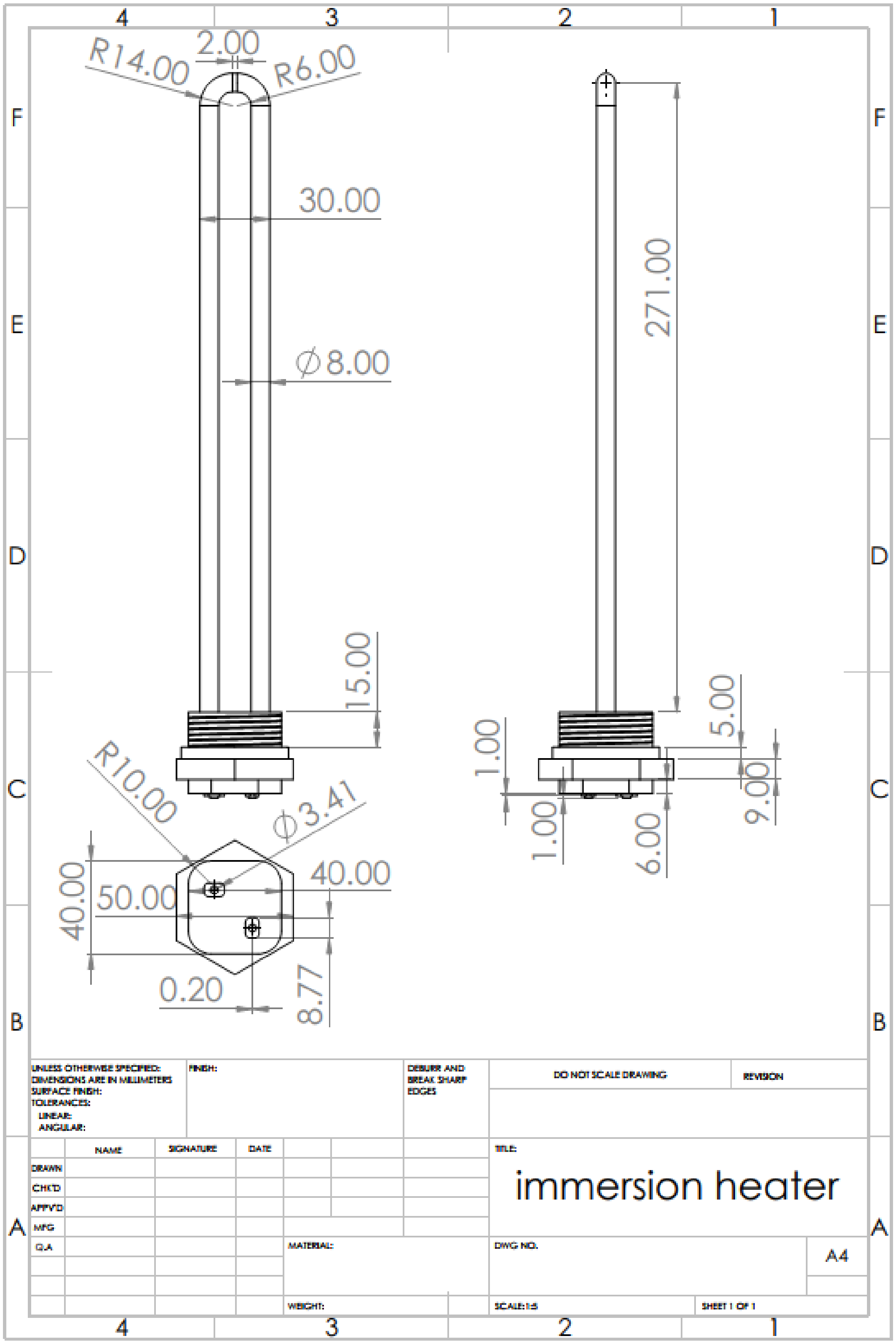

A9 Wheel and support drawing

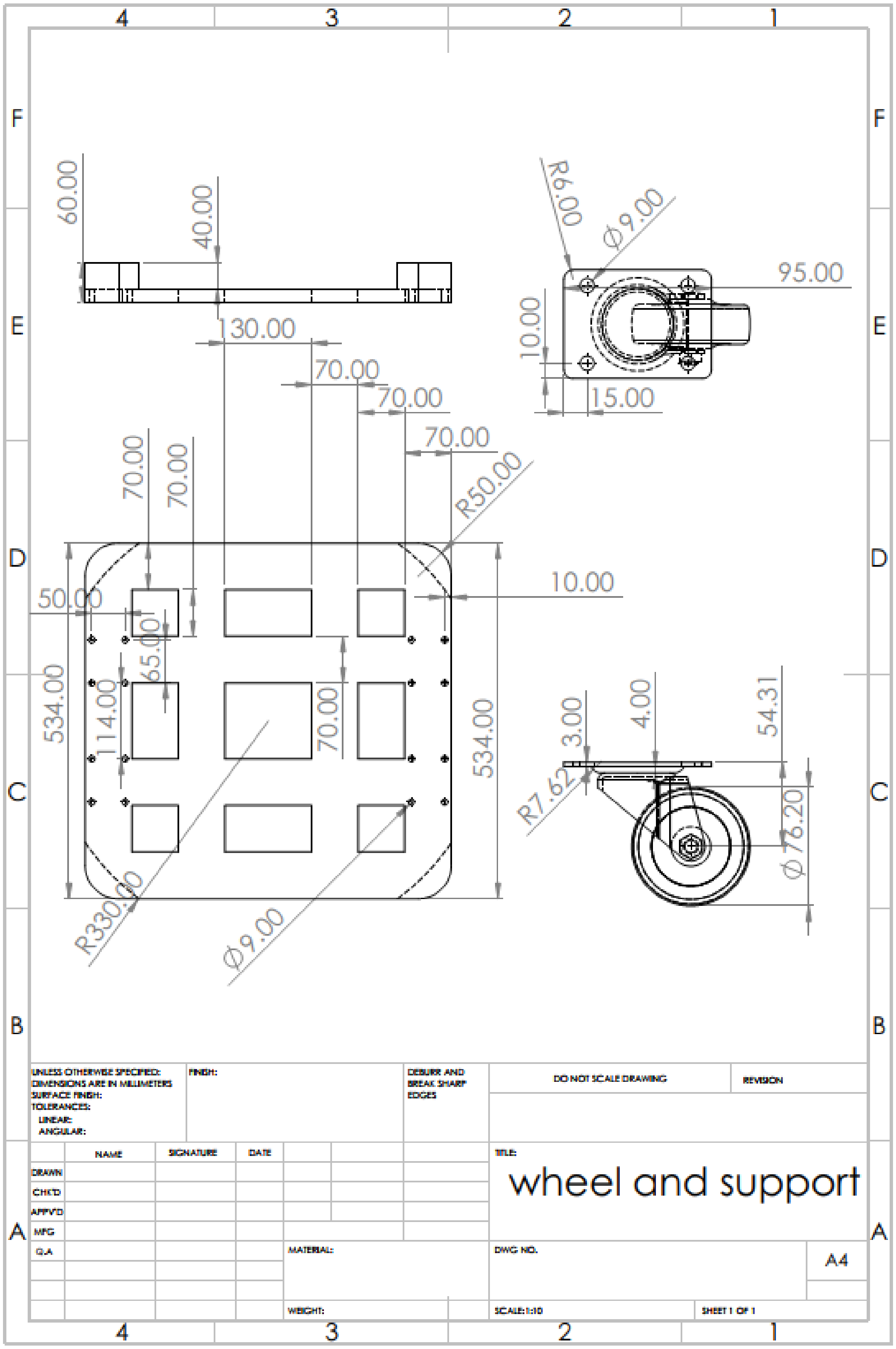

A10 Cooking pot drawing

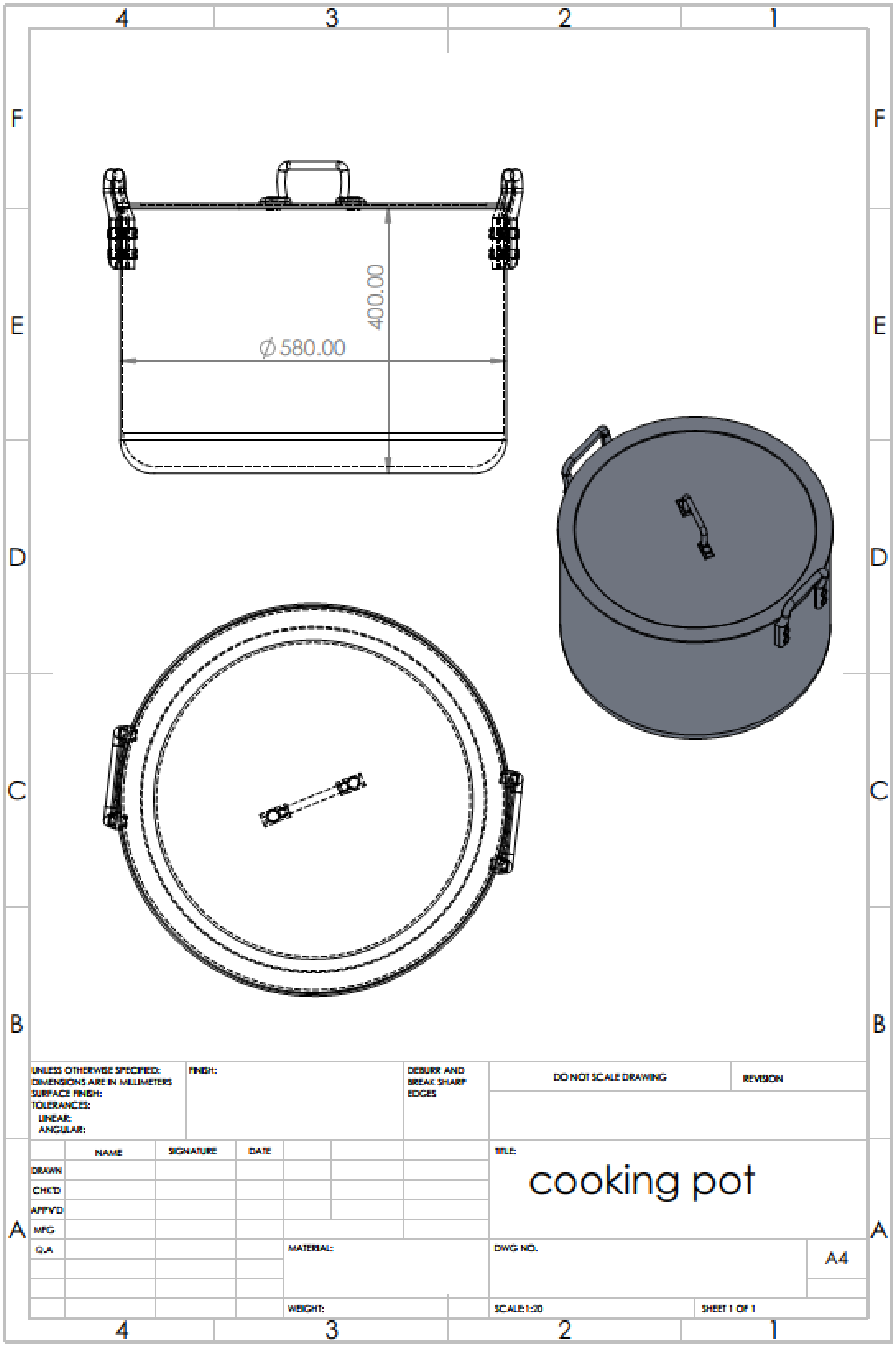

A 11 Insulation for Container

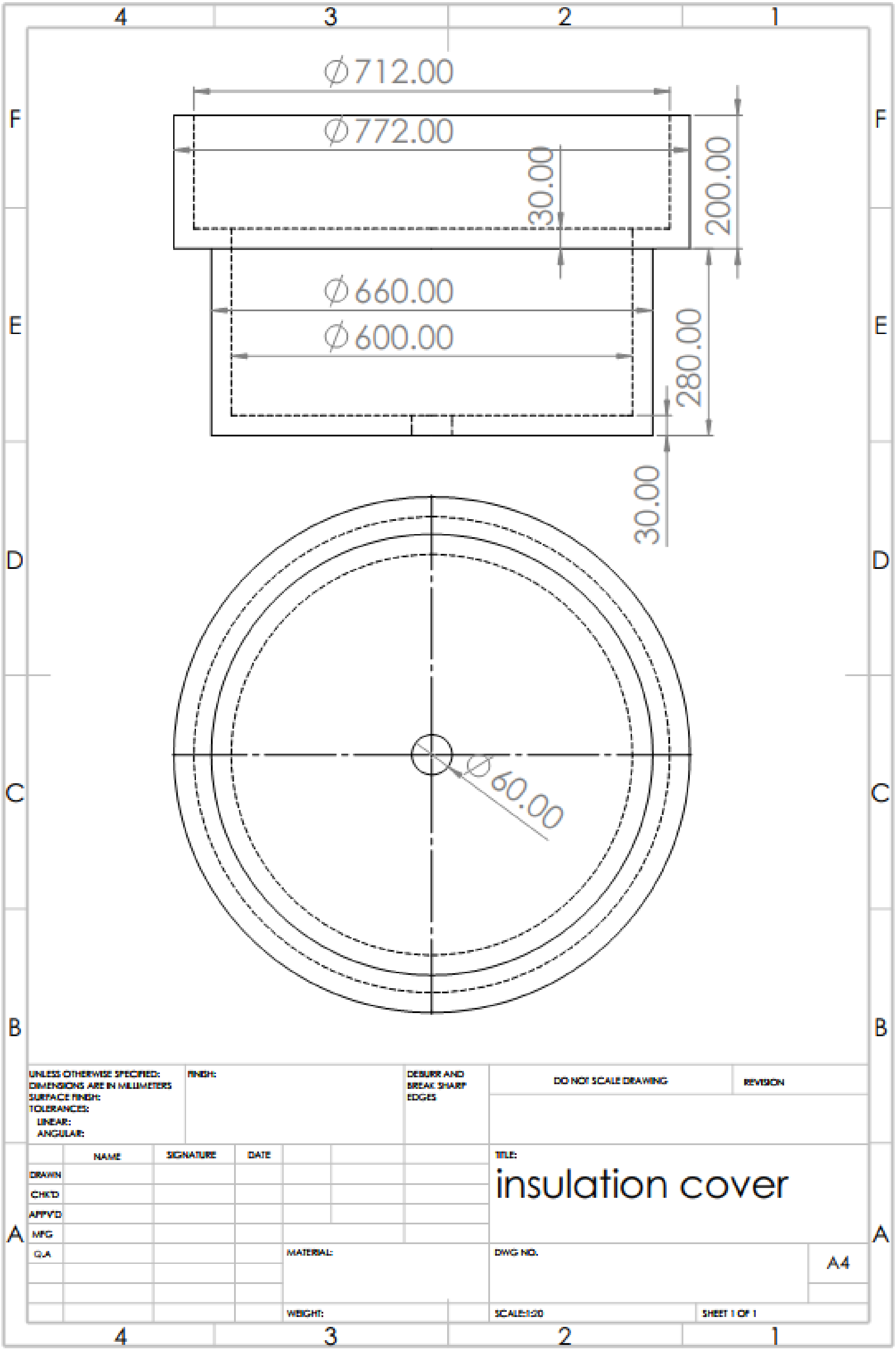

A12 Numerical approaches followed in Ansys fluent

Geometry

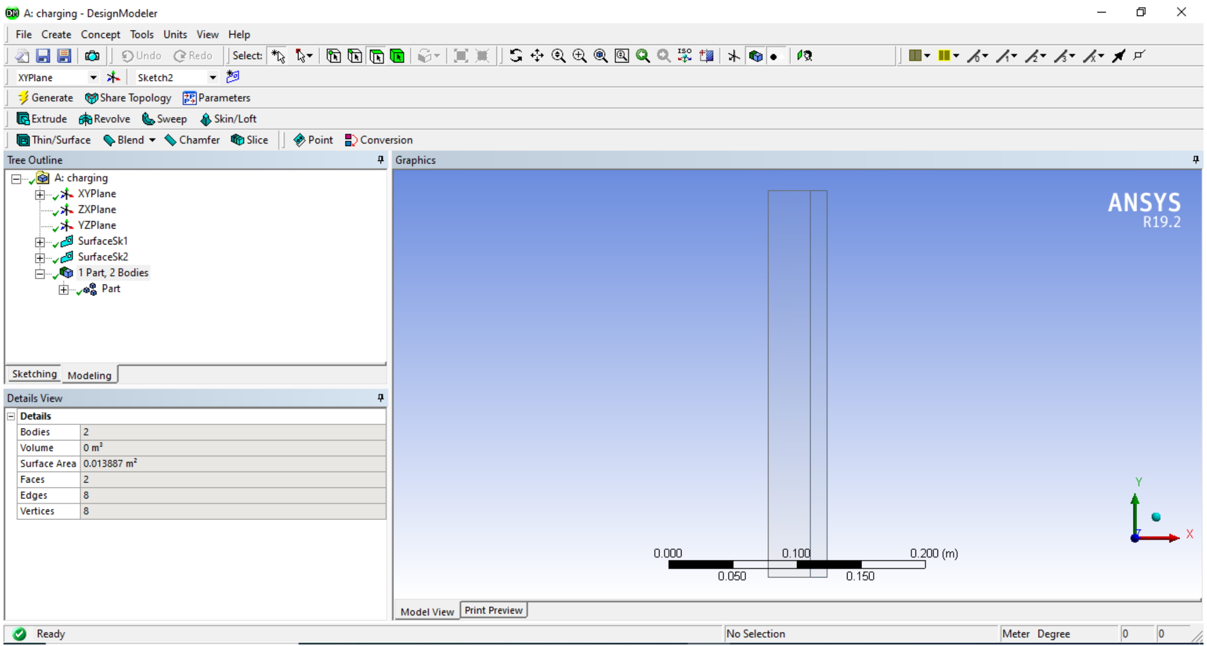

Mesh

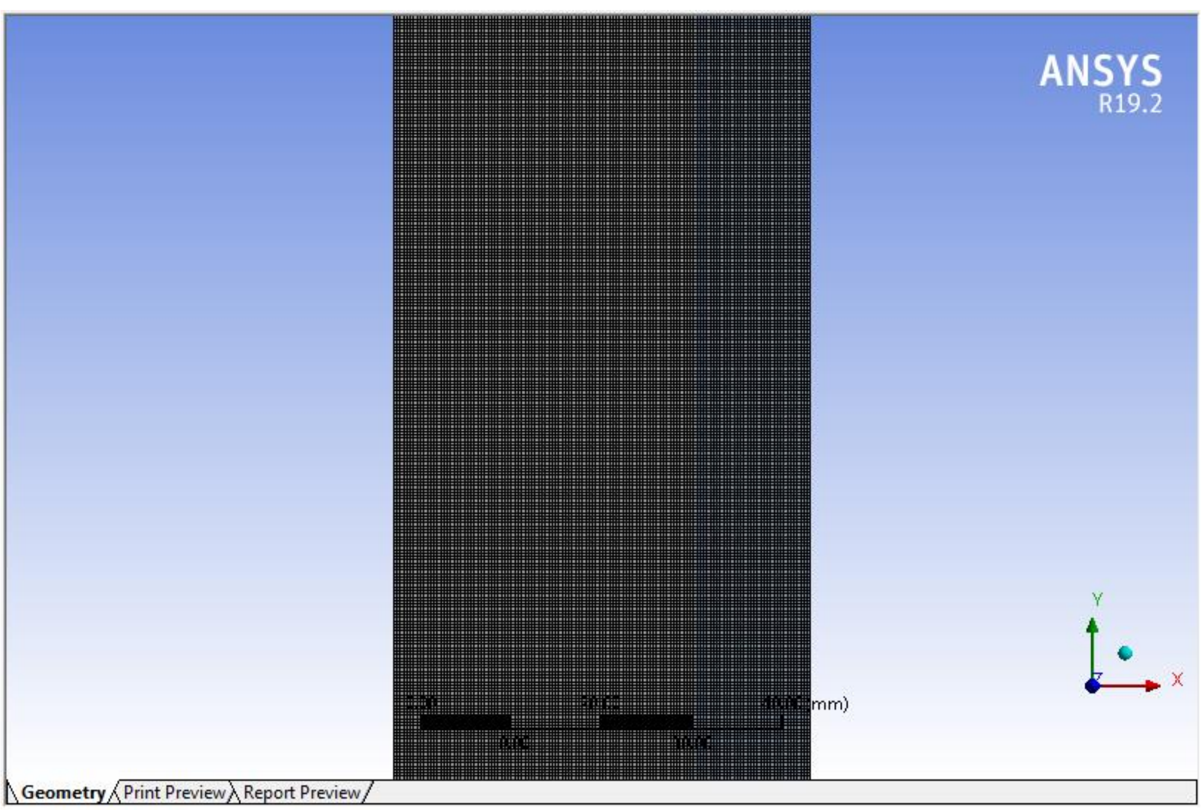

Named selection

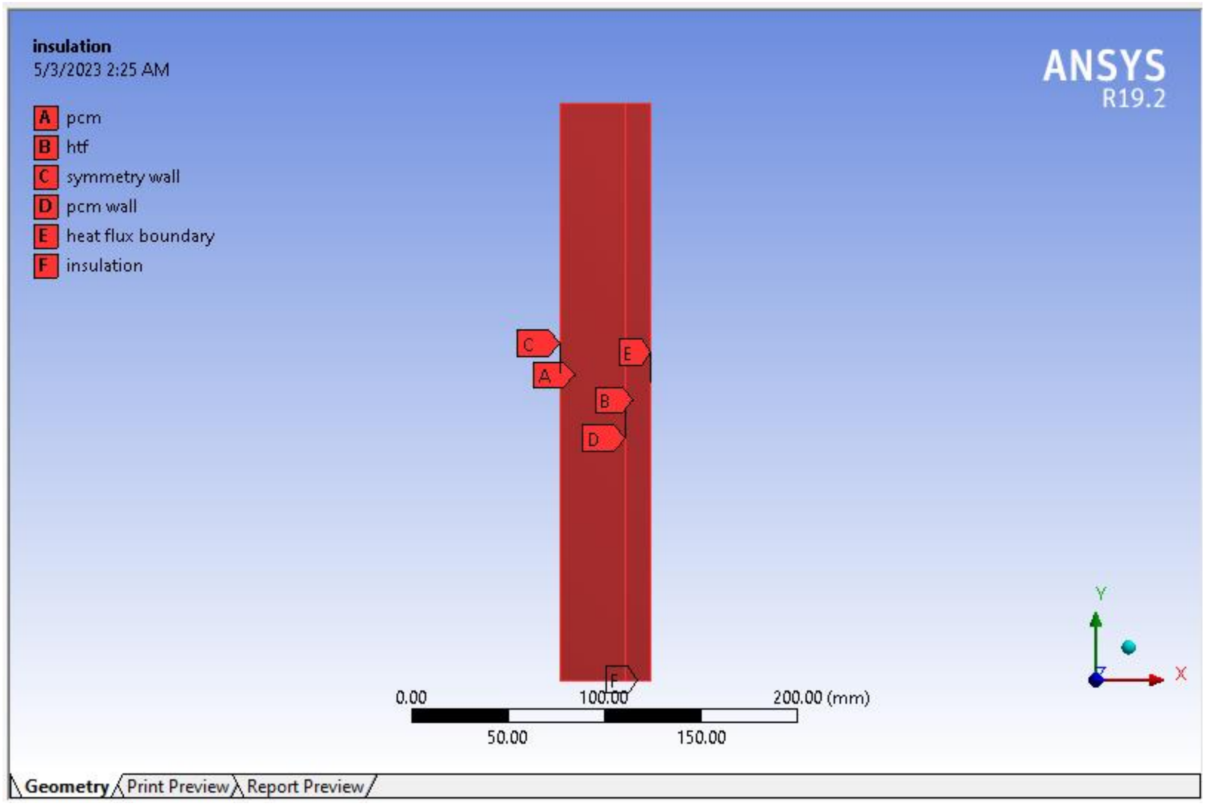

Ansys fluent launcher and models

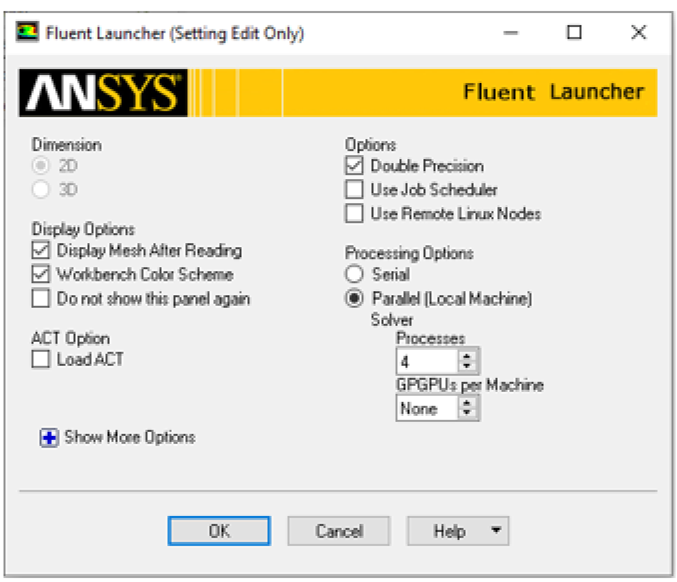

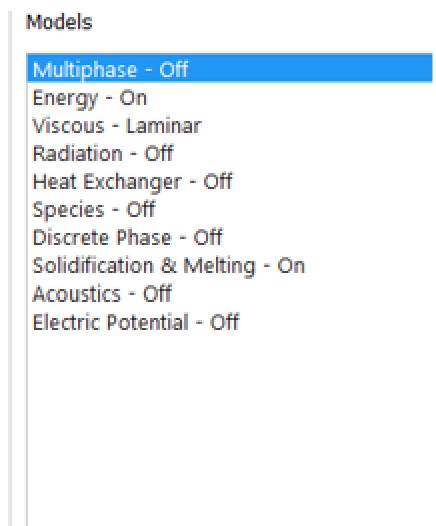

Materials

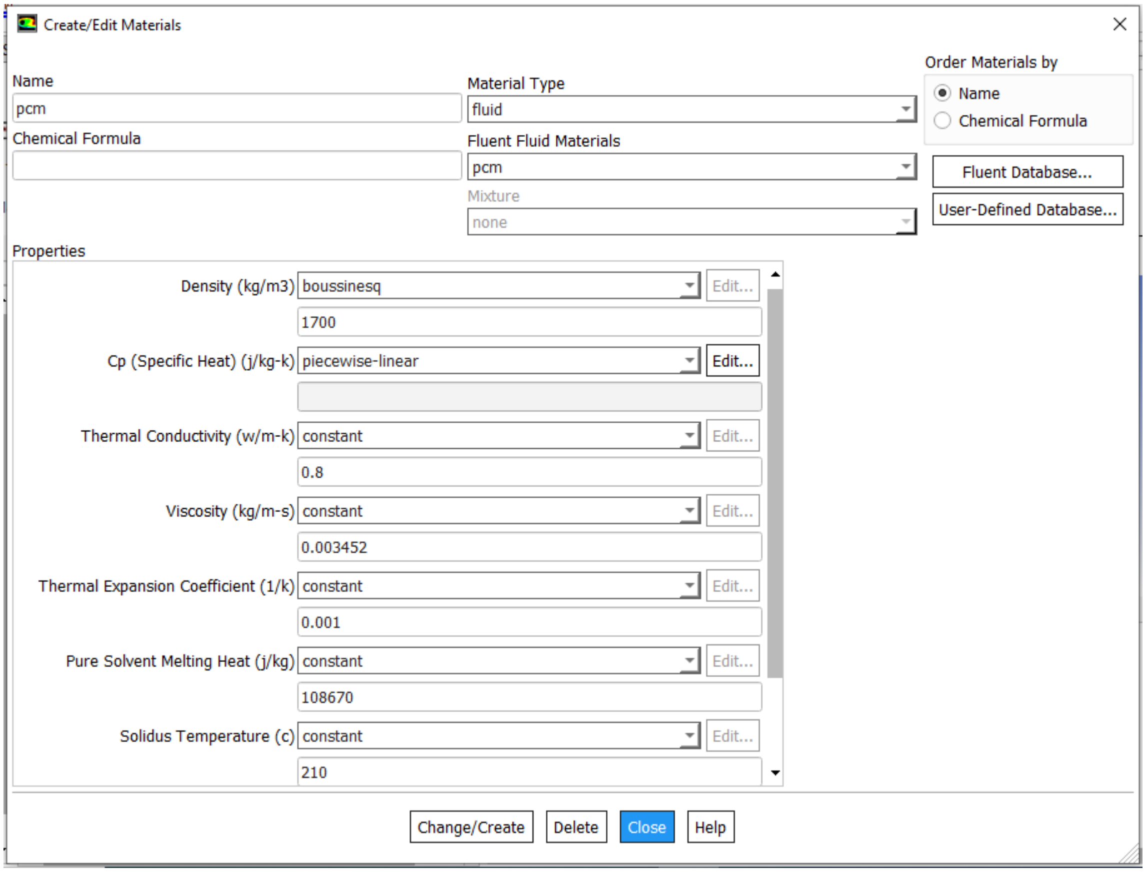
Create/Edit Materials
Name
pcm
Chemical Formula
Material Type
fluid
Fluent Fluid Materials
pcm
Mixture
none
Order Materials by
Name
Chemical Formula
Fluent Database...
User-Defined Database...
Properties
Density (kg/m3)
boussinesq
Edit...
1700
Cp (Specific Heat) (j/kg-k)
piecewise-linear
Edit...
Thermal Conductivity (w/m-k)
constant
Edit...
0.8
Viscosity (kg/m-s)
constant
Edit...
0.003452
Thermal Expansion Coefficient (1/k)
constant
Edit...
0.001
Pure Solvent Melting Heat (j/kg)
constant
Edit...
108670
Solidus Temperature (c)
constant
Edit...
210
Change/Create
Delete
Close
Help

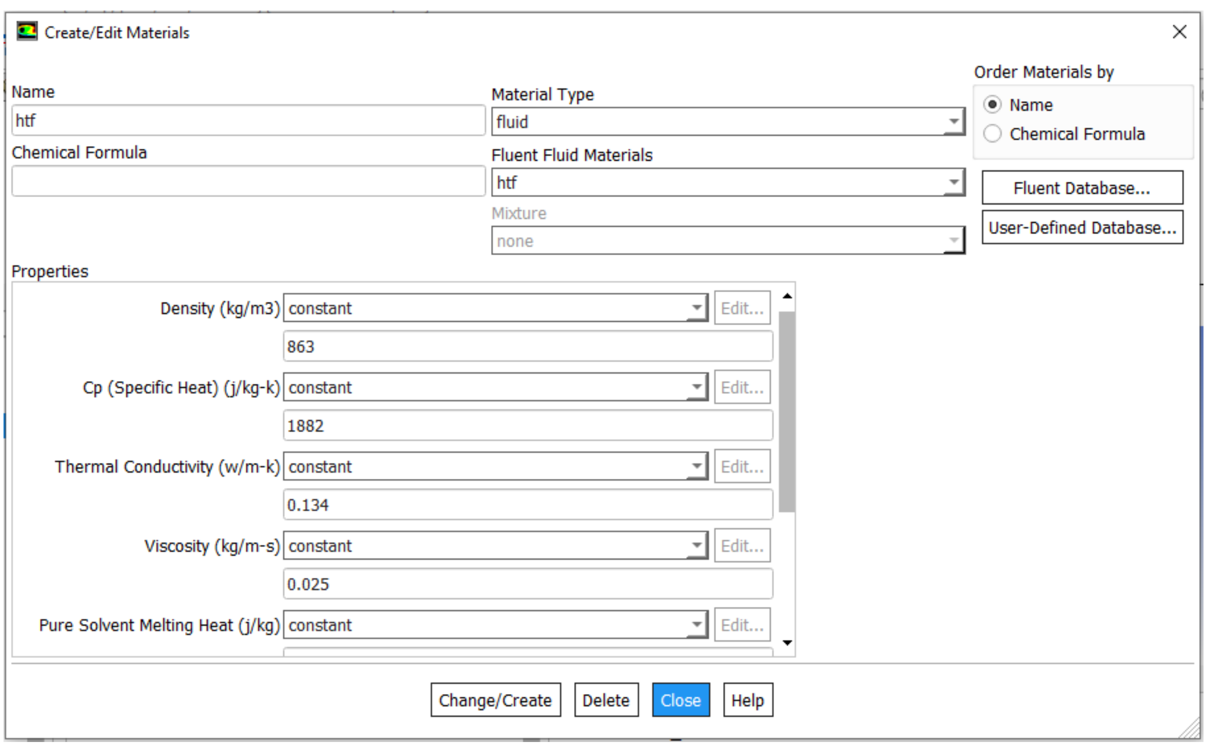
Create/Edit Materials
Name
htf
Chemical Formula
Material Type
fluid
Fluent Fluid Materials
htf
Mixture
none
Order Materials by
Name
Chemical Formula
Fluent Database...
User-Defined Database...
Properties
Density (kg/m3)
constant
Edit...
863
Cp (Specific Heat) (j/kg-k)
constant
Edit...
1882
Thermal Conductivity (w/m-k)
constant
Edit...
0.134
Viscosity (kg/m-s)
constant
Edit...
0.025
Pure Solvent Melting Heat (j/kg)
constant
Edit...
Change/Create
Delete
Close
Help

Boundary condition for charging

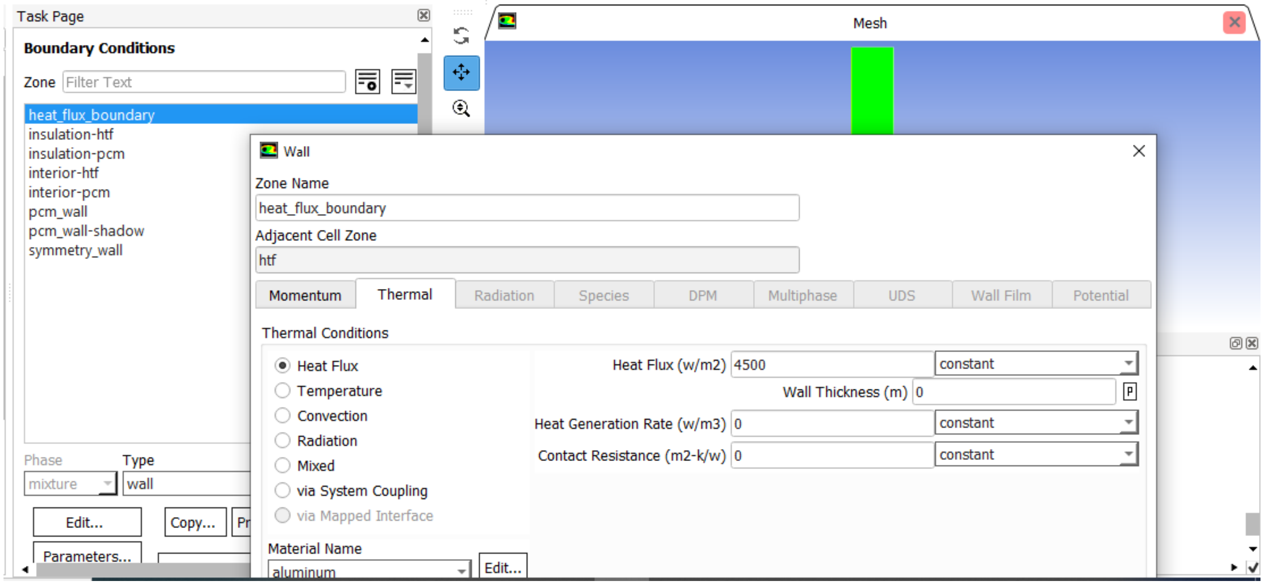

Boundary condition for discharging

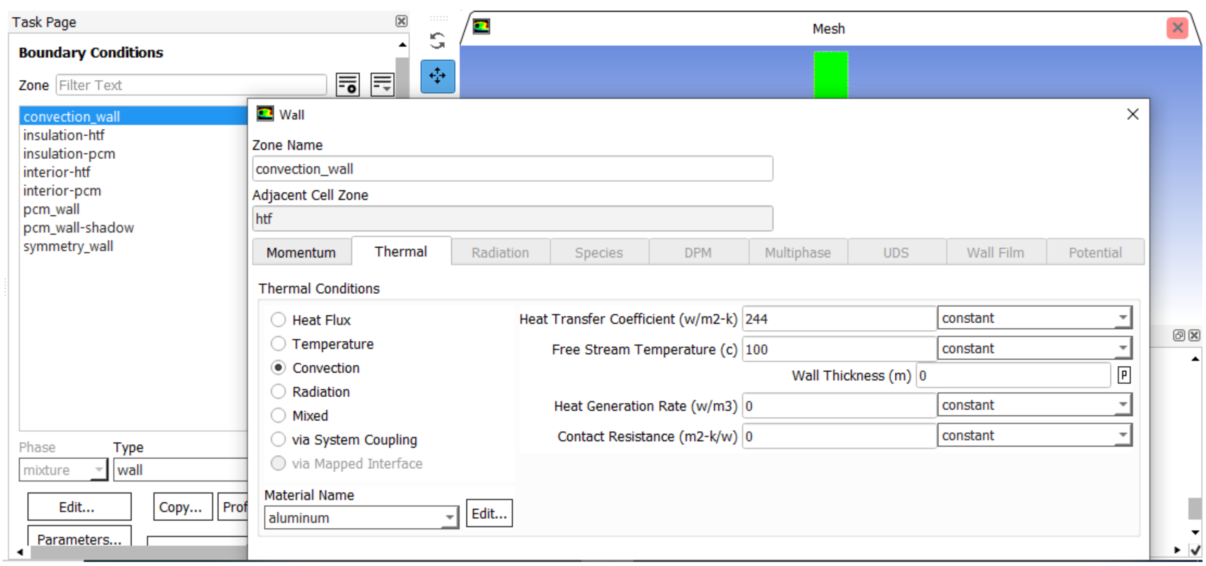

turnitin

Digital Receipt

This receipt acknowledges that Turnitin received your paper. Below you will find the receipt information regarding your submission.

The first page of your submissions is displayed below.

Submission author:	Tihun Birhanu
Assignment title:	Revised Thesis
Submission title:	Revised Design and Simulation of Institutional Solar-powere...
File name:	final_thesis_2.docx
File size:	10.13M
Page count:	125
Word count:	23,526
Character count:	130,124
Submission date:	27-Jun-2023 12:37PM (UTC+0300)
Submission ID:	2119577474

Addis Ababa University

Addis Ababa Institute of Technology

School of Mechanical & Industrial Engineering

Design and Simulation of Institutional Solar-powered Cookstove Using Thermal Storage System

A Thesis Submitted to the School of Graduate Studies of Addis Ababa Institute of Technology, Addis Ababa University in partial fulfillment for the Degree of Master of Science in Mechanical Engineering (Thermal engineering)

By: Tihun Birhanu Beyene

Advisors: Abdulkadir A. (PhD) & Kamil D. (PhD)

Addis Ababa, Ethiopia
June, 2023

Revised Design and Simulation of Institutional Solar-powered Cookstove Using Thermal Storage System

ORIGINALITY REPORT

19%	14%	13%	3%
SIMILARITY INDEX	INTERNET SOURCES	PUBLICATIONS	STUDENT PAPERS

PRIMARY SOURCES

1	www.researchgate.net Internet Source	1%
2	etd.aau.edu.et Internet Source	1%
3	etd.astu.edu.et Internet Source	1%
4	spectrum.library.concordia.ca Internet Source	1%
5	edisciplinas.usp.br Internet Source	<1%
6	dokumen.pub Internet Source	<1%
7	F. Fornarelli, V. Ceglie, B. Fortunato, S.M. Camporeale, M. Torresi, P. Oresta, A. Miliozzi. "Numerical simulation of a complete charging-discharging phase of a shell and tube thermal energy storage with phase change material", Energy Procedia, 2017 Publication	<1%